

DISCLAIMER

This report was prepared as an account of work sponsored by an agency of the United States Government. Neither the United States Government nor any agency thereof, nor any of their employees, makes any warranty, express or implied, or assumes any legal liability or responsibility for the accuracy, completeness, or usefulness of any information, apparatus, product, or process disclosed, or represents that its use would not infringe privately owned rights. Reference herein to any specific commercial product, process, or service by trade name, trademark, manufacturer, or otherwise does not necessarily constitute or imply its endorsement, recommendation, or favoring by the United States Government or any agency thereof. The views and opinions of authors expressed herein do not necessarily state or reflect those of the United States Government or any agency thereof.

Available to DOE and DOE contractors from the Office of Scientific and Technical Information, P.O. Box 62, Oak Ridge, Tennessee 37831; prices available from (615)576-8401, FTS 626-8401.

Available to the public from the National Technical Information Service, U.S. Department of Commerce, 5285 Port Royal Rd., Springfield, Virginia 22161.

Price: Printed Copy A05
Microfiche A01

EFFECT OF METALLIC ADDITIVES ON IN SITU COMBUSTION
OF HUNTINGTON BEACH CRUDE EXPERIMENTS

SUPRI TR 78

By
C. J. Baena
L. M. Castanier
W. E. Brigham

August 1990

Work Performed Under Contract No. FG19-87BC14126

Prepared for
U.S. Department of Energy
Assistant Secretary for Fossil Energy

Thomas B. Reid, Project Manager
Bartlesville Project Office
P.O. Box 1398
Bartlesville, OK 74005

Prepared by
Stanford University
Petroleum Research Institute
Stanford, CA 94305-4042

TABLE OF CONTENTS

	<u>Page</u>
LIST OF TABLES	iii
LIST OF FIGURES.....	iii
ACKNOWLEDGEMENTS	iv
ABSTRACT	v
1. INTRODUCTION.....	1
2. LITERATURE SURVEY	4
2.1 Kinetic Studies with Metals and Metallic Additives	5
2.2 Field Studies using Metallic Additives.....	7
3. PROBLEM STATEMENT	9
4. EXPERIMENTAL SYSTEM.....	12
5. EXPERIMENTAL PROCEDURE.....	19
6. EXPERIMENTAL DESIGN.....	25
7. EXPERIMENTAL OBSERVATIONS	27
7.1 Produced Gas Composition	27
7.2 Temperature Profiles.....	33
7.3 Recovery Data	39
8. EXPERIMENTAL RESULTS	45
8.1 Analysis of Gas Composition Data	45
8.1.1 Hydrogen to Carbon Ratios and Carbon Dioxide to Carbon Monoxide Ratios	45
8.1.2 Combustion Efficiency	47
8.1.3 Air Requirement at 100% Combustion Efficiency	49
8.1.4 Actual Air Requirements.....	49
8.1.5 Fuel Consumption	52
8.1.6 Fuel Availability.....	54
8.1.7 Air-Oil Ratios.....	58
8.1.8 Heat of Combustion	58
8.2 Combustion Front Temperature.....	61
8.3 Combustion Front Velocity	66
8.4 Discussion	66
8.4.1 Instabilities Early In-Situ Combustion Type Runs.....	66
8.4.2 Packing Technique for Sand Pack.....	68
8.4.3 Variations in Packing the Insulation	68
9. CONCLUSIONS AND RECOMMENDATIONS	69
REFERENCES	72
APPENDIX A	74

LIST OF TABLES

	<u>Page</u>
3.1 Summary of Qualitative Results of Kinetic Studies.....	10
4.1 Specifications of Components in Experimental System.....	14
5.1 Properties of Huntington Beach Crude Oil.....	20
5.2 Sieve Analysis of Ottawa Sand	21
6.1 Summary of Combustion Tube Runs	26
9.1 Results of Combustion Tube Runs	70

LIST OF FIGURES

1.1 Cross Section of a Reservoir Subjected to In-Situ Combustion.....	2
4.1 Schematic Diagram of the Experimental System.....	13
4.2 Details of the Combustion Tube Assembly	16
5.1 X-Ray Diffraction Patterns of Clay Showing Kaolinite Peaks.....	22
7.1 Produced Gas Composition for the Control Run.....	28
7.2 Produced Gas Composition for the Ferrous Chloride ($FeCl_2 \cdot 4H_2O$) Run	29
7.3 Produced Gas Composition for the Stannic Chloride ($SnCl_4 \cdot 5H_2O$) Run.....	30
7.4 Produced Gas Composition for the Zinc Chloride ($ZnCl_2$) Run	31
7.5 Packing Techniques Used for the Runs.....	32
7.6 Temperature Profiles for the Control Run	34
7.7 Temperature Profiles for the Ferrous Chloride ($FeCl_2 \cdot 4H_2O$) Run.....	35
7.8 Temperature Profiles for the Stannic Chloride ($SnCl_4 \cdot 5H_2O$) Run	36
7.9 Temperature Profiles for the Zinc Chloride ($ZnCl_2$) Run.....	37
7.10 Comparison of Combustion Front Temperatures	38
7.11 Recovery Data for the Control Run	40
7.12 Recovery Data for the Ferrous Chloride ($FeCl_2 \cdot 4H_2O$) Run.....	41
7.13 Recovery Data for the Stannic Chloride ($SnCl_4 \cdot 5H_2O$) Run.....	42
7.14 Recovery Data for the Zinc Chloride ($ZnCl_2$) Run.....	43
8.1 Plot of m and n Values.....	46
8.2 Oxygen Utilization Efficiencies	48
8.3 Air Requirements at 100% Efficiency (scf/lb of fuel burned).....	50
8.4 Actual Air Requirements (scf/cu ft reservoir).....	51
8.5 Fuel Consumption (lb of fuel/100 lbs of rock).....	53
8.6 Carbonaceous Residue for the Control Run	55
8.7 Carbonaceous Residue for the Ferrous Chloride ($FeCl_2 \cdot 4H_2O$) Run.....	56
8.8 Carbonaceous Residue for the Zinc Chloride ($ZnCl_2$) Run.....	57
8.9 Air Oil Ratio.....	59
8.10 Heat of Combustion (BTU/lb of fuel burned).....	60
8.11 Front Temperature and Heat Liberated for the Control Run.....	62
8.12 Front Temperature and Heat Liberated for the Ferrous Chloride ($FeCl_2 \cdot 4H_2O$) Run.....	63
8.13 Front Temperature and Heat Liberated for the Stannic Chloride ($SnCl_4 \cdot 5H_2O$) Run.....	64
8.14 Front Temperature and Heat Liberated for the Zinc Chloride ($ZnCl_2$) Run.....	65
8.15 Velocities of the Combustion Front.....	67

ACKNOWLEDGEMENTS

Financial support for this research was provided by the U.S. Department of Energy through contract DE-FG19-87BC 14126 and the Industrial Affiliates Committee of SUPRI A. Special thanks are due to Shell Oil Company for providing the crude oil from its Huntington Beach lease for use in these experiments and to Petrolite Corporation for supplying Tretolite RN-3003 used as a de-emulsifying agent for treating the crude oil-water emulsions produced during the tube runs.

ABSTRACT

The economics and applicability of an in-situ combustion process for the recovery of crude oil are dictated to a large extent by the nature and the amount of fuel formed during the process. If the amount of fuel deposited is insufficient, as in the case of light oil reservoirs, the combustion front will not be self sustaining. If excessive fuel is deposited, as in the case of very heavy oil reservoirs, the air requirements will be excessive and the process may not be economically viable. Through kinetic studies on crude oil oxidation in porous media, metals have been shown, on a qualitative basis, to affect the nature and the amount of fuel formed. The aim of this work is to use combustion tube studies to determine on a quantitative basis, how the nature and the amount of fuel formed could be changed by the presence of metallic additives.

These experiments follow from the qualitative observations on the effect of metallic additives on the in-situ combustion of Huntington Beach crude oil made by De los Rios (1987) at SUPRI. He performed kinetic studies on the oxidation of Huntington Beach crude in porous media and showed that the nature of the fuel formed changed when metallic additives were present.

In this study, combustion tube runs were performed using the metallic additives: ferrous chloride ($\text{FeCl}_2 \cdot 4\text{H}_2\text{O}$), zinc chloride (ZnCl_2) and stannic chloride ($\text{SnCl}_4 \cdot 5\text{H}_2\text{O}$). Soluble salts of these metals were selected from the results observed in De Los Rios' kinetic studies. Unconsolidated cores were prepared by mixing predetermined amounts of an aqueous solution of the metal salt, Huntington Beach crude oil, Ottawa sand and clay in order to achieve the desired fluid saturations. The mixture was then tamped into the combustion tube. Dry air combustion tube runs were performed keeping the conditions of saturation, air flux and injection pressure approximately the same during each run.

The nature of the fuel formed and its impact on the combustion parameters were determined and compared with a control run - an experiment performed with no metallic additive. It was found that the presence of metallic additives increased the atomic hydrogen to carbon ratio of the fuel from 0.07 for the control run to 0.13 in the presence of ferrous chloride, 0.61 with zinc chloride and 0.79 with stannic chloride. The H/C ratio of the fuel coupled with the extent to which the oxidation formed CO_2 in preference to CO affected the following combustion parameters: velocity of the combustion front, heat of combustion of the deposited fuel, air requirements at 100% combustion efficiency, the air/oil ratio and the oil recovery rates. As a result of the increased hydrogen content of fuel, the heat of combustion and the air requirements at 100% combustion efficiency increased as the H/C ratio increased. The metallic additives increased the burning front velocity and the oil recovery rate. However these were found to be affected by the oxygen utilization efficiency, the nature and the amount of fuel formed and the air flux.

1. INTRODUCTION

Thermal recovery is one of the principal enhanced oil recovery techniques used to recover low API gravity, viscous crude oils. Its objective is to bring about a reduction in the viscosity of the crude oil by heating in order to improve the mobility of the crude. This enhances the displacement efficiency increasing the amount of oil that can ultimately be produced. Thermal recovery in which heat is generated in the reservoir by burning a part of the oil in place is known as fireflooding or in-situ combustion.

Figure 1.1 shows a schematic cross section of a reservoir during dry, forward in-situ combustion. In this process ignition is usually initiated by the use of gas or electric heaters in the injection well while air or oxygen is injected to initiate and sustain combustion. The fuel that is burnt is the unrecoverable carbon rich residue that is deposited behind the steam front as a result of distillation, thermal cracking and some catalytic cracking. The heat that is generated partially distills the crude oil. The distilled light ends of the crude oil along with the water vapor that is generated through the vaporization of the residual water and also as a combustion product, move ahead of the region of the combustion front. The region ahead of the combustion front is heated by the conduction of heat, by the convection of the combustion gases, and by the condensation of volatiles and the generated steam. The oil ahead of the combustion front is displaced toward the production well by gas drive provided by the combustion gases, by hot water and steam drive provided by the condensing steam, and by miscible drive provided by the condensed light ends.

In-situ combustion is applicable to a wide range of reservoir fluid characteristics. The absence of wellbore heat losses in the injection well allows in-situ combustion to be carried out in deeper reservoirs having thinner, tighter sand sections which are not amenable to steam injection. The oil that is produced is also lighter than the oil in place as a result of cracking and distillation. In-situ combustion also has a higher energy utilization ratio than cyclic steam injection or steam drive. However, the applicability of the in-situ combustion process is limited by the nature and the amount of the fuel formed ahead of the combustion front. If insufficient fuel is deposited, as is likely in light oil reservoirs, the combustion front will not be self sustaining. If excessive fuel is deposited, as is likely in very heavy oil reservoirs, the air requirements will be excessive and the front velocity and the oil recovery rate will be too slow to be economically viable. The nature of the fuel formed determines the amount of heat liberated per mole of fuel burned, which in turn determines the extent of visbreaking and thermal cracking. It thus follows that if the nature and amount of fuel formed could be changed by some economical technique, the process of in-situ combustion could be adopted to recover crude oil from a wider variety of reservoirs having different fluid characteristics.

Earlier work done by a number of researchers, particularly De Los Rios (1987), has shown, on a qualitative basis, that the use of metallic additives affects the nature of the fuel formed; this, in turn, will affect the heat of combustion, the air-oil ratio, the air requirements, the front velocity and the oil recovery rate. To determine on a quantitative basis the nature of the fuel formed and the impact of metallic additives on the combustion parameters, combustion tube experiments are needed. In this work, combustion tube experiments were performed on Huntington Beach crude oil in the presence of water soluble iron ($\text{FeCl}_2 \cdot 4\text{H}_2\text{O}$), tin ($\text{SnCl}_4 \cdot 5\text{H}_2\text{O}$) and zinc (ZnCl_2) salts, and the results of these runs were compared to a control run with no additive.

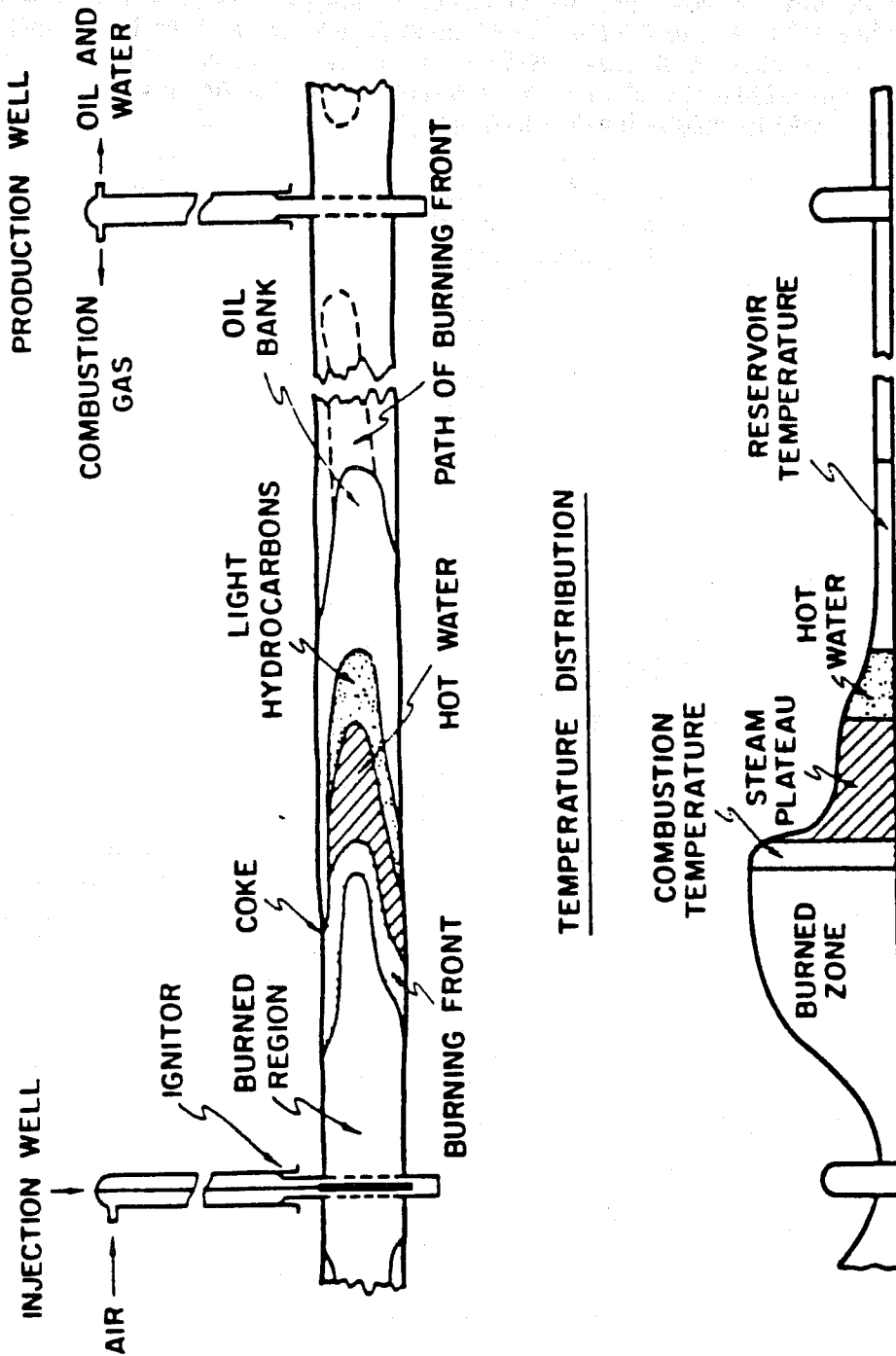


Figure 1.1 Cross Section of a Reservoir subjected to In-Situ Combustion.

The sections that will be encountered in this thesis are as follows. Section 2 contains a literature survey which outlines the work done by prior researchers on the effect of metallic additives on in-situ combustion. Section 3 provides a description of the results of De Los Rios's kinetic studies and the study undertaken herein. Section 4 provides a description of the experimental apparatus used. Section 5 describes the experimental procedure used to perform the combustion tube runs. Section 6 provides details of the design of the experiments. Section 7 discusses the observed effects of the metallic additives on the nature of the fuel formed and its impact on the combustion parameters. Section 8 provides a summary of the conclusions made and the recommendations for future work. Appendix A outlines the method of Dew and Martin (1965) that is used to analyze the data from the runs.

2. LITERATURE SURVEY

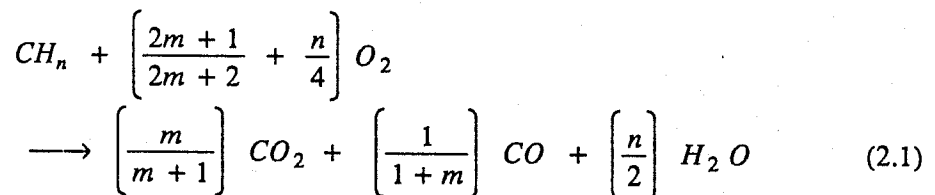
The study of the effects of metallic additives on in-situ combustion emerged in the late nineteen seventies as a result of the observations of increased fuel deposition and increased air requirement in reservoirs having minerals with high metallic content in the rock matrix (Burger and Sahuquet, 1974; Bardon and Gadelle, 1977; Earlougher *et al.*, 1970 and Hardy *et al.*, 1972). Researchers first attempted to understand the reactions involved in the combustion reaction through determination of the kinetics of crude oil oxidation in porous media when metallic additives were present (Burger and Sahuquet, 1974; Fassihi, 1981; Sidqi *et al.*, 1985; Racz, 1985). Their observations that metallic additives increased fuel deposition encouraged investigation of such additives in reservoirs to modify the nature of the fuel formed and to change the combustion parameters involved in the in-situ combustion reaction (Racz, 1985). This section will discuss the qualitative observations made during such kinetic studies and the field studies that were performed using metals and metallic additives.

In order to understand the discussion of the effects of metallic additives on in-situ combustion, it is necessary to briefly explain how the oxidation reactions that take place have been modeled in the kinetic studies, for several references to these modeled reactions will be made throughout this thesis. The reaction kinetics have been modeled into three sets of reactions: (1) low temperature oxidation, (2) medium temperature reactions and (3) high temperature oxidation. A discussion of these reactions and the research findings follows.

Low temperature reactions (LTO) result in the formation of chemicals such as peroxides, hydroperoxides, aldehydes, ketones, carboxylic acids and alcohols (Burger and Sahuquet, 1972). Alexander *et al.* (1962) and Al-Saadon (1970) showed that fuel availability was increased when low temperature oxidation of the crude oil took place. Dabbous and Fulton (1974) also found this to be true. They found that LTO causes a substantial decline in recoverable oil from the distillation and cracking zones, an increase in the fuel deposition and marked changes in the fuel characteristics and coked sand properties.

Medium temperature reactions involve distillation, visbreaking and coking of the fuel along with partial oxidation of the products formed (Bardon and Gadelle, 1977; Fassihi, 1981; Sidqi *et al.*, 1985). The amount of coking and the atomic H/C ratio of the fuel were found to decrease with increasing coking temperature (Bousaid, 1967). Increasing pressure was found to increase the amount of hydrocarbon residue formed; but the fuel deposited had a lesser hydrogen content (Sidqi *et al.*, 1985).

High temperature oxidation (HTO) reactions involve oxidation of the cracked hydrocarbon residue. HTO takes place according to the following equation:



In Eq. (2-1), m is the ratio of carbon dioxide to carbon monoxide formed upon oxidation of the fuel, and n is the atomic hydrogen to carbon ratio of the fuel burned.

The analysis of the reaction rates of the three modeled in-situ combustion reactions has traditionally been expressed in terms of oxygen concentration rather than in terms of carbon oxides formed because oxygen is partially consumed in the low temperature reactions resulting in the formation of oxidized products not found in the produced gas.

The reaction rate R_r is expressed as:

$$R_r = k P_{O_2}^a C_f^b \quad (2.2)$$

In Eq. (2-2), a is the order of the reaction with respect to the partial pressure of oxygen present, P_{O_2} ; b is the order of the reaction with respect to the concentration of the fuel, C_f , k is the rate constant related to the Arrhenius (1889) constant, A_r , and the energy of activation, E , given by the expression:

$$k = A_r \exp(-E/RT) \quad (2.3)$$

In Eq. (2-3), R is the universal gas constant and T is the absolute temperature. The Arrhenius rate constant, A_r , was found to be dependent on the grain size distribution of the porous medium (Burger and Sahuquet, 1971; Bardon and Gabelle, 1977). The energy of activation, E , was found to be insensitive to the type of crude and the porous medium (Dabbous and Fulton, 1974).

The reaction rate has been found to be first order with respect to the fuel concentration and was found to have an order of 0.5 to 1 with respect to the oxygen partial pressure (Dabbous and Fulton, 1974). Weijdema (1968) and Fassihi (1981) found that the order for the LTO reaction, in terms of the partial pressure of oxygen, was close to unity.

With this brief review of the modeling of the oxidation reactions, the discussion now focuses on the effect of metals and metallic additives on in-situ combustion. Metals have long been known to catalyze hydrocarbon oxidation and cracking reactions and have been extensively used as catalysts in the chemical and petroleum refining industries. Gureyev and Sublina (1965) found that by adding metals such as copper, brass, iron, aluminum, tin, lead or zinc, oxidation of the crude oil was promoted by destroying the antioxidants naturally present in the crude.

The oxidation of hydrocarbons has been found to be catalyzed by metals through a chain reaction mechanism involving initiation, propagation and termination steps. The classical steps are outlined by Racz (1985), and repeated in De Los Rios's thesis (1987) and will not be repeated here.

2.1 Kinetic Studies with Metals and Metallic Additives

Several kinetic studies have been performed to determine the influence of metals and metallic additives on the oxidation characteristics of crude oils. The work performed and the observations made during these experiments are described below.

In two separate experiments, Burger and Sahuquet (1972) studied the influence of 1% nickel oxide and 2,000 ppm copper in sand on the oxidation of a 27° API crude. They found that the activation energy of the low temperature reaction was reduced with a corresponding

increase in the amount of fuel deposited. This was evident from the occurrence of oxidation at a lower temperature with a high peak for the high temperature reaction.

Fassihi (1981) studied the oxidation of a 27° API crude and the effect of adding 2,000 ppm copper to the sand. He found that the activation energy of the low temperature reaction was unaffected, but higher reaction rates were observed in the low temperature reaction as a result of an increased Arrhenius rate constant, A_r . The activation energy of the medium temperature reaction increased by about fifty percent, but that of the high temperature reaction decreased by fifty percent.

Thermogravimetric analysis (TGA) and differential scanning calorimetric (DSC) analysis have been used to determine important combustion parameters such as the combustion front temperature, the heat value of the crude oil, amount of fuel deposited, and the average H/C ratio during combustion. In thermogravimetric analysis, a sample is weighted continuously as it is heated at a constant rate. The resulting curve of weight change versus time or temperature gives the TGA thermogram. Kinetic data may be derived from analysis of the TGA plot (McCarthy *et al.* 1971). In differential scanning calorimetry, the energy changes in a sample are detected and measured as a function of time or temperature. In practice the temperature of a sample is compared continuously with a reference material at a constant temperature.

Racz (1985) studied the influence of iron pentacarbonyl, and a mixture of manganese, vanadium and other metals using TGA and DSC. He found that iron generated the greatest heat at a lower temperature, implying that the low temperature oxidation reaction rate was increased and hence more fuel was deposited during the medium temperature reaction. Iron pentacarbonyl was successfully used in a pilot study on the Demjen-Kelet field where recovery was increased from 15% under primary recovery to 60% using iron-catalyzed in-situ combustion initiated by tertiary butyl hydroperoxide (TBH). TBH was injected along with air into the reservoir and its pressure was raised to 2-4 MPa. Once the combustion front was stabilized, a 1% solution of iron pentacarbonyl was injected to catalyze the combustion process. A detailed discussion of this pilot study will be provided in the next sub-section on field tests in the presence of metallic additives.

Drici and Vossoughi (1985) studied the influence of vanadium, titanium, nickel, copper and iron oxides on the oxidation of a 20° API crude using TGA and DSC. Oxidation reactions were first carried out with increasing amounts of the metal oxides present. As the amount of metal oxides in the mixture increased, they made two significant observations: (1) the fractional amount of heat released in the low temperature region gradually increased and attained a maximum level; (2) the coke combustion peak shifted to a lower temperature and became smaller. They then carried out experiments on mixtures of metal oxide (1% by weight), crude oil (5% by weight) and coarse sand having grain size less than 48 mesh and found that, in contrast, the heat released during the high temperature oxidation was increased as a result of increased fuel deposition. Finally they studied the oxidation characteristics of the crude oil using mixtures of metal oxide (1% by weight), crude oil (5% by weight) and fine silica powder (90 mesh) and found the effect of the metal oxide to be insignificant primarily because of the large surface area offered by the fine silica powder.

The precursor to the work done in this thesis has been the kinetic studies on Huntington Beach crude oil performed by De Los Rios at SUPRI (1987). He performed kinetic studies using 1% and 2% concentration water soluble solutions of salts of iron, tin, magnesium, zinc, potassium, copper, manganese, nickel and cadmium. A discussion of his observations will be found in the Section 3 of this thesis wherein the purpose and results of this work has been reviewed.

2.2 Field Studies Using Metallic Additives

Observations on the influence of metals and their salts on in-situ combustion were initially made through in-situ combustion studies on reservoirs having a high metallic content in clays and minerals found in the rock matrices of the reservoirs. Results from the Fry Test showed increased air requirement as the reservoir had a matrix which contained both clays and iron derivatives such as pyrite and siderite that increased the fuel deposition (Earlougher *et al.*, 1970). Similar results were also observed for the field tests performed in May Libby reservoir in the Delhi field (Hardy *et al.*, 1972).

Such observations encouraged the investigation of the feasibility of in-situ combustion in reservoirs having high concentration of metals. Carcoana *et al.* (1983) reported that Romania planned to recover 41% of its total EOR recoverable oil by the process of in-situ combustion. Reservoirs in Romania have been found to contain a high concentration of metals such as vanadium, nickel and chromium. These metals were found to act as natural catalysts in laboratory studies run to determine the effect of these naturally occurring minerals. Carcoana *et al.* have not published quantitative results of these studies.

A comprehensive description of a technique tested in the field has been published by Racz (1985) on work done in Hungary. In this field test an initiator was used to enhance the chain reaction mechanism involved in the metal catalyzed oxidation of hydrocarbons in in-situ combustion. The next paragraphs discuss his technology which used tertiary butyl-hydroperoxide (TBH) as initiator in the presence of iron pentacarbonyl catalyst. When his test pattern in the Demjen-Kelet field was produced by in-situ combustion with iron pentacarbonyl catalyzed by TBH, oil recovery increased to 60% from an estimated primary recovery of 15%.

In developing his new technology, the reaction kinetics was first determined through TGA studies for different oil grades in porous media and different air flow rates using a wide range of additives. The aim of these experiments was to determine additives that would bring about a decrease in the activation energy of the low temperature oxidation process, thereby improving the feasibility of in-situ combustion for recovering crude oil from the Demjen-Kelet field.

Racz also studied the influence of the mineral content of the reservoir rocks on the in-situ combustion process. An analysis of the mineral content of the reservoir showed trace elements of Ba, As, Mn, Ti, V, Cu, Na, Ni, Zr, Co, Sr, K, Fe and Cr. TGA and DSC studies showed iron and iron compounds had a marked exothermal effect as compared to the other metallic additives.

Using the knowledge that, with metals present, oxidation of hydrocarbons follows a chain reaction mechanism, it was deduced that, if easily decomposing compounds like peroxides, metal carbonyls and azo-compounds were added to the system, as initiators, the oxidation reactions would be further enhanced. The influence of tertiary-butyl-hydroperoxide (TBH) was studied. Laboratory experiments were performed to determine the amount of oxygen adsorbed with 5% TBH at 140 °C and 160 °C at atmospheric pressure (100 KPa), and at 4 atmospheres (400 KPa). At atmospheric pressure, (100 KPa), the rate of oxidation was found to be significantly increased at temperatures above 200 °C. At a pressure of 400 KPa, the rate of oxidation increased at temperatures above 170 °C.

Dynamic microcalorimetric measurements were performed on mixtures of the distillation residue of Demjen-Kelet oil having a boiling point above 200 °C, quartz sand and different metallic additives. The greatest heat generations were observed in systems containing iron and

a mixture of magnesium, vanadium and other metals. Both systems exhibited a shift in the low temperature oxidation peak to lower temperatures, suggesting that the activation energy of the low temperature oxidation reaction was decreased, which, in turn, implies that higher fuel deposition will occur.

A series of wet combustion tube experiments were performed to determine the influence of iron pentacarbonyl. It was found that the combustion front temperature was 450 °C when no catalyst was used. When a 1% solution of iron pentacarbonyl catalyst was used, the combustion front temperature was reduced by 120-150 °C.

The technology developed in the laboratory was field tested in a 50x50 m pilot inverted five spot pattern 280 m in depth in the Demjen-Kelet field. TBH was injected along with air into the reservoir and its pressure was raised to 2-4 MPa. Once the combustion front was stabilized, a 1% solution of iron pentacarbonyl was injected. The results were good. Ultimate recovery was increased to 60% from the anticipated 15% primary recovery. Because of the success of the pilot study, a full scale operation is now being planned in the Demjen Kelet field.

This publication by Racz (1985) has been the only one that has described the use of a metal catalyst and also the use of an initiator to enhance the chain reactions typical in the oxidation of hydrocarbons in the presence of metallic additives. The literature is sparse regarding such work.

3. PROBLEM STATEMENT

The economics and applicability of an in-situ combustion process is largely determined by the nature and the amount of fuel formed. The nature of the fuel formed affects: (1) the heat of combustion and hence the extent of visbreaking, (2) the combustion front velocity and hence the oil recovery rate, and (3) the air requirement and hence the operating cost of the in-situ combustion process. The effect of metallic additives on the nature of the fuel formed and the combustion parameters can be determined on a quantitative basis by performing combustion tube studies in the presence of metallic additives.

Only a few combustion tube experiments have been performed to determine the effect of metallic additives as catalyzing agents to regulate the nature of the fuel formed and to change the combustion characteristics of the fuel. Increases in the amount of fuel deposited have been reported when metals are present in the rock matrix (Earlougher *et al.*, 1970; Hardy *et al.*, 1972; Racz, 1985). Racz (1985) was the first to propose the addition of iron pentacarbonyl to catalyze an in-situ combustion of the crude in the Demjen-Kelet field in Hungary. The existing literature has so far not addressed the quantitative determination of the influence of metallic additives on the nature of the fuel formed and its impact on the combustion parameters.

The present work addresses this deficiency. In this study, 1% solutions of stannic chloride ($\text{SnCl}_4 \cdot 5\text{H}_2\text{O}$), ferrous chloride ($\text{FeCl}_2 \cdot 4\text{H}_2\text{O}$) and zinc chloride (ZnCl_2) have been added to determine this effect on the in-situ combustion characteristics of Huntington Beach crude oil. These metallic additives were selected based on the kinetic studies by De Los Rios (1987) when used these additives with Huntington Beach crude oil. His observations are summarized in Table 3.1 and briefly discussed in the following paragraphs.

De Los Rios (1987) found that metallic salts of iron, tin and aluminum induced similar effects on the oxidation of Huntington Beach crude oil, but to differing extents. Addition of iron or tin produced significant increases in the rates of oxidation. In the case of aluminum, the effects were less pronounced.

When ferrous chloride was used by De Los Rios, lower activation energies were observed. This resulted in increased oxidation and fuel deposition in the LTO reaction. The medium temperature reaction exhibited greater reaction rates as a result of a larger pre-exponential constant. The activation energy was larger in the medium temperature range, but the pre-exponential constant was very large causing an increase in the reaction rate. The high temperature combustion reaction was found to peak at a lower temperature and it occurred over a narrower temperature range with no significant change in the energy of activation. However the increased fuel deposition at lower temperatures led to larger pre-exponential constants and thus higher reaction rates in the HTO reaction. When stannic chloride was used by De los Rios (1987), effects similar to those of iron were observed. Increased reactivity to oxygen occurred at a lower temperature for all the reactions. Greater reaction rates occurred in the LTO reaction with increased fuel deposition due to reduced activation energy. Larger pre-exponential constants were observed in the medium and high temperature reactions.

Zinc, magnesium, chromium and manganese caused similar effects on the oxidation of HBO (De los Rios, 1987). Their relative effects varied during the low and medium temperature reactions; but these reactions occurred at a much higher rate. As a result of low temperature oxidation, fuel deposition increased. When zinc chloride was used, increased oxygen consumption and carbon oxide production occurred at a lower temperature. However this was not

Table 3.1

SUMMARY OF QUALITATIVE RESULTS OF KINETIC STUDIES

(after De Los Rios, 1987)

Metallic Additive	Low Temperature	High Temperature
$FeCl_2$ $SnCl_2$ $AlCl_3$	Increased CO_x Production & O_2 Consumption	Increased CO_x Production & O_2 Consumption Shift to Lower Temperature
$ZnCl_2$ $MgCl_2$ $MnCl_2$ $K_2 Cr_2 O_7$	Increased CO_x Production & O_2 Consumption	Decreased CO_x Production & O_2 Consumption Shift to Lower Temperature
$CuSO_4$ $CdSO_4$ $Ni(NO_3)_2$	Increased O_2 Consumption	Decreased CO_x Production & O_2 Consumption

because of a reduction in activation energy, but rather because of an increase in the pre-exponential constant. Higher activation energy in the medium temperature reaction resulted in a higher, narrower temperature peak. A reduction in the activation energy was observed in the high temperature reaction. As a result, a broad high temperature peak was observed. Magnesium and chromium produced effects similar to zinc; however manganese produced a much reduced effect.

Copper, nickel and cadmium produced only a small effect on the effluent gas composition. In the case of copper, De Los Rios observed an increase in the activation energy of the low temperature reaction leading to a decrease in the LTO reaction rate for Huntington Beach crude. This observation is different from that observed by Burger and Sahuquet (1972). They reported that the energy of activation decreased in the LTO reaction resulting in increased fuel deposition in their kinetic studies on a 27° API crude. In contrast, Fassihi (1981) observed that there was no change in the energy of activation in the LTO reaction during his kinetic experiments on a 27° API French crude. Such differences in the effects of copper on the reactivity of crudes could be explained on the basis that the reactivity of a crude may differ depending on the crude oil composition. Cadmium exhibited an effect opposite to copper for the LTO reaction. However for both nickel and cadmium, slightly larger activation energies in the HTO reaction resulted in sharper and narrower high temperature peaks.

Of the nine metallic additives studied by De Los Rios, stannic chloride ($\text{SnCl}_4 \cdot 5\text{H}_2\text{O}$), zinc chloride (ZnCl_2) and ferrous chloride ($\text{FeCl}_2 \cdot 4\text{H}_2\text{O}$) were used in this study. These additives were chosen after studying their influence on the oxidation reactions as characterized by the effluent gas composition and the cell temperature seen during the kinetic experiments of De Los Rios. Stannic chloride and ferrous chloride were chosen because they exhibited a considerable effect on the LTO reaction increasing the fuel deposited by reducing the activation energy of the LTO reaction. Zinc chloride was chosen as representative of those metallic additives which increased the LTO rate as a result of an increase in the pre-exponential constant rather than a decrease of the activation energy.

The next section describes the experimental system used to acquire the data. The experimental procedure and the observations and results will be discussed in the sections following the description of the experimental system.

4. EXPERIMENTAL SYSTEM

The experimental system is similar to that used by a number of researchers at SUPRI (Satman, 1979; Fassihi *et al.*, 1982; Andrade, 1984; Sidqi *et al.*, 1985). A schematic diagram of the system is shown in Figure 4.1. Table 4.1 describes the major components of the equipment used. Details of the combustion tube assembly are shown in Figure 4.2.

The combustion tube is 7.6 cm O.D. and 99.6 cm long and is made of stainless steel (SS 316) with a 0.041 cm wall thickness. Flanges are silver soldered to its ends. The flange covers are secured to the flanges by means of eight 0.64 cm diameter nuts and bolts and the pressure seal is accomplished by custom made brass ring gaskets.

Two 240 V, 1000 W Watlow heater coils are wound around the combustion tube at distances of 10 and 15 cms from the top flange. The second coil serves as a standby in case of failure of the first or extinction of the combustion front. Voltage to the heaters is controlled by a 240 V Powerstat variable autotransformer.

When packing the combustion tube, a thermowell is placed along its center. It runs from the bottom flange through the center of the top flange of the combustion tube, and leaves the top flange of the pressure shell in which the combustion tube is placed. Before and during the combustion run, a thermocouple is passed through the thermowell to record the axial temperature profile. At the lower end of the thermowell, two wire screens are attached around the thermowell. These occupy the annular space between the thermowell and the combustion tube. The upper screen is of 200 Tyler mesh size and is used to restrict the sand from being carried out along with the outlet stream. The lower screen, of 10 Tyler mesh, is used to provide support to the 200 mesh screen above it.

The combustion tube is placed in a thermally insulated unpressurized external shell. The purpose of the shell is to contain a fire in case of an emergency and to minimize accidents which might arise from mechanical failure of the combustion tube which is operated at 100 psig. The annular space between the tube and the shell is insulated with Dacotherm insulation. Dacotherm is an all mineral powdery form of insulation manufactured by Diamond Shamrock.

Three Brisket electrical heating tapes are wound around the pressure shell in order to heat the sandpack within the combustion tube. These heating tapes are controlled by three Love temperature controllers. The Brisket heating tapes, used in conjunction with the Love temperature controllers, are used to heat the sandpack to the "reservoir temperature" before combustion is begun and also to maintain this temperature ahead of the condensation zone during the experiment. The sandpack is maintained at a sufficiently high temperature, around 50-75 °C, to reduce the possibility of fluid blockage arising from the high saturation and viscosity of the crude oil.

The combustion tube and the pressure cell are mounted onto an angle iron frame on which inlet and outlet pressure gauges, temperature controllers, cold water circulating system and other associated equipment are mounted.

A Matheson mass flow controller is placed upstream of the combustion tube in order to control the air flow rate to the tube. Air for the combustion is supplied by a cylinder provided with a two stage pressure regulator.

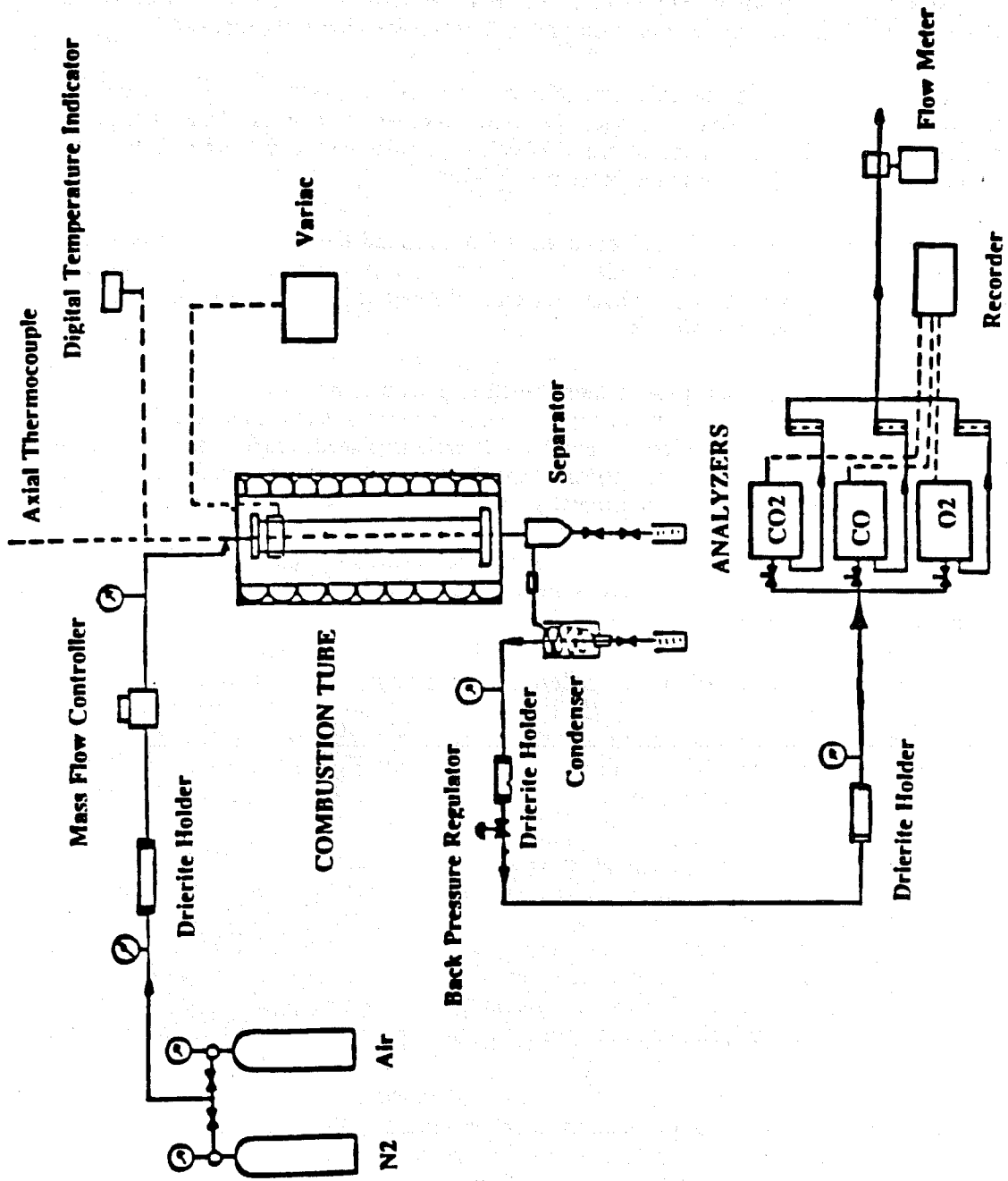


Figure 4.1 Schematic Diagram of the Experimental System

Table 4.1

SPECIFICATIONS OF COMPONENTS IN EXPERIMENTAL SYSTEM

Combustion Tube	Stainless Steel (SS 316), 7.5 cm O.D., 0.041 cm wall thickness, 99.6 cm length. Flanges SS 304, 12.1 cm diameter, 1.27 cm thick, eight 0.64 cm bolt holes located at a diameter of 10.8 cm.
Pressure Shell	SS 304, 16.8 cm O.D., 0.71 cm wall thickness, 111.8 cm length. Flanges 22.2 cm diameter, 1.27 cm thick, eight 1.27 cm bolts located at a diameter of 20.9 cm.
Thermowell	SS 321, 1.65 cm O.D., 0.025 cm wall thickness
Screens	200 Tyler mesh screen above, 10 Tyler mesh screen at bottom.
Igniter	Watlow, coil type, 1,000 Watts, 240 Volts, 50 Hz. Part Number 125CH93AUX.
Igniter Controller	Powerstat 3PF236 Variable Autotransformer 240/110 Volts, 50/60 Hz, 0-280 output Volts, 9 Ampere, maximum 2.5 KVA, specification BP57502.
Heating tape	Three Brisket Weave, flexible heating tapes four and six feet long, 2.54 cm width, maximum 10 Ampere.
Temperature Controllers	Three Love Proportional Temperature Controllers, Model 71, 10 amp, -17.8-760 °C
Axial Thermocouple	Omega Type J (Iron-Constantan), 0.102 cm O.D., 127 cm length.
Temperature Indicator	Omega 2176A Digital Temperature Indicator having range -17.8-537.8 °C, with °C/°F indicating capabilities, maximum of 10 channels, 115 Volts AC, for J-type thermocouple.
Gas Analyzers	Teledyne Oxygen Analyzer 326A with 0-5, 0-10, 0-25 % range capabilities, with micro-fuel cell A-5. Beckman Model 864, Non-dispersive Infrared Carbon Monoxide Analyzer with linearized circuit, 0-2 & 0-5 % range. Beckman Model 864, Non-dispersive Infrared Carbon Dioxide Analyzer with linearized circuit, 0-5 & 0-20 % range. Beckman Model 755 Paramagnetic Oxygen Analyzer with 0-5, 0-10, 0-25, 0-50 % range with suppressed ranges of 20-21, 19-21, 16-21 and 11-21%. Replaced by Teledyne Oxygen Analyzer.

Data Acquisition	Hewlett Packard 3497A, having capabilities of scanning 17 channels and taking 300 readings per second. Has 20 analog input channels per card. Used in conjunction with IBM XT personal computer. Esterline Angus PD 2064 data acquisition machine. Replaced by Hewlett Packard 3497A.
Pressure Regulator	Tescom Back Pressure Regulator Model 26-1727-24-014, range 0-500 psi Moore Absolute Pressure Relief Valve, model 43R, 0-20 psi, used after analyzers.
Recorders	Soltec 3-pen Precision Recorder, Model 12434 for recording gas analyses.
Flow Controller	Matheson Electronic Mass Flow Controller, Model 8240, range 100-5,000 sccm, with digital output. Uses sensor 8142, for up to 5 slpm air.
Flow Meters	Matheson Model 8160, Electronic Mass Flow Indicator, range 100-2,000 sccm, with digital output uses sensor 8141, for up to 5 slpm air. Two Matheson 220A Rotameters, capacity 2.0 scfh, 15 psig.
Totalizer	Matheson Totalizer, Model 8122, 100 CPM at 5 Volts D.C.
Balance	Fischer Gram-Atic Balance, accuracy 0.0005 gram; Mettler P11N Balance, capacity 10,000 gram, accuracy 0.01 gram
Centrifuge	Damon IEC PR-6000 Centrifuge with speeds up to 6,000 rpm, with thermostat control capability (-10 to 25 °C).

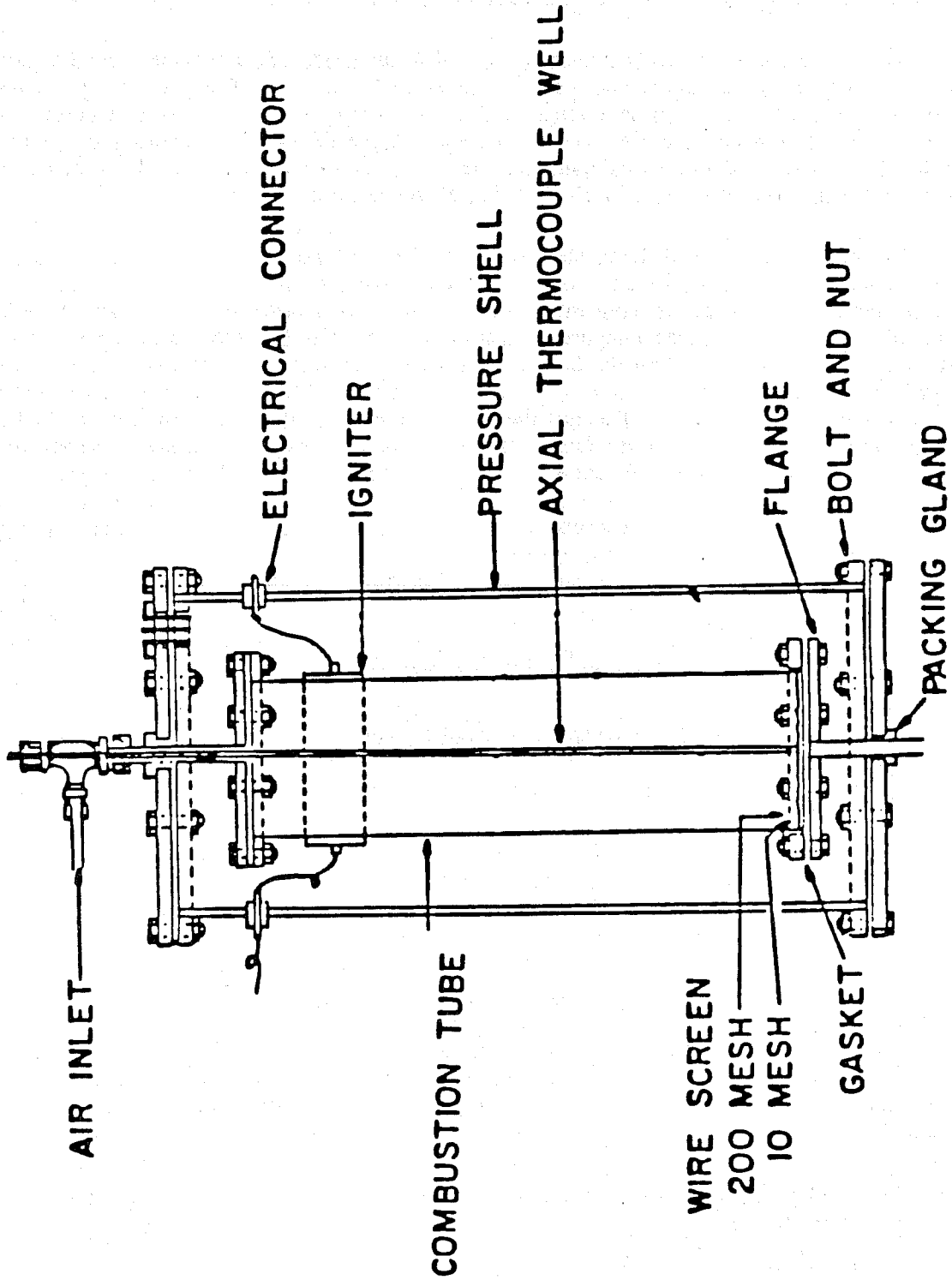


Figure 4.2 Details of the Combustion Tube Assembly.

At the outlet end of the combustion tube, two separators with a condenser in between, are connected in series to efficiently separate the liquid products and condensibles from the gaseous products of the outlet stream. At the base of both separators, a piping system containing three valves, is provided to prevent the escape of the gas from the outlet stream when draining the liquid from the separators. The top valve is a 1.91 cm gate valve while the bottom two valves are 1.91 cm ball valves. The liquid leaving the separators is collected into 50 ml. centrifuge tubes, filled approximately 20 ml. each time, for analyses in later steps.

The first separator collects the crude oil and water produced, while the second separator collects whatever condensibles that were not collected in the first. The gas leaving the upper portion of the first separator is cooled further by passing it through the condenser which removes any of the condensible material present. The condenser is cooled by circulating a cooled 1% aqueous solution of calcium chloride. This solution is used since the freezing point of water is depressed to -2°C with the addition of the calcium chloride.

The gas and condensed fluids then pass from the condenser through the second separator. The condensed liquid is collected through the three-valve system located at the bottom of this second separator. The gas leaving the second separator then flows through a Drierite holder, containing 8 Tyler mesh size anhydrous calcium sulfate. The Drierite removes any moisture present. The gas from the Drierite holders then passes through two filters of 60 microns followed by 5 microns, which remove any particulate matter. These filters are used to prevent damage to the gas analyzers. The gas then passes through three gas analyzers: a Beckman carbon dioxide analyzer and a Beckman carbon monoxide analyzer connected in series, and a Teledyne oxygen analyzer connected in parallel with the carbon oxides analyzers. The analyzers are connected in this series-parallel arrangement to accommodate the fact that oxygen reacts with the fuel cell of the Teledyne oxygen analyzer. In addition, there are maximum flow rate requirements of the oxygen analyzer that have to be met.

The gas from the analyzers is recombined and then flows through a Matheson gas flow meter. A 0-500 psi back pressure regulator is used to fix the system back pressure to 100 psig. A Soltec 3-pen recorder is used to record the gas analyses.

Data from the axial thermocouple is manually recorded at periodic time intervals, usually every half hour. These data are used to determine the combustion front location, the combustion front velocity, the steam zone location and temperature and the combustion front temperature.

A Hewlett Packard 3497A data logger, in conjunction with an IBM XT microcomputer, is used to log the produced gas composition data at intervals of one minute. These gas analyses are key data in the analysis of a combustion tube run.

A Damon IEC PR-6000 centrifuge is used to separate the water from the oil in the samples collected during the experiment. A couple of drops of Tretolite RN 3003 are added to aid the separation process. Water is sometimes added to improve the separation. Mineral spirits must not be added since it would change the composition of the crude oil and prevent further analyses of the crude. The amount of oil and water in each sample are used to determine the cumulative oil and water produced.

Other supporting equipment consist of the gas cylinders containing the calibration gases used to calibrate the gas analyzers.

Prior to the experiments that are reported in this thesis, a number of experiments were carried out which were unsuccessful. In the first unsuccessful experiment, the rubber gasket that sealed the combustion tube failed at the high temperature it encountered. It had to be abandoned for safety reasons, and because the desired operating pressure of 100 psig could not be maintained.

In the second experiment the igniter coils burned out during the process of raising the temperature around the igniters for initiating combustion. It was later learned that the digital thermometer, that was used to read the temperature around the igniters, was indicating the average of the igniter temperature and the atmospheric temperature because a thermocouple that was used in the kinetic experiments by De Los Rios had been accidentally connected in parallel with it. The coil heaters were subsequently replaced by the much more powerful 1000 W Watlow coil heaters.

The third experiment was going well until the Beckmann 775 Paramagnetic Oxygen Analyzer behaved erratically toward the end of the experiment and finally failed. This initiated a major revision of the system. The Esterline Angus PD 2064 data logger and the Beckman 755 Paramagnetic Oxygen Analyzer were replaced by the Hewlett Packard 3497A data acquisition system and the Teledyne Oxygen Analyzer 326A. The Teledyne Oxygen Analyzer, when it first arrived, was found to be connected for vacuum systems for flue gas analyses in stacks. It was repiped for pressure systems. When it was tested it showed erratic behavior. It was found that the equipment had not been properly grounded. Once all these problems had been solved, the runs described later could be made.

To those performing similar combustion tube experiments, the author recommends that proper control over the back pressure regulation system must be maintained throughout the experiment. It is essential that the analyzers be calibrated at the pressure expected during the experiments, because the gas analyzers have been found to be pressure sensitive. The experiment also needs a minimum of two assistants to perform the experiment comfortably. Proper planning for contingencies: ordering of spare parts, spare cylinders of calibration gas, air and nitrogen; should be done at least a couple of months in advance to avoid project delays.

5. EXPERIMENTAL PROCEDURE

This section outlines the steps used to carry out the combustion tube experiments on Huntington Beach crude oil whose properties are shown in Table 5.1. Sieve analysis of the Ottawa sand used for the pack is shown in Table 5.2. Figure 5.1 shows the x-ray diffraction pattern of the clay added to simulate natural reservoirs (Fassih, 1981). The clay was found to contain principally Kaolinite whose peaks are indicated on Figure 5.1 by the letter "K".

The steps used to carry out the in-situ combustion tube experiments are as follows:

1. The sand pack is first prepared by mixing known weights of 20-30 mesh Ottawa sand, clay, oil and water containing the dissolved metal salt at its desired concentration to achieve the desired saturations of the fluids. It is important that this should be done with care to ensure proper mixing for our observations have shown variations in fuel deposition as a result of local and zonal saturation variations.
2. The combustion tube is then filled by tamping the prepared sand into it, care being taken to avoid moving the axial thermowell. Samples are taken at the top, middle and bottom of the pack to check for the desired fluid saturations. Water saturation in the samples are determined using the ASTM D-95 extractive distillation technique. In this process, toluene is used as the agent to determine the water content in a core sample. The water boils out along with the toluene and separates out as a distinct layer in the graduated arm of the extractor tube. Crude oil dissolves into the toluene and remains in the toluene-crude oil mixture in the flask. Crude oil saturation is determined by difference using the knowledge of the weight of the sample taken, the water content of the sample and the weight of the sand after burning off the hydrocarbon residue on the sand at the end of the ASTM-D95 extraction. The sample is burned in a convective oven at 700 °C. The porosity of the pack is determined on the basis of the weight of the material put into the pack, and the volume of the pack. The sandpack is tamped to a height of 85 to 90 cm from the bottom of the tube.
3. Three millilitres of linseed oil are added to the top of the saturated pack in order to bring about a quick ignition and uniform combustion. The rest of the space above this is filled with clean sand, to prevent premature coking reactions.
4. The combustion tube is assembled by connecting the flanges and other accessories.
5. The combustion tube is then pressure tested to 150 psig by using nitrogen gas. The combustion tube is pressurized for over three hours and any leaks are corrected.
6. The combustion tube is placed inside the pressure cell and the annular space is uniformly filled with Dacotherm insulation to minimize heat losses.
7. The top flange of the pressure cell is secured by bolts and the air supply line is connected to the combustion tube. The separator is connected to the bottom of the combustion tube. The exit line for the gaseous products from the separator is connected to the condenser.
8. After assembly, checks are made for any leaks in the system using nitrogen at 150 psig.
9. Any blockages in the system lines are detected and rectified.
10. The gas analyzers are calibrated in accordance with manufacturers' instructions, while other equipment used for data collection are tested. One should note here that the analyzers

Table 5.1

PROPERTIES OF HUNTINGTON BEACH CRUDE OIL

Field	Zone	API Gravity	% C	% H	H/C Ratio	% N	MW
Huntington Beach	Lower Main Zone	22.9	84.5	11.53	1.64	0.86	386

Table 5.2 SIEVE ANALYSIS OF OTTAWA SAND

Ottawa Sand (20-30 mesh), Unisil Corporation

Density = 2.6509 gm/cm³

Sieve Size (Tyler Mesh)	Percent by Weight Retained
20	4.70
24	82.12
28	11.85
32	0.55
35	0.36
60	0.24
>60	0.18
	100.00

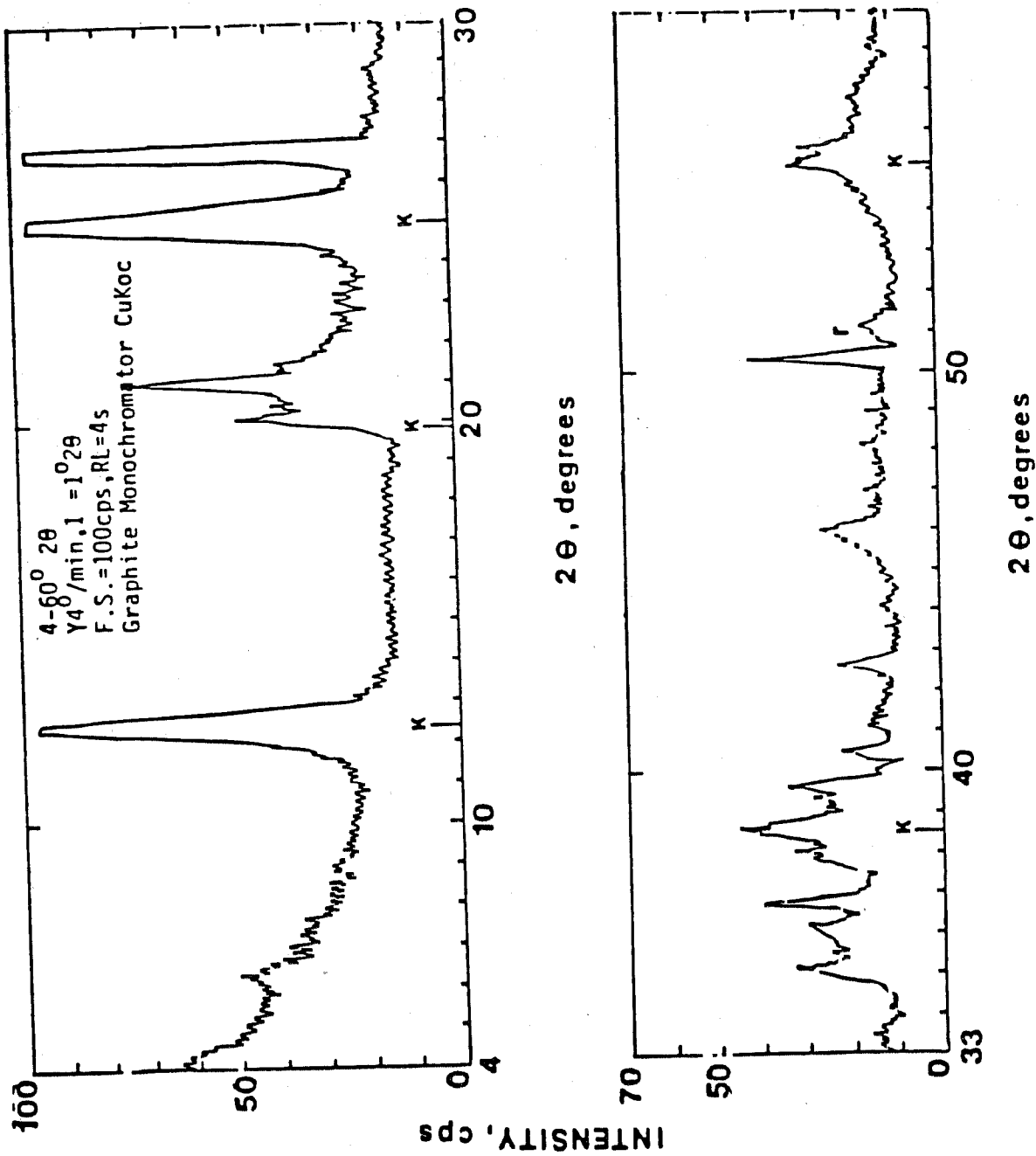


Figure 5.1 X-Ray Diffraction Patterns of Clay Showing Kaolinite Peaks
(after Fassihi, 1981)

should be calibrated at the pressure and flow rate at which they will be operated during the combustion tube runs, for they were found to be particularly sensitive to the pressure.

11. The reservoir is preheated by turning on the external heaters around the pressure shell and leaving it overnight. To maintain an average reservoir temperature between 50 to 75 °C, the Love temperature controllers are set so that the middle heater is kept at 60 °C, the top at 65 °C, and the bottom at 82 °C. These set points have been recommended by previous investigators using this experimental system, to counteract the heat losses in the system.

12. The next day the analyzers are checked for calibration and the data collection equipment is turned on. The igniter coil is turned on and nitrogen is injected at a flow rate of 3.0 slpm (standard litres per minute), while maintaining the pressure in the combustion cell at 100 psig. The axial thermocouple is raised to a point in the region around the top of the sand pack. When the temperature reaches around 315 °C, air is injected at 3.0 slpm. The pressure drop across the combustion cell, the injection pressure and the outlet gas composition are monitored on the Soltec recorder. The start of combustion is indicated by a jump in the temperature and a drop in the concentration of oxygen in the outlet stream with a corresponding increase in the concentration of carbon oxides. The air flow rate is maintained at 3.0 slpm, and the stop watch and the data acquisition system are started.

13. The igniter is turned off once the burning front is stable. This is indicated by plots of gas composition on the Soltec recorder. This happens when the front has moved approximately 3 to 5 cm from the point of ignition. Air injection is maintained at 3.0 slpm in order to propagate the front.

14. During the above steps, the outlet gas concentration is continuously monitored by the three gas analyzers and recorded on the multi-channel data logger. The data logger is programmed to record data every minute. The inlet and outlet pressures to the combustion cell are monitored continuously and recorded every half hour.

15. Every thirty minutes or when convenient, the entire length of the combustion cell is traversed from the top to the bottom of the combustion tube by the axial thermocouple in order to record the temperature distribution along the length of the combustion tube. This procedure usually takes about eight minutes depending on the number of data points taken. The temperature profiles help determine the velocity and location of the combustion front and the location of the steam plateau.

16. Every three hours the three gas analyzers are checked and recalibrated. The Beckmann oxygen analyzer especially had to be checked while the carbon monoxide and carbon dioxide analyzers usually maintained their calibration. The Teledyne oxygen analyzer that was purchased later was also found to work well without any need for recalibration during the experiment. The pressure and flow rate through the analyzers are maintained constant throughout an experiment.

17. The process of air injection and data taking is continued until the burning front sweeps through 90% of the combustion tube. The combustion front is then quenched by switching from air to nitrogen injection.

18. During the runs, the liquid produced is collected in graduated centrifuge bottles. Later these are centrifuged at 3,500 rpm for fifteen minutes. Water cut and mass of oil produced are determined.

19. After cooling, the equipment is dismantled and the data are analyzed. These data include analyses of the liquid produced and the core left in the combustion tube for determining the

hydrocarbon residue left behind the combustion front and the oil and water saturations ahead of the front. These data are needed to perform an overall material balance of the components used in the experiment.

6. EXPERIMENTAL DESIGN

Throughout the study, the objective was to operate each run at the same pressure, reservoir temperature, fluid saturation, metal salt concentration and air flow rate. In all, seven runs were performed. The first three were discarded because of equipment problems that arose during the experiments. In the first run the rubber gasket used to seal the combustion tube failed at the high temperature it encountered, resulting in the loss of operating pressure. The second run had band heater failures. Both heaters failed during the ignition period and the experiment had to be abandoned. For the first two runs excessive gravity drainage was observed and for later runs clay was added to minimize this problem, and also to create a sand pack more representative of a typical reservoir. The third run ran fairly well at first, but toward the end of the run the oxygen analyzer began malfunctioning and finally failed. This run was analyzed; however, the variations in the oxygen analysis were so significant that the evaluation was not felt to be accurate enough to be useful. Thus these three runs were abandoned.

The next four runs were successful and are reported here. The first was the control run, wherein the experiment was performed with no metallic salt. The next three runs used 1% by weight solutions of stannic chloride ($\text{SnCl}_4 \cdot 5\text{H}_2\text{O}$), zinc chloride (ZnCl_2) and ferrous chloride ($\text{FeCl}_2 \cdot 4\text{H}_2\text{O}$) for the "connate water."

Table 6.1 is a summary of the pack conditions used for the four successful runs performed. The operating pressure throughout the runs ranged between 100 and 105 psig. The initial reservoir temperature for each run was found to vary along the length of the combustion tube in the range of 50-75 °C.

In all four runs, the same amount of sand, oil and solution of the metallic additive was taken to prepare the sample. Thus the ratios of volume of oil to sand grain volume and volume of water to sand grain volume were constant. The ratio of volume of oil to sand grain volume was 20.82 and the ratio of volume of water to sand grain volume was 15.03. In packing the sample into the combustion tube, different packing techniques were used. In packing the combustion tube for the stannic chloride and ferrous chloride run, a large amount of the sand pack mixture was placed in the combustion tube before squeezing it in with the help of a tamper. In the case of the control and zinc chloride runs, small amounts of the sand pack mixture were placed in the tube and these were each vigorously tamped in. As a result, the total amount of sample put into the combustion tube was different for each run. Thus the saturations and porosities were somewhat different for each run as indicated in Table 6.1. The control run and the ferrous chloride run had porosities of 35.73 and 35 respectively and therefore had higher oil saturations of 37.47% and 38.67% respectively and were much alike in their saturation and porosities. The zinc chloride run and the stannic chloride run had porosities of 39.10 and 39.27 and therefore had lower oil saturations of 32.43 and 32.21 respectively, and were much like each other in their saturation and porosities.

The next section describes the observations and data collected during the four combustion tube runs.

Table 6.1

SUMMARY OF COMBUSTION TUBE RUNS

Operating Pressure: 100-105 psig
Operating Temperature: 50-75 °C
Air Flow Rate: 3.0 standard litres per minute.

Run Designation	Control Run	Ferrous Chloride $\text{FeCl}_2 \cdot 4\text{H}_2\text{O}$	Stannic Chloride $\text{SnCl}_4 \cdot 5\text{H}_2\text{O}$	Zinc Chloride ZnCl_2
Length of Pack, cm	90.77	83.06	91.15	89.90
Porosity	35.73	35.00	39.10	39.27
Oil Saturation, %	37.47	38.67	32.43	32.21
Water Saturation, %	27.05	27.92	23.41	23.25
Concentration of Metal Salt in Water, wt. %	0.00	1.0	1.0	1.0
Vol. Oil/Vol. Rock	20.828	20.824	20.821	20.828
Vol. Water/Vol. Rock	15.035	15.031	15.030	15.034

7. EXPERIMENTAL OBSERVATIONS

The data collected during the four combustion tube experiments on Huntington Beach crude oil are presented in this section. One run was the control run with no metallic additives, while the other three runs were with one percent water solutions of ferrous chloride ($\text{FeCl}_2 \cdot 4\text{H}_2\text{O}$), zinc chloride (ZnCl_2) and stannic chloride ($\text{SnCl}_4 \cdot 5\text{H}_2\text{O}$).

Three sets of data were periodically collected during each combustion tube experiment. They were the produced gas composition, the temperature profile along the length of the combustion tube, and the liquid production. These data sets are presented in the following subsections.

7.1 Produced Gas Composition

The produced gas composition was constantly monitored by the gas analyzers to determine its oxygen, carbon dioxide and carbon monoxide content. Figures 7.1 - 7.4 show the composition of the produced gas for the four runs. Figure 7.1 shows the produced gas composition for the control run with no metallic additive, Figure 7.2 shows the same data for ferrous chloride ($\text{FeCl}_2 \cdot 4\text{H}_2\text{O}$), Figure 7.3 is for stannic chloride ($\text{SnCl}_4 \cdot 5\text{H}_2\text{O}$), and Figure 7.4 is for the zinc chloride (ZnCl_2) run.

All graphs show some common features. Oxygen peaks are coupled with troughs in the carbon dioxide and carbon monoxide compositions. This is because oxygen is consumed in generating the carbon oxides. The concentration of oxygen in the produced gas provides an indication of the oxygen utilization efficiency of the run. The greater the concentration of oxygen in the produced gas, the lower is the efficiency of oxygen utilization. A comparison of the figures shows that the oxygen concentration in the produced gas was the lowest in the stannic chloride run. The oxygen concentration in the produced gas was higher for the ferrous chloride run and much higher for the zinc chloride run. The control run had the highest concentration of oxygen. The impact of the oxygen concentration in the produced gas on the oxygen utilization efficiency will be discussed in Section 8.

If we consider the graph of produced gas composition for the control run (Figure 7.1), one observes large cyclical variations in gas composition. The variations in gas composition for the control run, however, stabilize considerably after 2.75 hours. If we consider the graphs of produced gas composition for stannic chloride and the ferrous chloride runs (Figures 7.2 and 7.3), one observes fairly steady composition curves. Zinc chloride showed large cyclical variations in produced gas composition throughout the run (Figure 7.4). These variations are a result of the packing techniques used for each experiment.

Figure 7.5 illustrates the different packing techniques used. In packing the combustion tube for the stannic chloride and ferrous chloride runs, a large amount of sand pack mixture was placed in the combustion tube before squeezing it in with the help of a tamper. The steady values of gas composition for the stannic and ferrous chloride runs could have been the result of this packing technique. By contrast, for the control and zinc chloride runs, small amounts of the sand pack mixture were placed in the tube and each addition was vigorously tamped in. This method of packing could have led to saturation and porosity variations in smaller zones, resulting in the large cyclical variations in the produced gas composition for these two runs. The impact of the packing techniques on variations in the data will be discussed in Section 8.

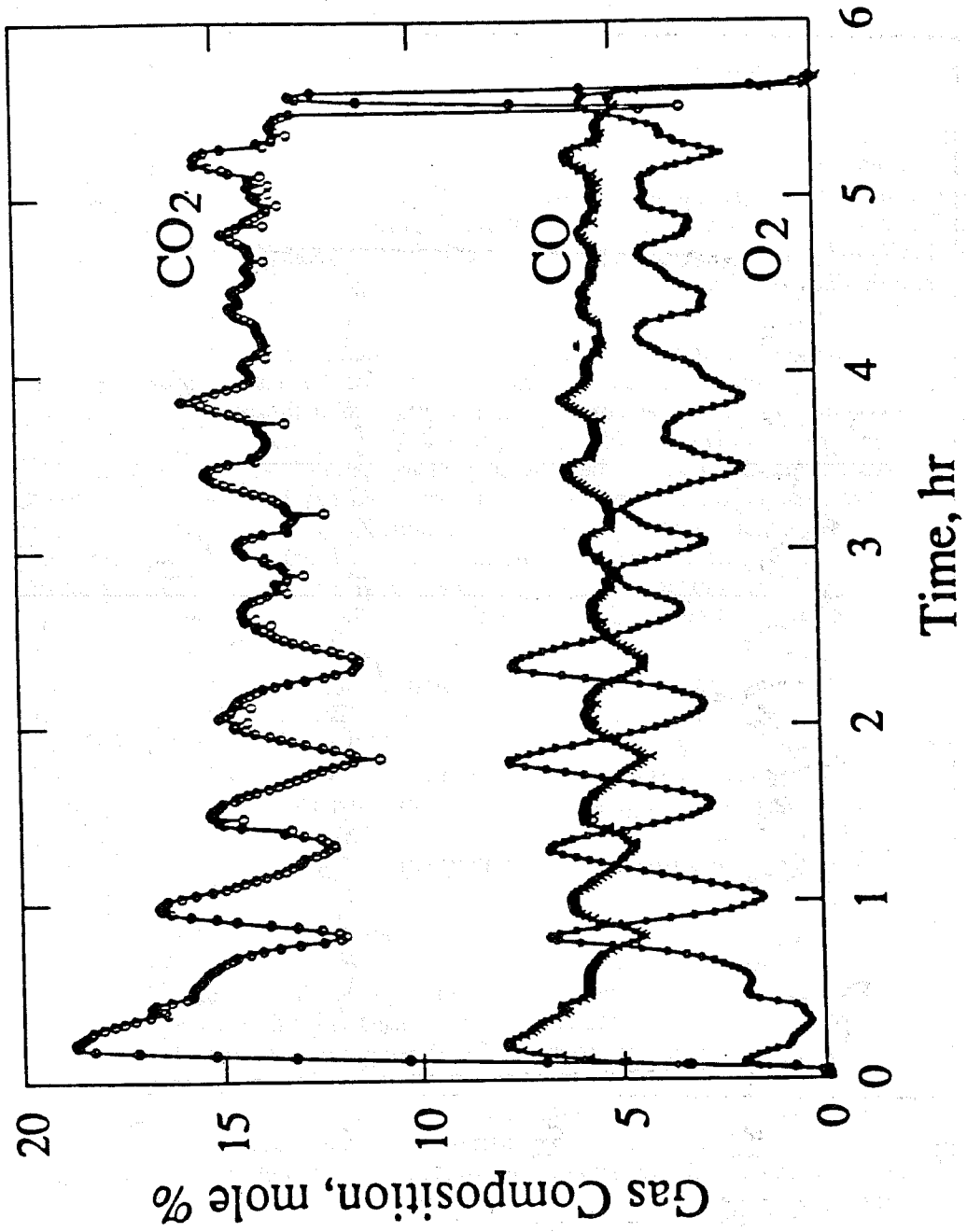


Figure 7.1 Produced Gas Composition for the Control Run

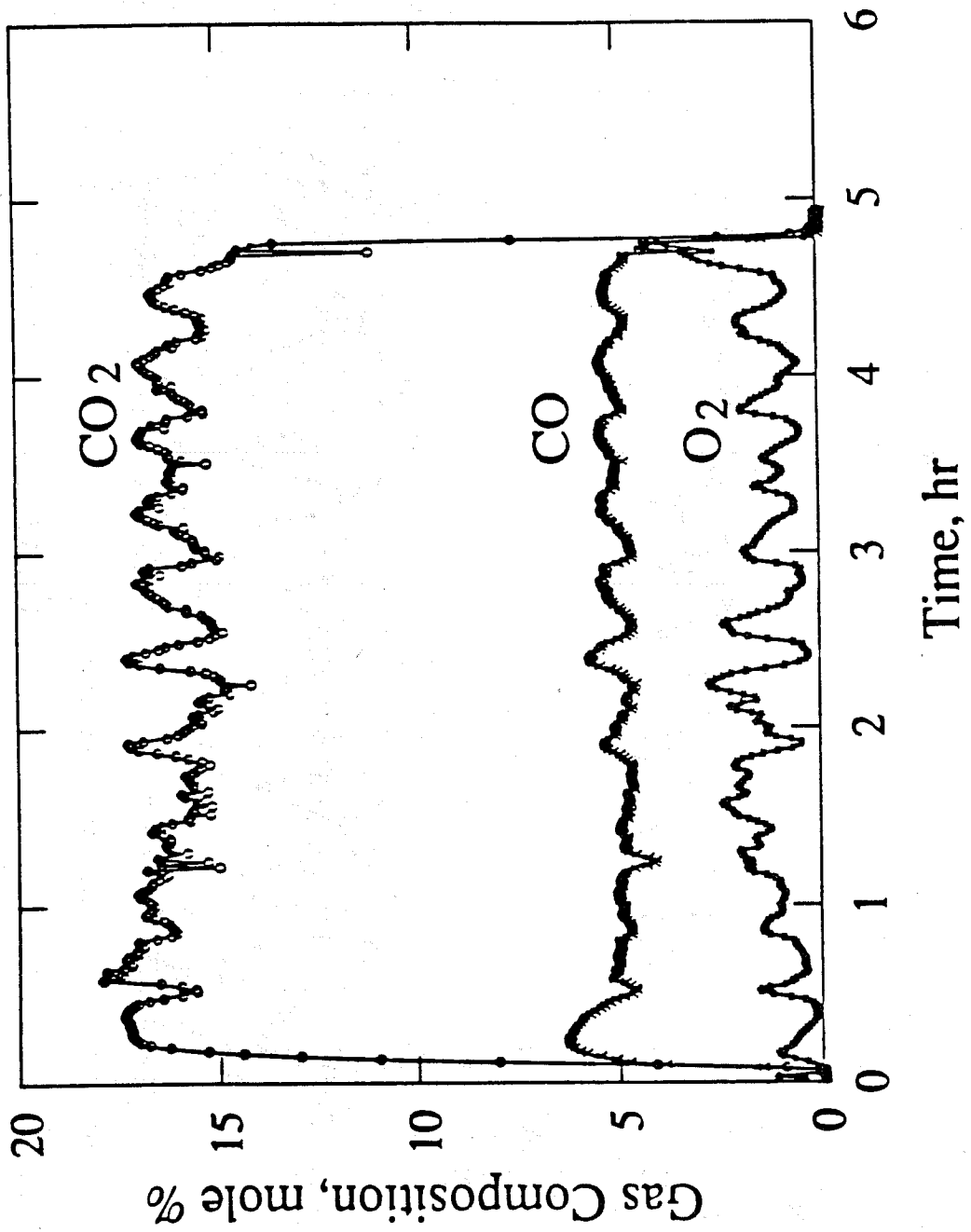


Figure 7.2 Produced Gas Composition for the Ferrous Chloride ($FeCl_2 \cdot 4H_2O$) Run

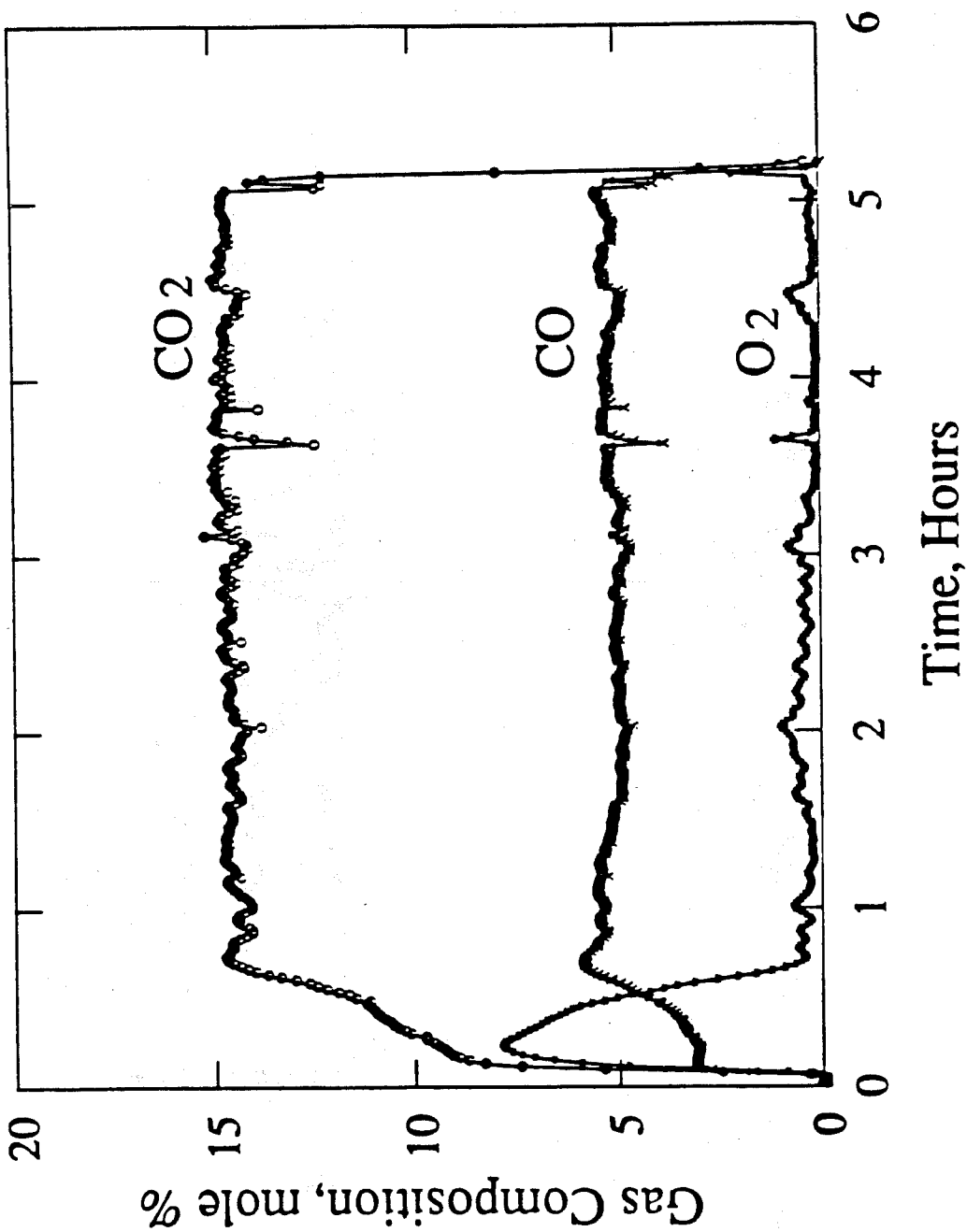


Figure 7.3 Produced Gas Composition for the Stannic Chloride ($\text{SnCl}_4 \cdot 5\text{H}_2\text{O}$) Run

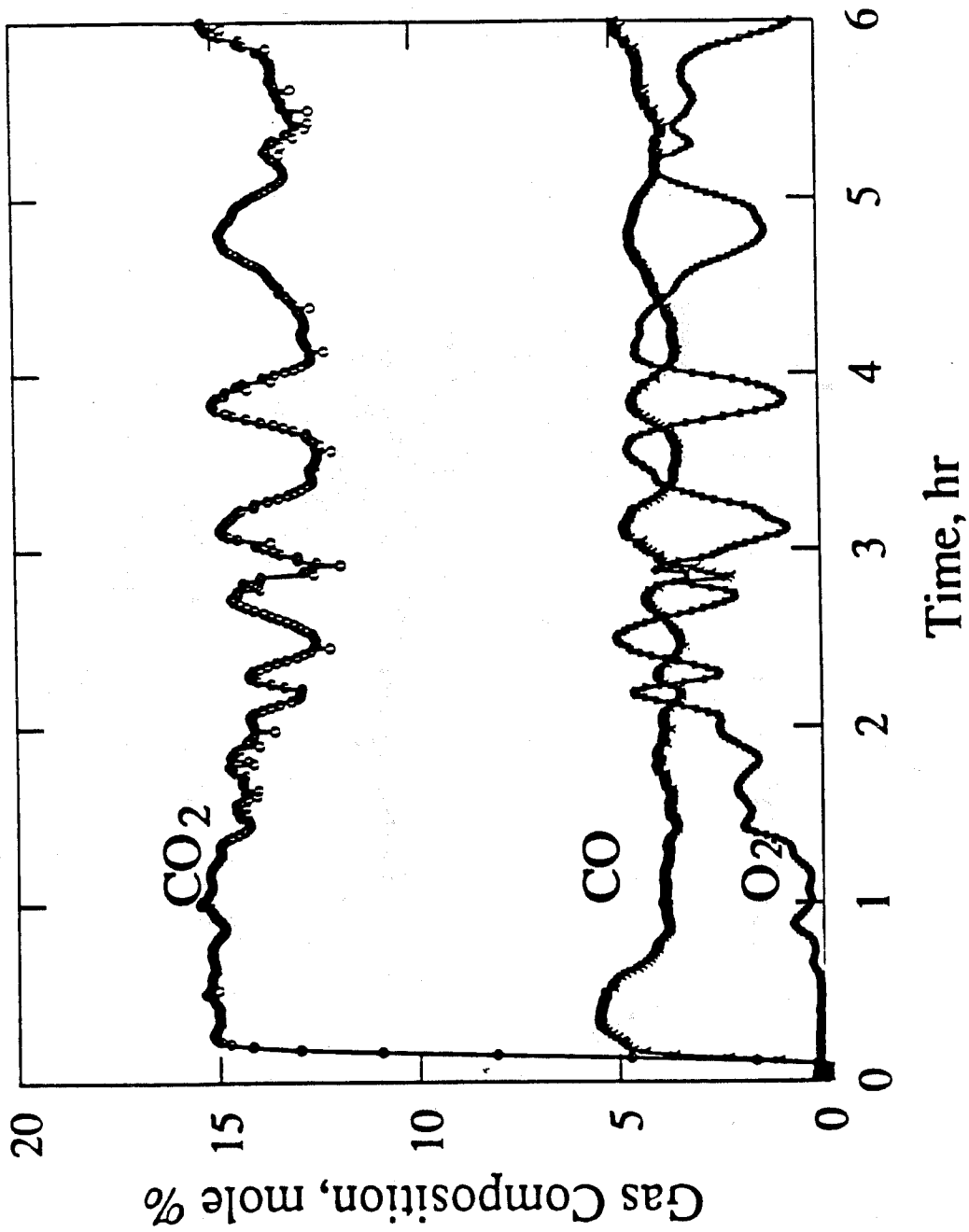
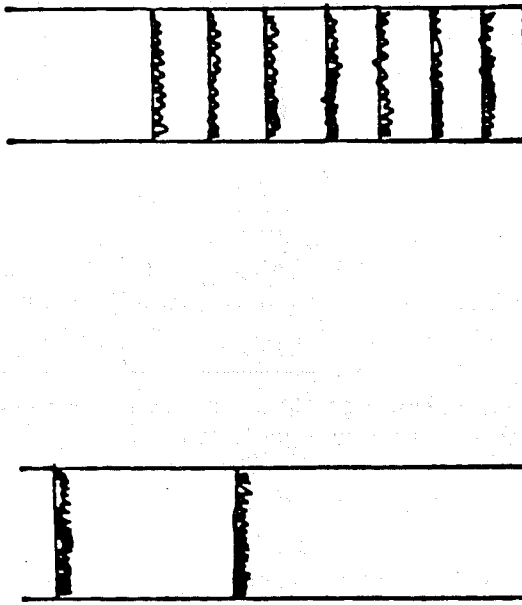


Figure 7.4 Produced Gas Composition for the Zinc Chloride ($ZnCl_2$) Run



PACK TYPE 1

PACK TYPE 2

Pack type 1: Larger Volume of pack put in and then squeezed

Pack type 2: Small Volume put in and tamped

Figure 7.5 Packing Techniques Used for the Runs

7.2 Temperature Profiles

Figures 7.6 - 7.9 show the axial temperature profiles taken for the four runs. Figure 7.6 is for the control run with no additive, Figure 7.7 is for the ferrous chloride ($\text{FeCl}_2 \cdot 4\text{H}_2\text{O}$) run, Figure 7.8 is for stannic chloride ($\text{SnCl}_4 \cdot 5\text{H}_2\text{O}$), and Figure 7.9 is for zinc chloride (ZnCl_2).

These graphs show that any given temperature profile exhibits distinct regions. There is a region ahead of the combustion front at the reservoir temperature. This is followed by a region wherein the temperature rises due to heat transfer ahead of the steam plateau. Next is the steam plateau where the temperature is constant over a region. For example, see the profile of Figure 7.6 at 1.575 hours in the region from about 35 cm. to 50 cm. Next, the steam plateau is followed by a region of rapidly increasing temperature until a peak is reached. This region is where the high temperature oxidation reaction takes place. It is known as the combustion front. The region behind the combustion front shows decreasing temperature as heat is lost to the surroundings and is used to heat the injected air.

From the graphs of temperature profile for the four runs, one can determine the steam plateau and combustion front temperatures. The steam plateau temperature for all four runs was found to range between 129 °C and 132 °C. In addition to data from axial temperature profiles, combustion front temperature data were also taken regularly by placing the junction of the axial thermocouple a short distance ahead of the combustion front and recording the maximum temperature as the front moved. The combustion front temperatures of the four runs are compared in Figure 7.10. Combustion front temperatures of all the runs lie in the range of 470 °C to 560 °C.

If we consider the graph of combustion front temperature for the control run (Figure 7.10), the temperature showed cyclic variations until a distance of 45 cms and then stabilized, producing temperatures between 490 °C and 510 °C thereafter. If we consider the temperature profiles for the control run (Figure 7.6), the time of stabilization was about 2.8 hours. This observation is consistent with the time the produced gas composition stabilized for the control run, as discussed in Section 7.1 and seen in Figure 7.1.

For stannic chloride, (Figure 7.10), the combustion front temperature was much higher than for the control run. The combustion front temperature was steady at about 507-516 °C as it burnt through a distance of about 30 cms. The front temperature then rose gradually to 559 °C and dropped gradually to 521 °C before rising again to 557 °C and falling to 524 °C.

For ferrous chloride, (Figure 7.10), front temperatures were slightly lower than for the control run. Variations were seen in the combustion temperature, however these variations were small.

For zinc chloride, significant temperature variation was observed, but combustion front temperatures were significantly lower than for the control run.

The variations seen in the combustion front temperature along the length of the combustion tube could be the result of variations in the amount of fuel consumed. This concept will be investigated in Section 8.

The combustion front temperatures for the four runs are related to their gas composition data, since the nature of the fuel formed is related to the produced gas composition. Additionally, the temperature depends on the amount of fuel deposited, which can be determined from the produced gas composition, and the air injection rate.

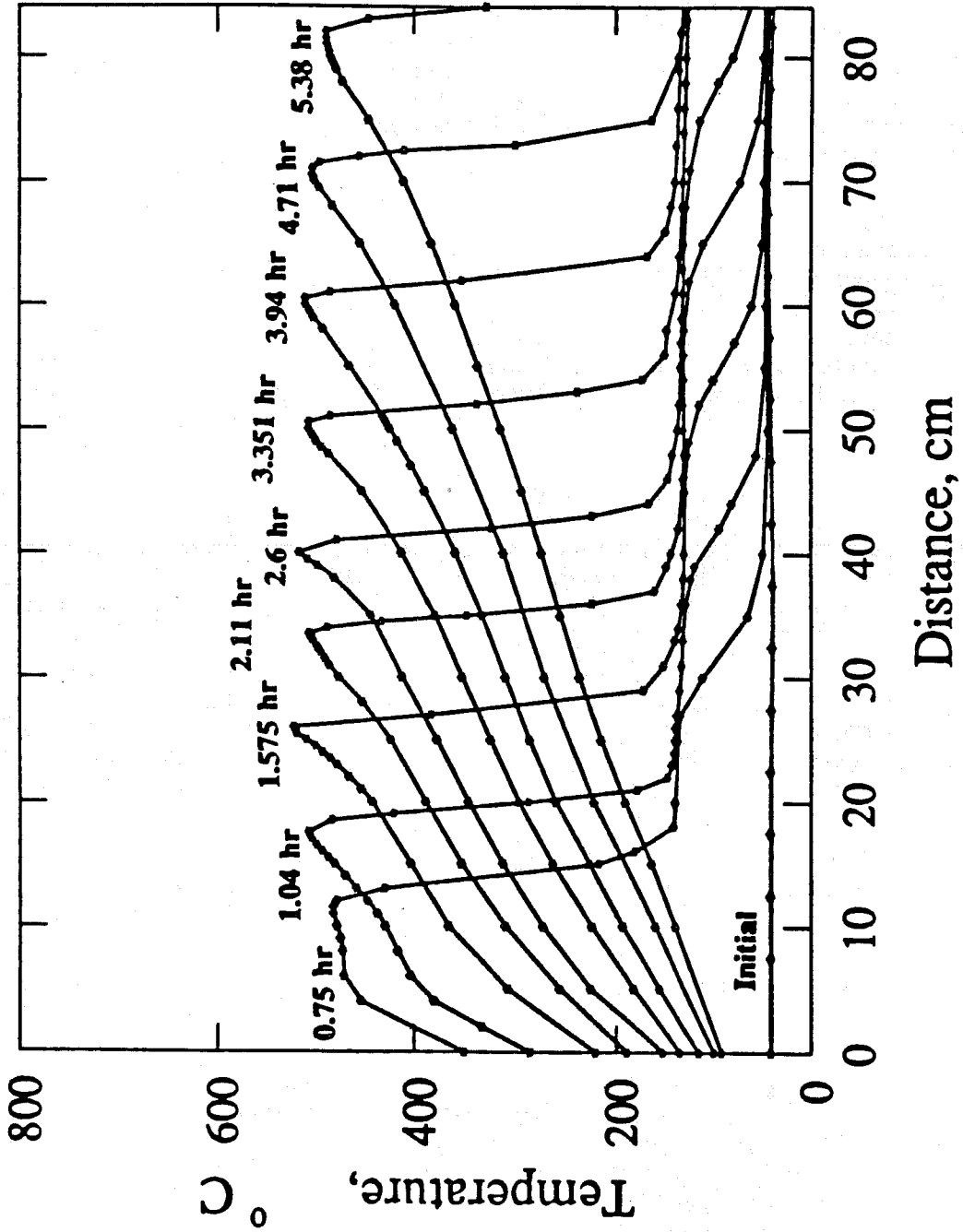


Figure 7.6 Temperature Profiles for the Control Run

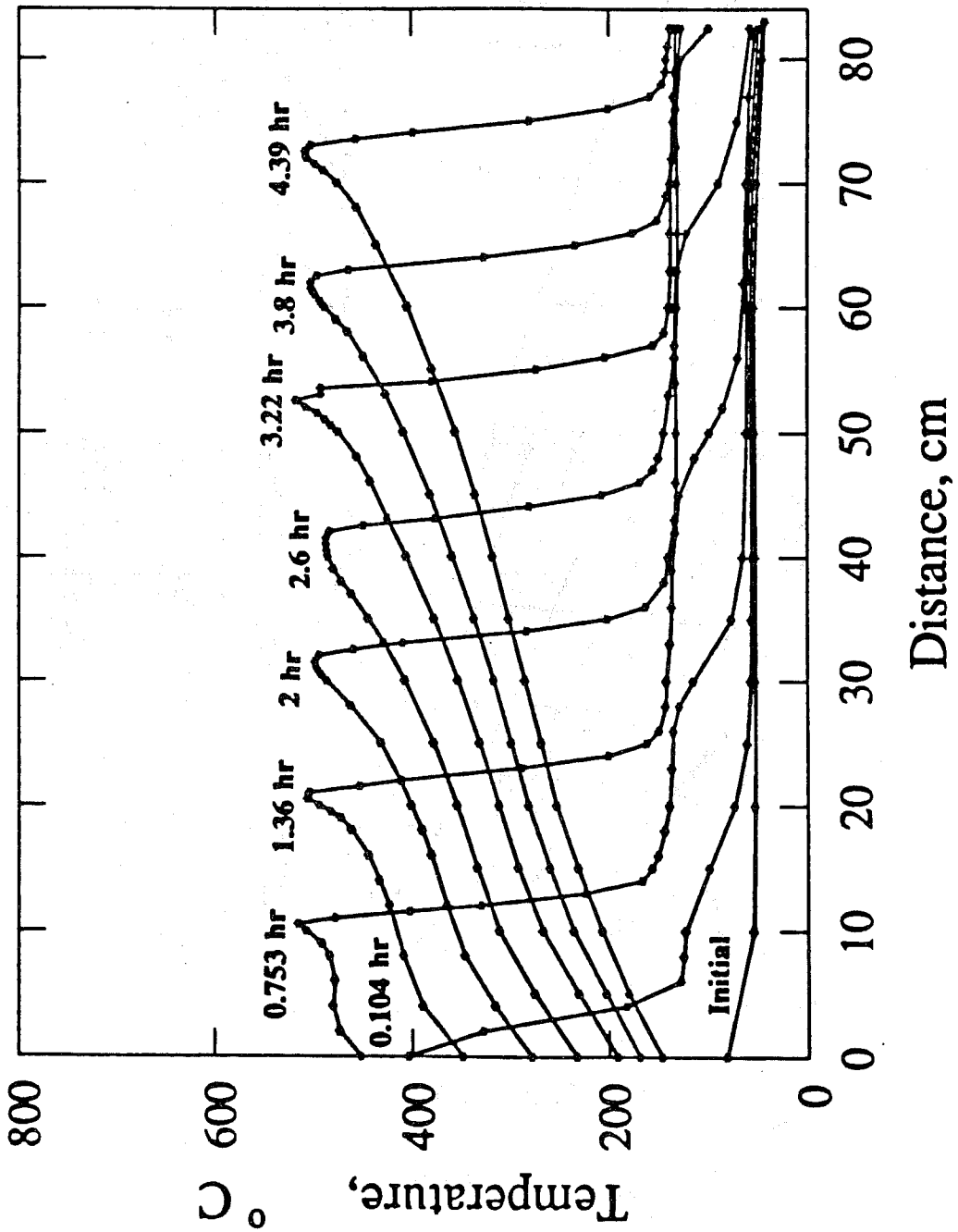


Figure 7.7 Temperature Profiles for the Ferrous Chloride ($FeCl_2 \cdot 4H_2O$) Run

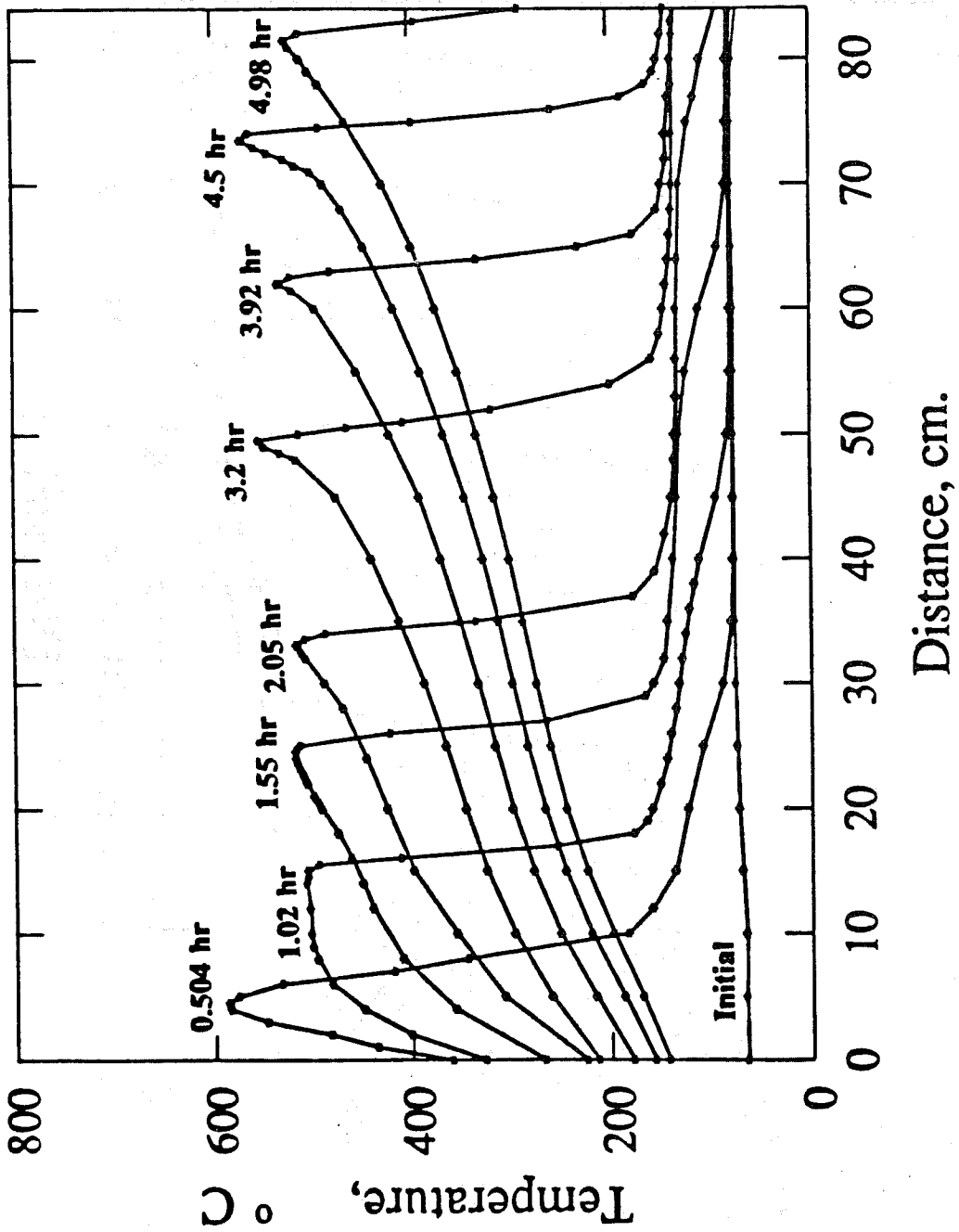


Figure 7.8 Temperature Profiles for the Stannic Chloride ($SrCl_4 \cdot 5H_2O$) Run

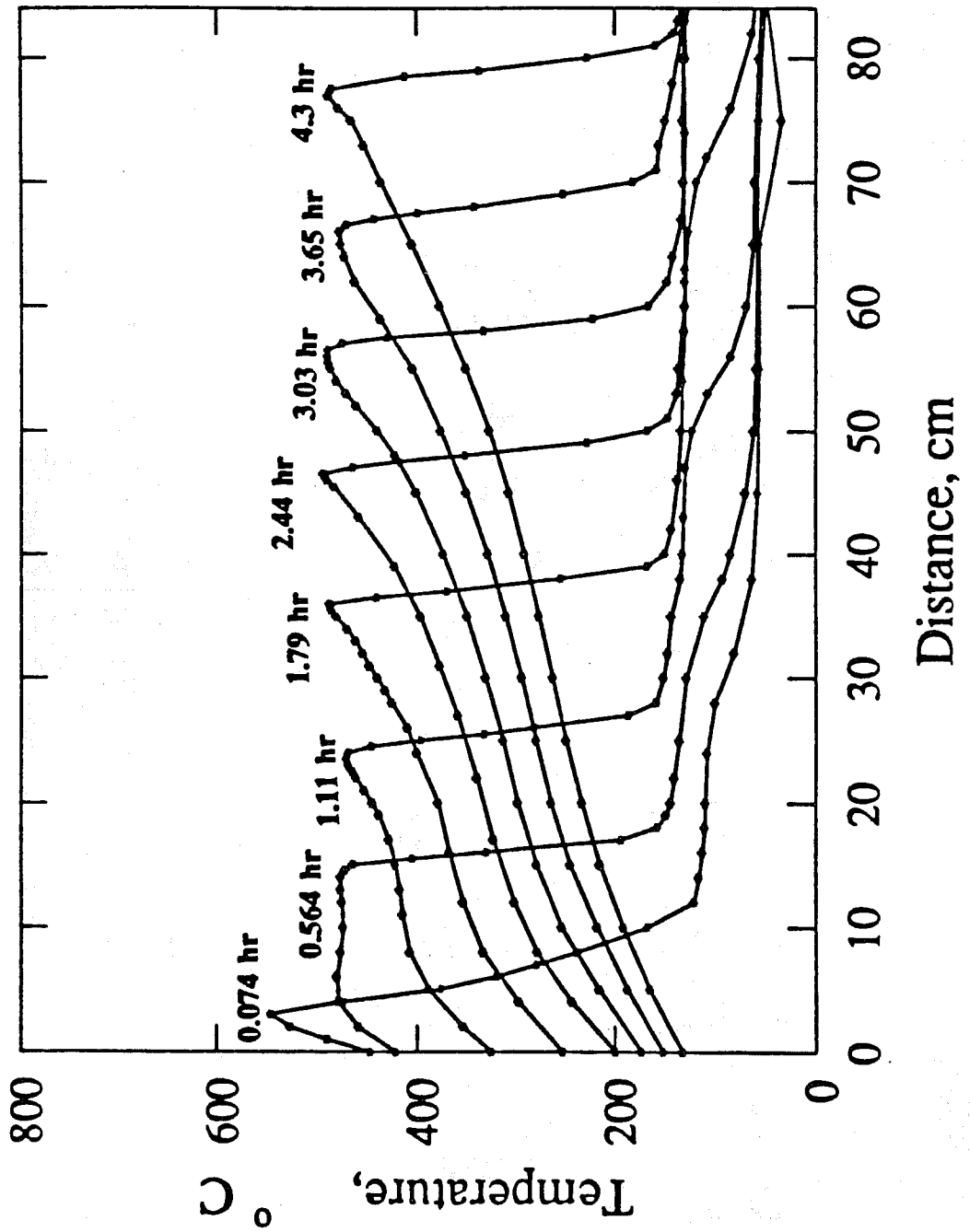


Figure 7.9 Temperature Profiles for the Zinc Chloride ($ZnCl_2$) Run

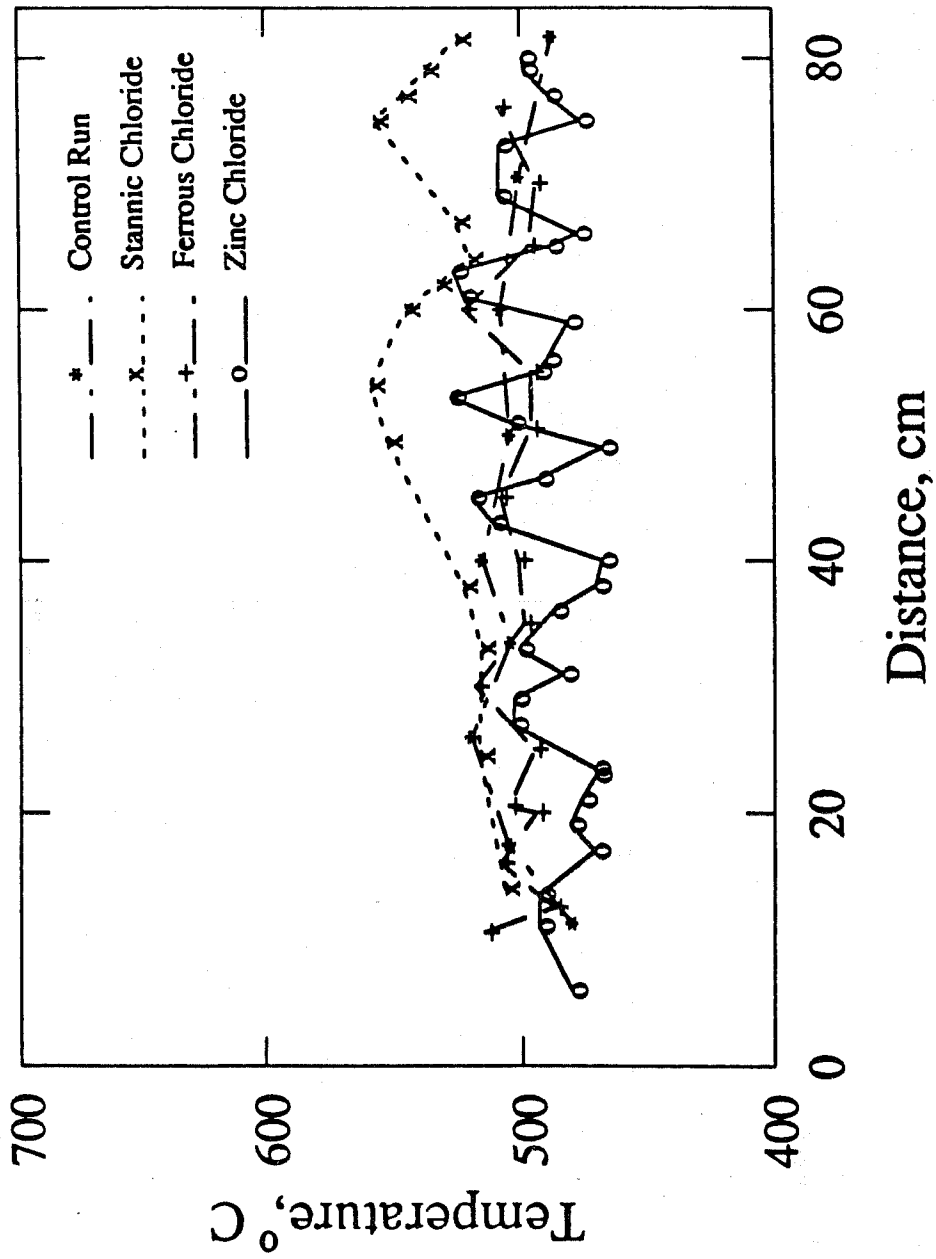


Figure 7.10 Comparison of Combustion Front Temperatures

For the control run, (Figure 7.10), small variations in combustion front temperatures are observed until about 2.75 hours, and then steady values of temperature are seen. If we consider the gas composition data for the control run, (Figure 7.1), variations in produced gas composition are observed, but these tend to stabilize after 2.8 hours. The ferrous chloride and stannic chloride runs showed large cyclical variations in the combustion front temperatures (Figures 7.10) but showed steady values of produced gas compositions (Figure 7.2 and 7.3). The variations in combustion front temperature could be a result of variations in the amount of fuel deposited and the heat lost locally. For zinc chloride, large cyclical variations are seen in the gas composition data and the combustion front temperature (Figures 7.4 and 7.10).

The combustion front temperature is a function of the amount of heat liberated and lost locally. The amount of heat liberated is related to the nature and amount of fuel formed. The nature of the fuel formed is determined through computation of its hydrogen to carbon ratio using produced gas composition data. The greater the hydrogen to carbon ratio of fuel, n , the greater would be the heat liberated on combustion of the fuel, and thus the higher would be the combustion front temperature. The effect of the hydrogen to carbon ratio of the fuel on the amount of heat liberated per pound of fuel will be discussed in Section 8. The heat lost locally is a result of insufficient or uneven packing of the insulation in the annulus around the combustion tube in the pressure shell. Heat losses are also greater around the flanges of the combustion tube. Heat losses will also be discussed in Section 8.

7.3 Recovery Data

The produced fluids were collected in centrifuge bottles and treated with Tretolite to break the emulsion. On centrifuging the produced fluid, the amounts of crude oil and water produced were estimated. Figures 7.11 - 7.14 show the oil recovery and water produced data for the four runs.

If we consider the recovery data for the control run, (Figure 7.11), one observes that the production rate for the oil and water was steady, and more or less the same. Initially oil was produced at a low flow rate as a result of drainage of the cold oil. As the oil was heated, it built up oil saturation ahead of the front before it began to move. Once the heated oil began to flow, the oil recovery rate increased and then attained a steady, constant value. This explains why the oil recovery data shows two slopes. The curve for water produced displays similar characteristics as that of the produced oil. Initially water is produced as a result of drainage along with the oil. As oil is heated, water gets displaced along with the oil, and is produced. The water that is generated as a result of combustion of the fuel is also produced. Once steady state is reached, the flow rates of water and oil remain constant. The oil recovery curve lies slightly above the water produced curve once the heated oil flows and is produced. This steady rate occurs after 2.7 hours, about the same time when the gas composition (Figure 7.1) and combustion temperature (Figure 7.10) are stabilized.

The recovery data for the ferrous chloride run, (Figure 7.12), show a similar increase in the oil recovery and water production rates as the crude oil is heated and is produced. The change in slopes occurs between 1.1 and 2.9 hours. The curve for oil recovery for the ferrous chloride run lies much higher than the water produced curve. This is in marked comparison to the control run. This is because oil is produced at a much higher rate in the presence of ferrous chloride. This is so because a greater amount of heat is liberated in the presence of ferrous chloride as will be seen later.

The fluid production data for the stannic chloride run produced two slopes in the oil and water production data (Figure 7.13) similarly to the control and ferrous chloride runs. The

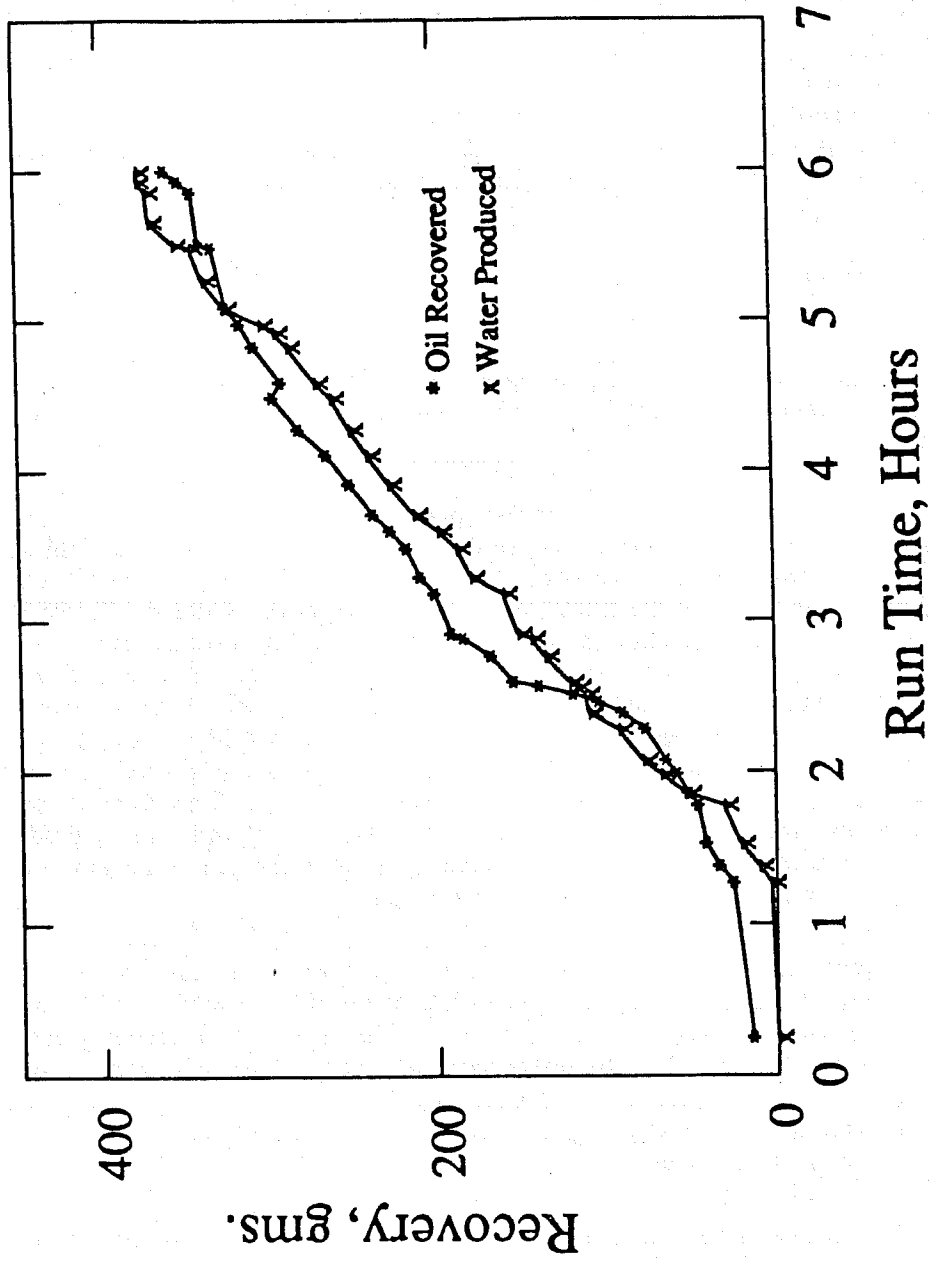


Figure 7.11 Recovery Data for the Control Run

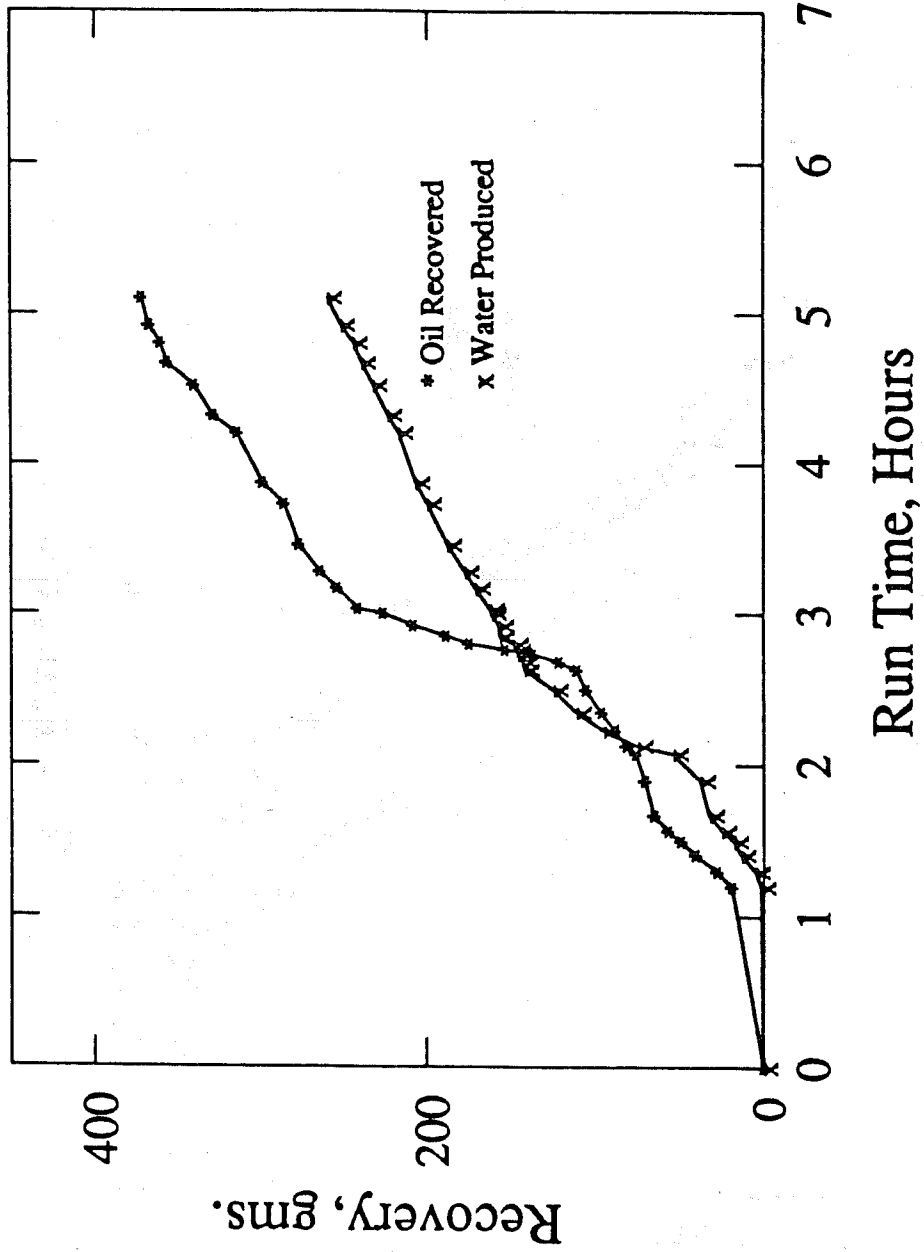


Figure 7.12 Recovery Data for the Ferrous Chloride ($FeCl_2 \cdot 4H_2O$) Run

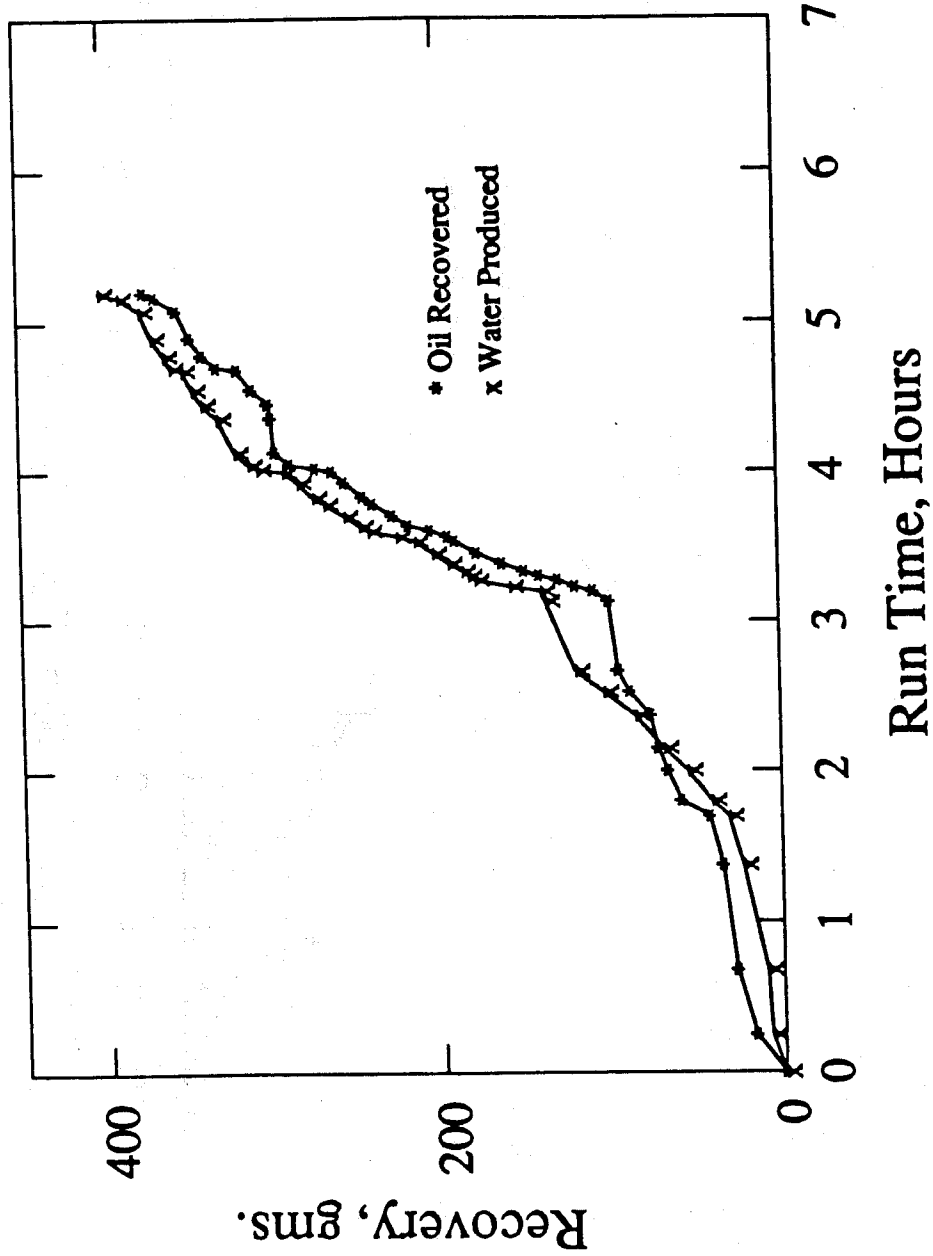


Figure 7.13 Recovery Data for the Stannic Chloride ($SnCl_4 \cdot 5H_2O$) Run

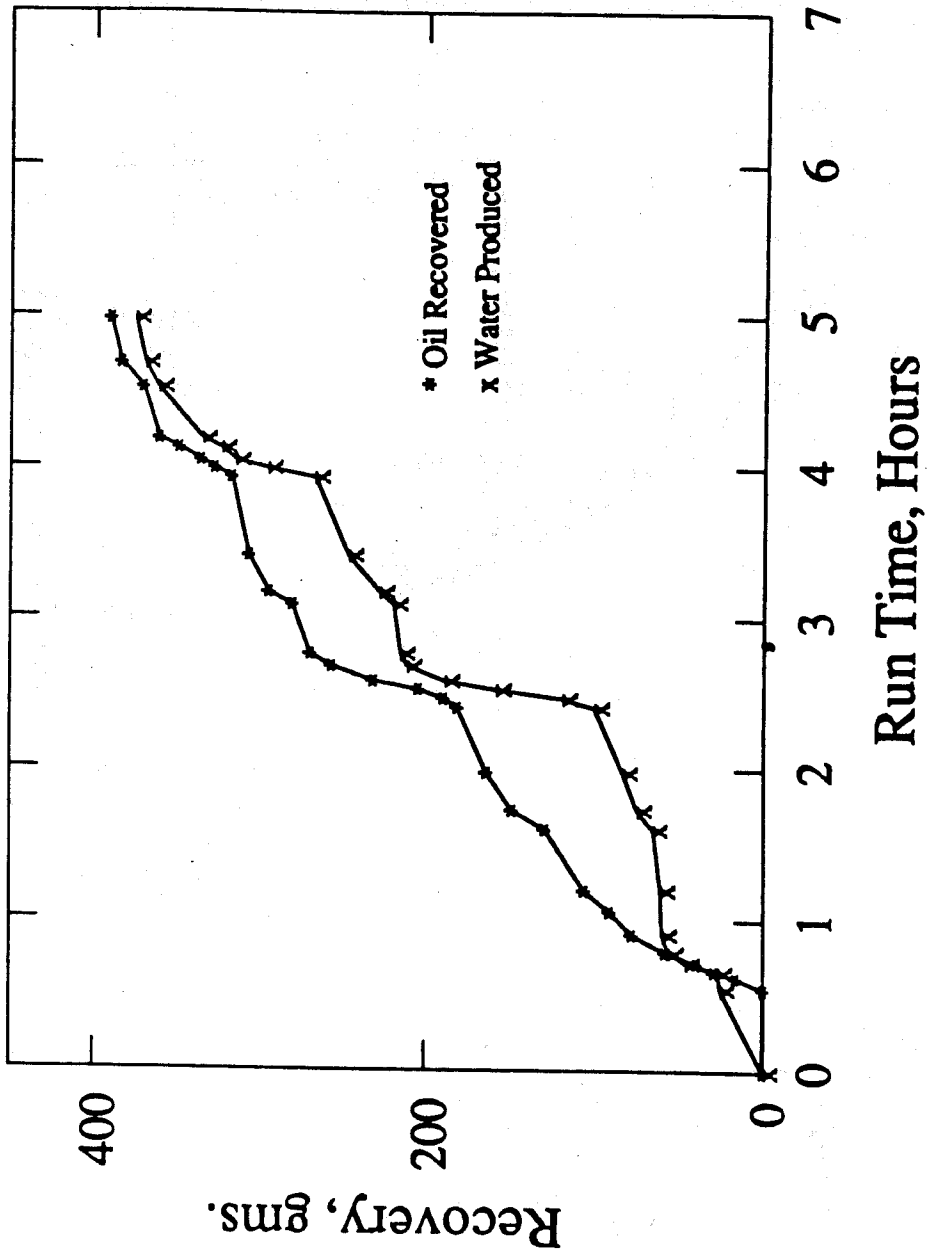


Figure 7.14 Recovery Data for the Zinc Chloride ($ZnCl_2$) Run

change in slope at 1.4 hours implies that the heated oil began flowing at this time. The water production curve lies above the oil recovery curve. This is because the fuel formed in the stannic chloride run has a higher hydrogen content in the fuel, (as seen in Section 8), producing a greater amount of water on burning, thus increasing the amount of water produced. Hydrogen to carbon ratio calculations will be discussed in Section 8.

For the zinc chloride run, (Figure 7.14), the change in slopes is not obvious. Large variations are seen in the fluid production data. This observation is consistent with the large variations in the combustion front temperature and produced gas compositions throughout the run (Figures 7.4, and 7.9). These variations are a result of packing which possibly led to variations in the amount of fuel deposited along the length of the combustion tube. Fuel deposited will be discussed in detail in Section 8. The water production curve lies below the oil production curve for the zinc chloride run. The ferrous chloride and control runs also show water production curves lying below their oil production curves. This is because the hydrogen contents of the fuels they form are lower than that of the stannic chloride run whose water production curve lies above the oil production curve. Smaller H/C ratios of the fuel implies that smaller amounts of water would be formed as a result of combustion, and produced along with the water that is displaced.

From the graph of the oil recovery, one can determine the oil recovery rate once the heated oil begins to flow. The order of increasing oil recovery rates was: control run, stannic chloride, ferrous chloride and zinc chloride. The oil recovery rate would be expected to be proportional to the combustion front velocity. Front velocities will be discussed in Section 8.

The experimental observations presented in this section are analyzed next in Section 8.

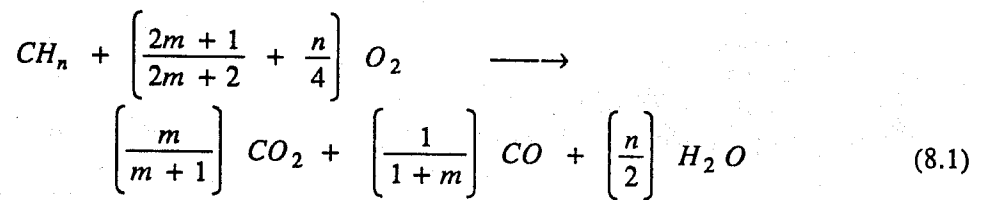
8. EXPERIMENTAL RESULTS

In this section the observations presented in Section 7 are analyzed for the four combustion tube experiments. First the gas composition data are analyzed to determine the hydrogen to carbon ratios of the fuels and the ratios of carbon oxides produced. These data are then used to determine the combustion parameters that affect the in-situ combustion process.

8.1 Analysis of Gas Composition Data

The produced gas composition history recorded during the combustion tube runs is analyzed using Martin and Dew's model (1964, 1965). The equations used in this analysis are found in Appendix A.

The high temperature oxidation combustion reaction is modeled as follows:



Based on this model, the data on the produced gas composition is used to determine the "apparent" atomic hydrogen to carbon ratio, n , of the fuel and the ratio of the carbon dioxide to carbon monoxide, m , in the produced gas. The H/C ratio, n , is determined using Equation A.3 in Appendix A, while m is determined directly from the concentrations of carbon oxides in the produced gas. The m and n values are used to determine the combustion parameters as discussed in the following subsections.

8.1.1 Hydrogen to Carbon Ratios and Carbon Dioxide to Carbon Monoxide Ratios

Figure 8.1 is one of the most important graphs in this study. It shows the ratio of hydrogen to carbon of the fuel, n , and the ratio of carbon dioxide to carbon monoxide, m , in the produced gas, for all four runs. The control run produced the lowest hydrogen to carbon ratio and carbon dioxide to carbon monoxide ratio of all the runs. The average H/C ratio of the fuel increased from 0.07 for the control run to 0.13 in the presence of ferrous chloride, 0.61 with zinc chloride and 0.79 with stannic chloride. These differences in the H/C ratios indicate that the nature of the fuel formed has been altered when metallic additives are present. The small value of the H/C ratio in the control run indicates that the fuel formed was nearly pure carbon.

A study the H/C ratios shows that the control run and the ferrous chloride run produced fairly constant values of the H/C ratio. For the stannic chloride and zinc chloride runs, variations occurred in the values of H/C ratios. However, the variations were much larger with zinc chloride, consistent with the large variations in its gas composition data (Figure 7.4), discussed earlier.

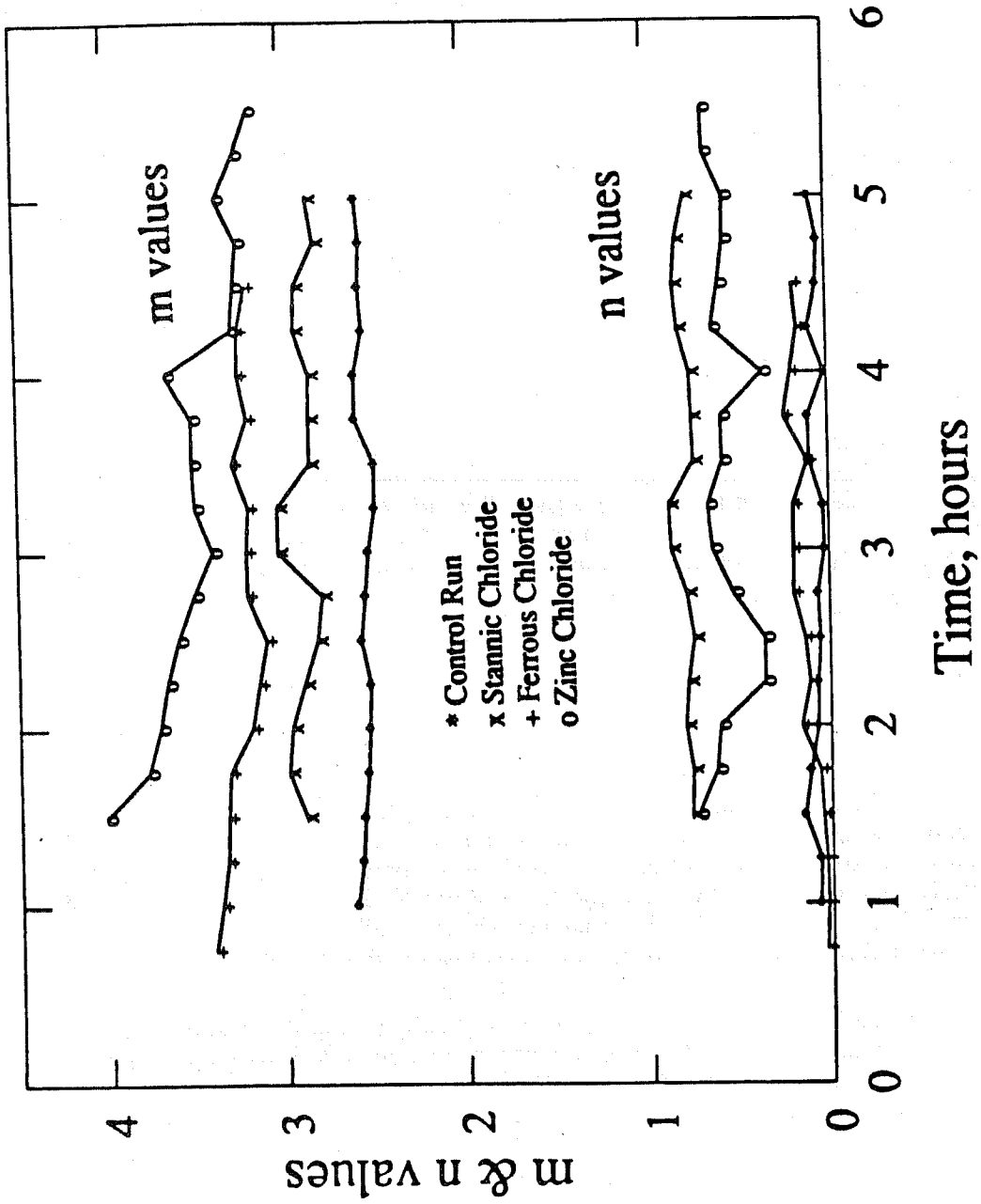


Figure 8.1 Plot of m and n Values

If we consider the average carbon oxide ratios, the order of increasing m values was control run, stannic chloride, ferrous chloride and zinc chloride. The average values were 2.55 for the control run, 2.90 for stannic chloride, 3.25 for ferrous chloride and 3.29 for zinc chloride. The control run and the ferrous chloride run produced fairly steady values of m . Stannic chloride and zinc chloride showed slight variations.

The H/C ratio affects the heat of combustion of the fuel. It also affects the amount of air required for combustion. Thus the combustion front temperature and the combustion front velocity are affected. The effect of the H/C ratio of the fuel, n , on combustion front temperature and velocity will be discussed in later subsections.

No indications on the nature of the fuel formed can be obtained from the ratio of carbon oxides. The ratio of carbon oxides provides an indication of the extent to which the oxidation to carbon dioxide is complete when the fuel burns. The ratio of carbon oxides, m , gives an indication of the amount of heat given off by burning the fuel and the amount of air needed to burn the fuel. This affects the combustion front temperature and the combustion front velocity and will also be discussed in later subsections.

8.1.2 Combustion Efficiency

The fraction of oxygen in the injected air that is consumed during combustion is known as the oxygen utilization efficiency. In performing combustion tube experiments, the calculation of the oxygen utilization efficiency is necessary, because combustion tube experiments are usually less than 100% efficient, while most field projects operate at near 100% efficiency. The concentration of oxygen in the produced gas gives an indication of the efficiency of the in-situ combustion process. From the produced gas composition graphs (Figures 7.1 to 7.4), one observes that the oxygen concentration in the produced gas was the lowest in the stannic chloride run. The oxygen concentration was higher for ferrous chloride run, and much higher for zinc chloride and highest for the control run. Equation A.7 in Appendix A was used to calculate the oxygen utilization efficiencies. Figure 8.2 shows results of computations for the four runs. The run using stannic chloride averaged 98.6% combustion efficiency, ferrous chloride averaged 94.2%, zinc chloride run averaged 86.9%, and the control run had the lowest average of 82.3%.

The graph of oxygen utilization efficiencies (Figure 8.2), shows that stannic chloride had a steady and gradually increasing combustion efficiency. Its value increased from 98% to nearly 100%. These results are also seen in the oxygen concentration in the produced gas for the stannic chloride run, (Figure 7.3). There is a gradually decreasing concentration of oxygen in the produced gas.

In the ferrous chloride run, the combustion efficiency decreased from about 97% to 91% at 1.4 hours and then it gradually increased to 94% at 2.6 hours and remained fairly steady. These results can be compared with the oxygen concentration in the produced gas for the ferrous chloride run, (Figure 7.2). The oxygen concentration gradually increased until about 1.4 hours, then decreased until about 2.6 hours and then remained steady.

The steady values of oxygen utilization efficiencies for stannic chloride and ferrous chloride are consistent with the gas composition data. In the the control run and the zinc chloride run, large variations were seen in the oxygen utilization efficiency. This result is consistent with the variations in the oxygen concentration seen in the produced gas for these runs (Figures 7.1 and 7.4).

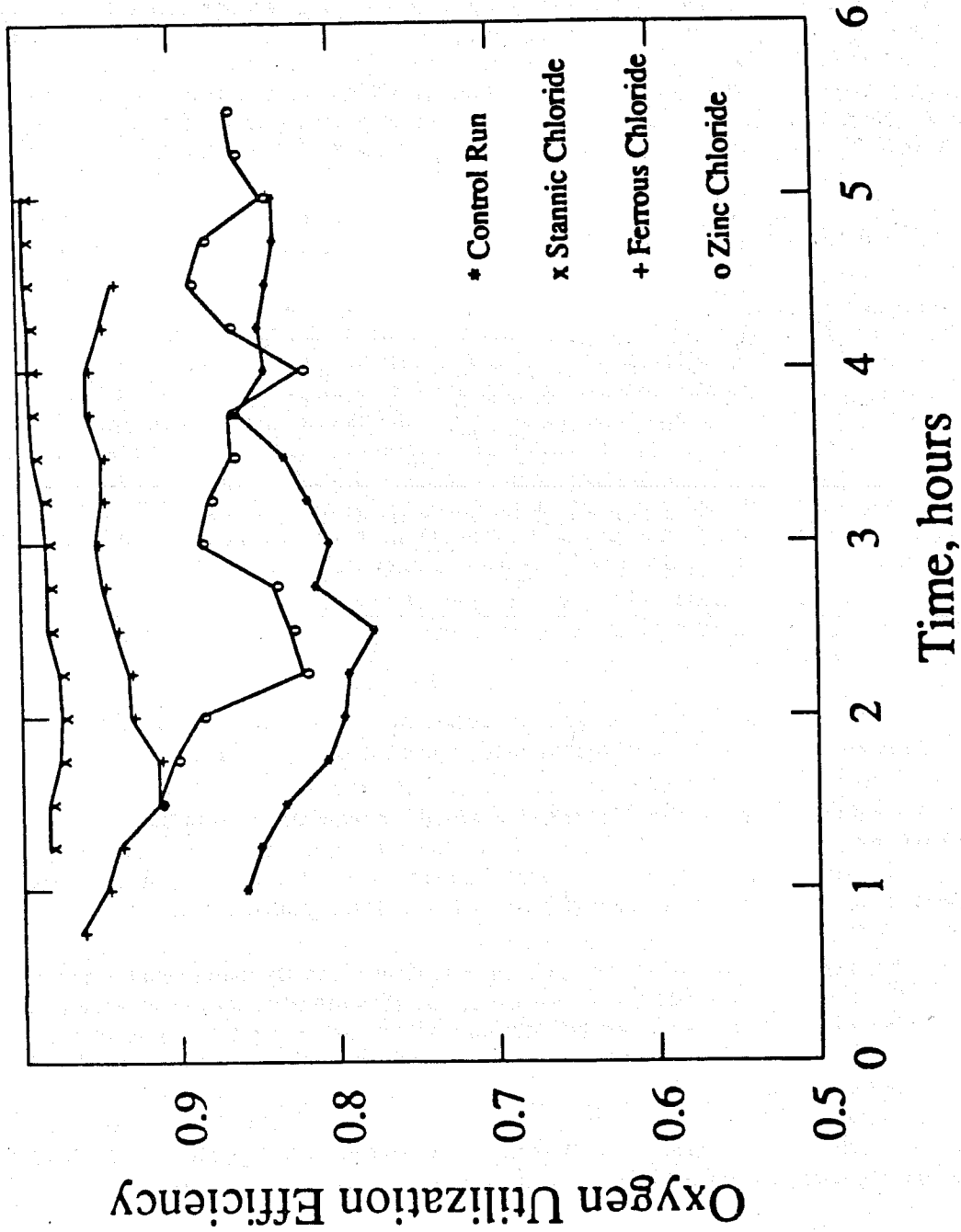


Figure 8.2 Oxygen Utilization Efficiencies

It appears as if two sets of efficiencies are produced based on the manner in which the combustion tubes were packed. In the stannic chloride and ferrous chloride runs, large amounts of sand were put into the tube and were gently squeezed in with the help of a tamper. In the control run and the zinc chloride run, small quantities of the sand pack were put into the tube and were vigorously tamped (Figure 7.5). It appears as if this second method of packing produced lower combustion efficiencies as well as greater variations in operating conditions.

8.1.3 Air Requirement at 100% Combustion Efficiency

The air requirement at 100% combustion efficiency is an important parameter because the overall economic feasibility of an in-situ combustion project depends upon the cost of injecting air. It is important to extrapolate the laboratory results to 100% combustion efficiency because most field projects in California operate at this condition while combustion tube runs often do not. In doing so, the laboratory data are being extrapolated to expected field results. The air requirement at 100% efficiency is determined using Equation A.8 in Appendix A.

Figure 8.3 shows the air requirements at 100% oxygen utilization efficiency in terms of scf/lb of fuel burned for all the runs. The air requirements averaged 130.6 scf/lb of fuel burned for the control run with no metallic additive, 135.8 scf/lb for ferrous chloride, 147.4 scf/lb for zinc chloride and 150.4 scf/lb for stannic chloride. The order of increasing air requirements at 100% combustion efficiency (Figure 8.3) was similar to the order of increasing H/C ratios of the fuel consumed (Figure 8.1). One also observes that for a given run, the variations observed for the air requirement are identical to the variations of the H/C ratio. Note that the variations in the carbon dioxide to carbon monoxide ratio had little effect on the runs. The H/C ratio was the major parameter affecting the air required. One would therefore expect that the variations observed for the air requirement at 100% efficiency to be similar to those in-situ combustion parameters that are affected significantly by the H/C ratio of the fuel. The heat of combustion is one such parameter. The variations in the heat of combustion in relation to the H/C ratio of its fuel will be discussed in a later subsection.

8.1.4 Actual Air Requirements

The amount of air actually used to burn a cubic foot of the reservoir, a_R , is computed using Equation A.16 in Appendix A. The computed values are shown in Figure 8.4.

Figure 8.4 shows that the order of increasing actual air requirement was the same as the air requirements at 100% efficiency. The control run had the highest average air requirements of 275 scf/cu ft of reservoir. Average air requirements were 241.4 scf/cu ft for ferrous chloride, 240.9 scf/cu ft for zinc chloride and 240.5 scf/cu ft for stannic chloride.

One would expect that the actual air requirements depend on the nature and amount of fuel formed and the combustion efficiency. While the combustion efficiency does play a role in the actual air requirements, the nature and amount of fuel formed plays a greater role in field projects. This is because most field projects operate at near 100% combustion efficiencies. Considering the combustion efficiencies of the four runs, one observes that the order of increasing actual air requirements is not in reverse order of the combustion efficiencies. The order of increasing efficiencies were zinc chloride, control run, ferrous chloride and stannic chloride (Figure 8.2).

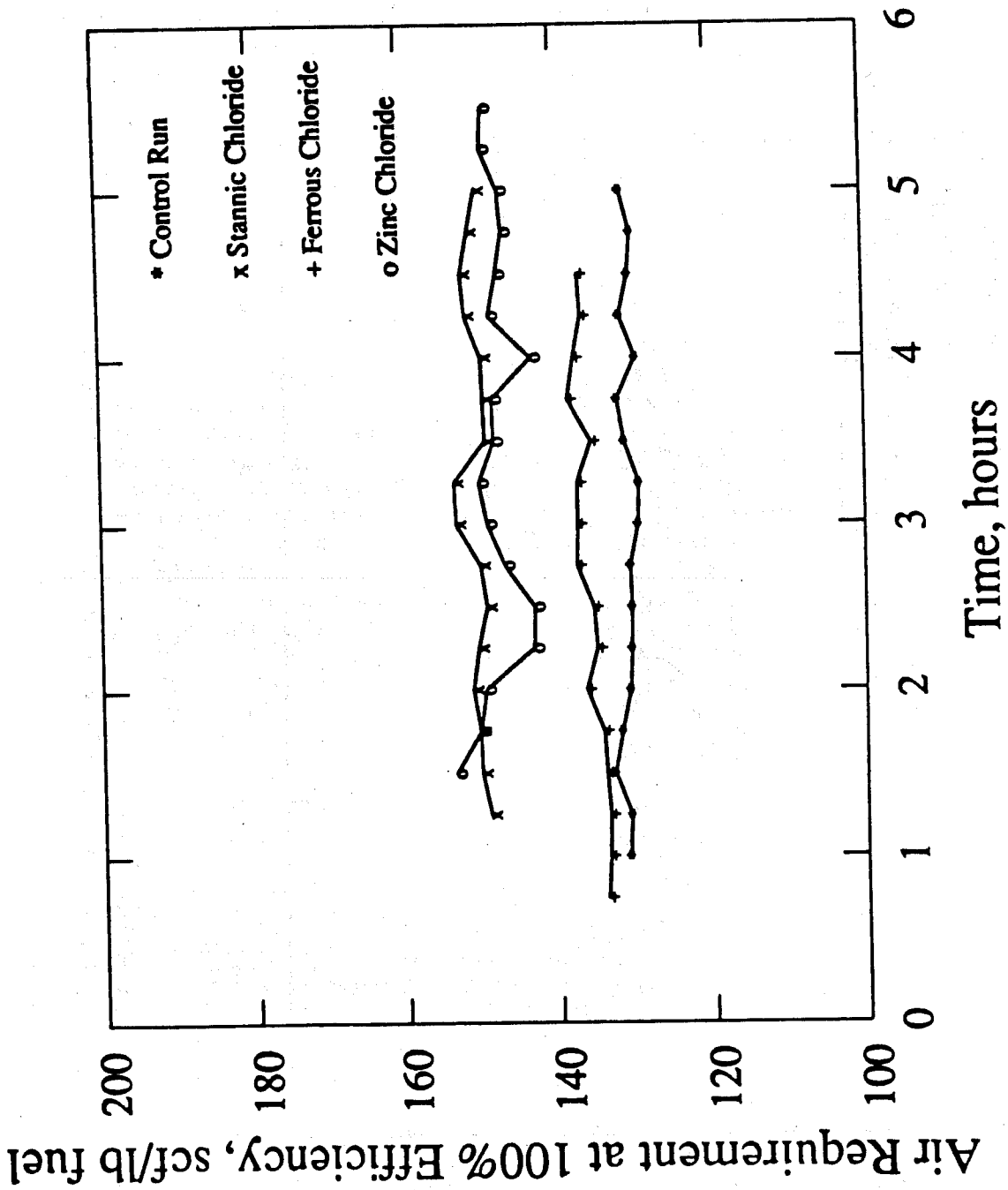


Figure 8.3 Air Requirements at 100% Efficiency (scf/lb of fuel burned)

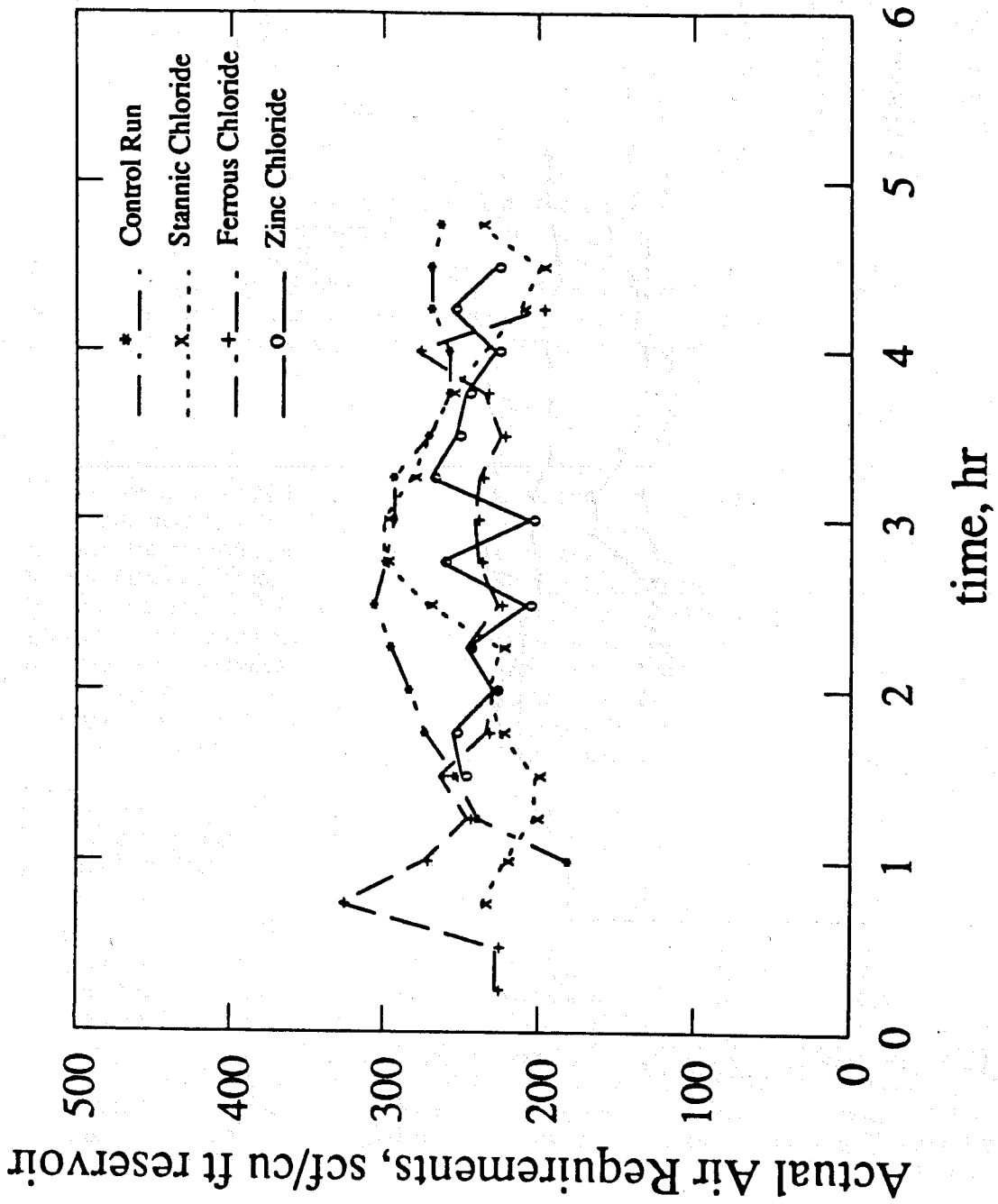


Figure 8.4 Actual Air Requirements (scf/cu ft reservoir)

The H/C ratios, n , of the fuels indicated increasing n values with the same order as that of the actual air requirements (Figure 8.1). This arises from the fact that a greater hydrogen content per mole of the fuel will require a greater amount of air to burn.

If the amount of fuel burned increases, the amount of air that would be required would increase. Computations of the fuel consumption are performed next, wherein the relationship between the actual air required and the fuel consumption will be established.

8.1.5 Fuel Consumption

Laboratory data on crushed rock and cores has shown that the amount of fuel burned depends upon the fuel-rock ratio on a weight basis, but is not affected by porosity variations over a practical range (Dew and Martin 1964, 1965). The amount of fuel consumed can be presented on the basis of pounds of fuel deposited per 100 pounds of the reservoir rock, thereby correcting for porosity, to relate laboratory data to the field.

Equations A.11 through A.15 in Appendix A are used to determine the fuel consumption during the runs. Figure 8.5 shows the fuel consumption in pounds of fuel per 100 pounds of reservoir rock for the four runs. If we consider the fuel consumption for the control run, we observe that the fuel consumption increases from a value of 1.1 lbs/100 lb rock and then stabilizes between 1.7 and 1.55 lbs/100 lb rock at about 2.5 hours. This observation is consistent with the stabilization time of the gas composition (Figure 7.1), the combustion front temperature data (Figure 7.6) and the oil recovery graph (Figure 7.11) for the control run.

If we consider the fuel consumption for stannic chloride, (Figure 8.5), large cyclical variations are observed. Fuel consumption decreases from 1.51 lbs/100 lb rock to 0.55 lbs/100 lb rock at 1.5 hours and then increases to a maximum of 1.8 at 2.5 hours. It then decreases to 1.33 at 4.5 hours and increases to 1.55 thereafter. The gas composition data for stannic chloride (Figure 7.3), however show steady values. The variations in fuel consumption indicate that the fuel deposited during the run was not uniform. This is manifested in the combustion front velocity (Figure 8.15) discussed later. Variations in the fuel deposited result in variations in the combustion front velocity and oil recovery rates (Figure 7.13). The oil recovery graph for stannic chloride showed variations similar to that of the combustion front velocity, but opposite to that of the fuel consumption. This is because the combustion front velocities and oil recovery rates decrease as the fuel consumed increases. Figure 7.13 shows that oil begins to flow at 1.4 hours. This result implies that stability was attained at this time (1.4 hours) and therefore data after this time should be evaluated.

The fuel consumption for the zinc chloride run, (Figure 8.5), showed large variations, consistent with the gas composition data (Figure 7.4), combustion front temperature (Figure 7.10) and oil recovery data (Figure 7.14). These variations are a result of the packing technique used for the zinc chloride run, discussed earlier.

Ferrous chloride produced large variations in fuel content initially, however the fuel content became more stable after about 1.1 hours (Figure 8.5). This observation is consistent with the time the heated oil began to flow (Figure 7.12). At around 4 hours, the fuel consumption increases to 1.78 lb/100 lb rock and then decreases to 1.24 lb/100 lb rock at 4.25 hours. This uneven fuel deposition at the end of the run is inherent. The combustion efficiency (Figure 8.2) decreases around this time. Actual air requirements (Figure 8.4) reflect the variations in fuel deposition. The amount of residue remaining unburnt is opposite to that of the fuel consumption at this time (Figure 8.7).

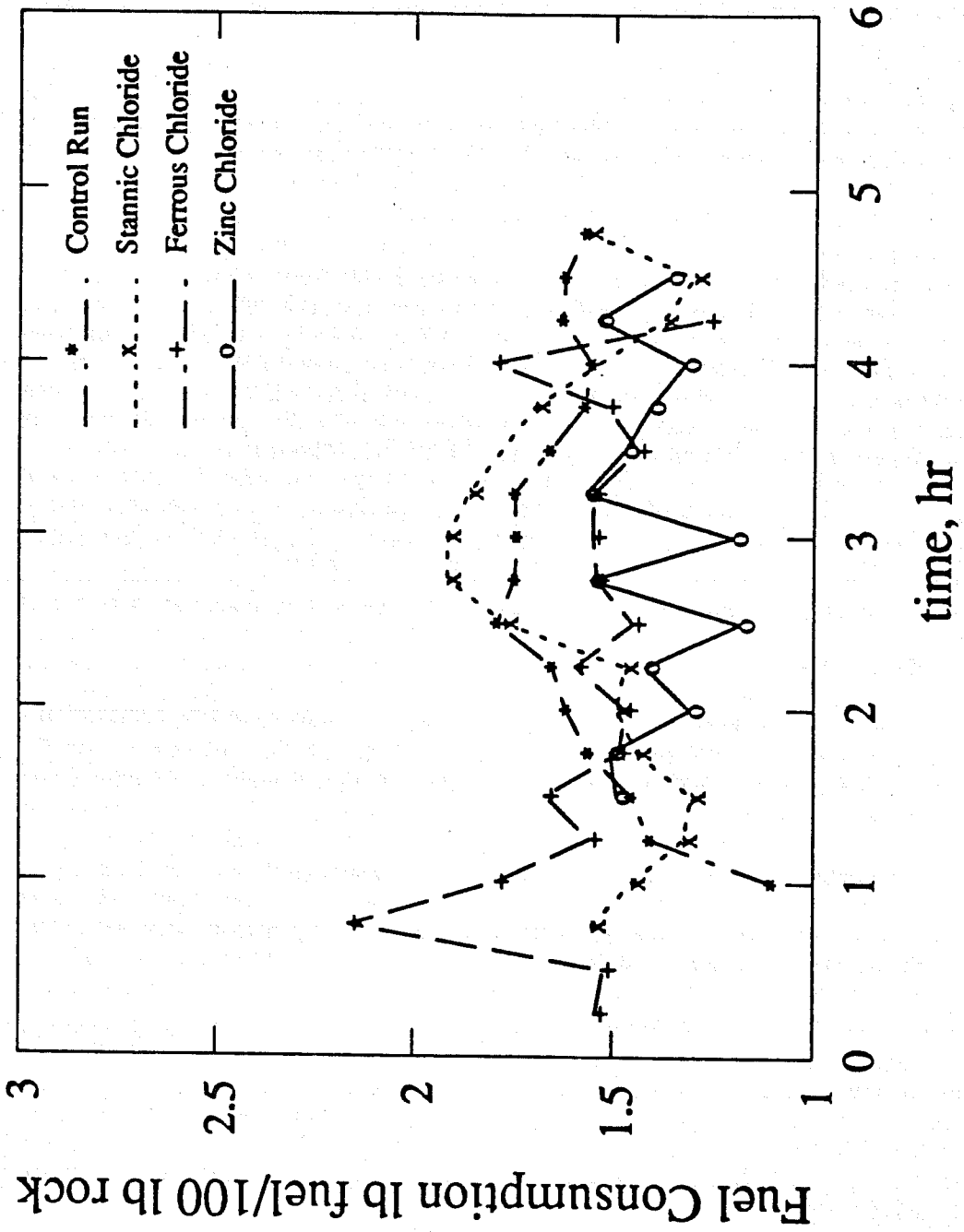


Figure 8.5 Fuel Consumption (lb of fuel/100 lbs of rock)

The average values of the fuel consumption were 1.41 lb/100 lb rock for zinc chloride, 1.50 lb/100 lb for the control run, 1.52 lb/100 lb for stannic chloride and 1.55 lb/100 lb for ferrous chloride. Fuel consumption decreased in the presence of zinc chloride. Stannic chloride and ferrous chloride increased the amount of fuel consumption. The fuel consumption was the highest with ferrous chloride.

Comparing Figure 8.4 and 8.5, one observes that the order of increasing actual air requirement is the same as the order of increasing fuel consumption. In addition, the shapes of the actual air requirement graphs are strongly influenced by the amount of fuel deposited. The shape of the graph for the control run and stannic chloride run for the fuel consumption in Figure 8.5, is the same as the shape of the actual air requirements in Figure 8.4. For example the hump in fuel consumption for the stannic chloride run is reproduced in the graph of actual air requirements. The variations in the fuel consumption for the zinc chloride run are also reproduced in the actual air requirement graph. Similar observations can be made for the other two runs.

Increased fuel was deposited for stannic and ferrous chloride. This result is consistent with the results of the kinetic studies on Huntington Beach crude oil by De los Rios (1987). He observed that when ferrous chloride and stannic chloride were used, lower activation energies were observed compared to a control run with no metallic additives. This resulted in increased oxidation and fuel deposition in the LTO reaction, making more fuel available for the high temperature oxidation or combustion reactions. The observation that the fuel consumption was the highest with ferrous chloride is also consistent with the results presented by Racz (1985). De los Rios also found a slight increase in the fuel deposition for zinc chloride. However this was not because of a reduction in activation energy, but rather because of an increase in the pre-exponential constant of the low temperature reaction. In our case, zinc chloride produced a slight reduction in the amount of fuel consumed, contrary to the observation of De Los Rios. This difference needs to be investigated by future researchers.

8.1.6 Fuel Availability

It is important to determine the amount of fuel available in in-situ combustion experiments in the laboratory. Sometimes not all fuel is burned and some unburned fuel is left on the sand. Field projects, however, usually burn all the fuel available, leaving behind clean sand.

Fuel availability may be estimated from the fuel consumption data and the analysis of the unburned carbonaceous residue left unburned behind the combustion front. The amount of unburned carbonaceous residue on the sand was determined by burning it in an oven at 700 °C, and determining its weight by difference.

Figures 8.6, 8.7, and 8.8 show the analyses of the sand for unburned carbonaceous residue left behind the burning front for the control, ferrous chloride and zinc chloride runs. The analyses of stannic chloride residue could not be performed, as the sample was accidentally discarded.

The amount of carbonaceous residue remaining unburned was approximately 0.5% of the weight of the sand for all the runs. Since the amount of unburned fuel was about the same for all runs, the relative values of fuel availability from the four runs are valid without need for correction.

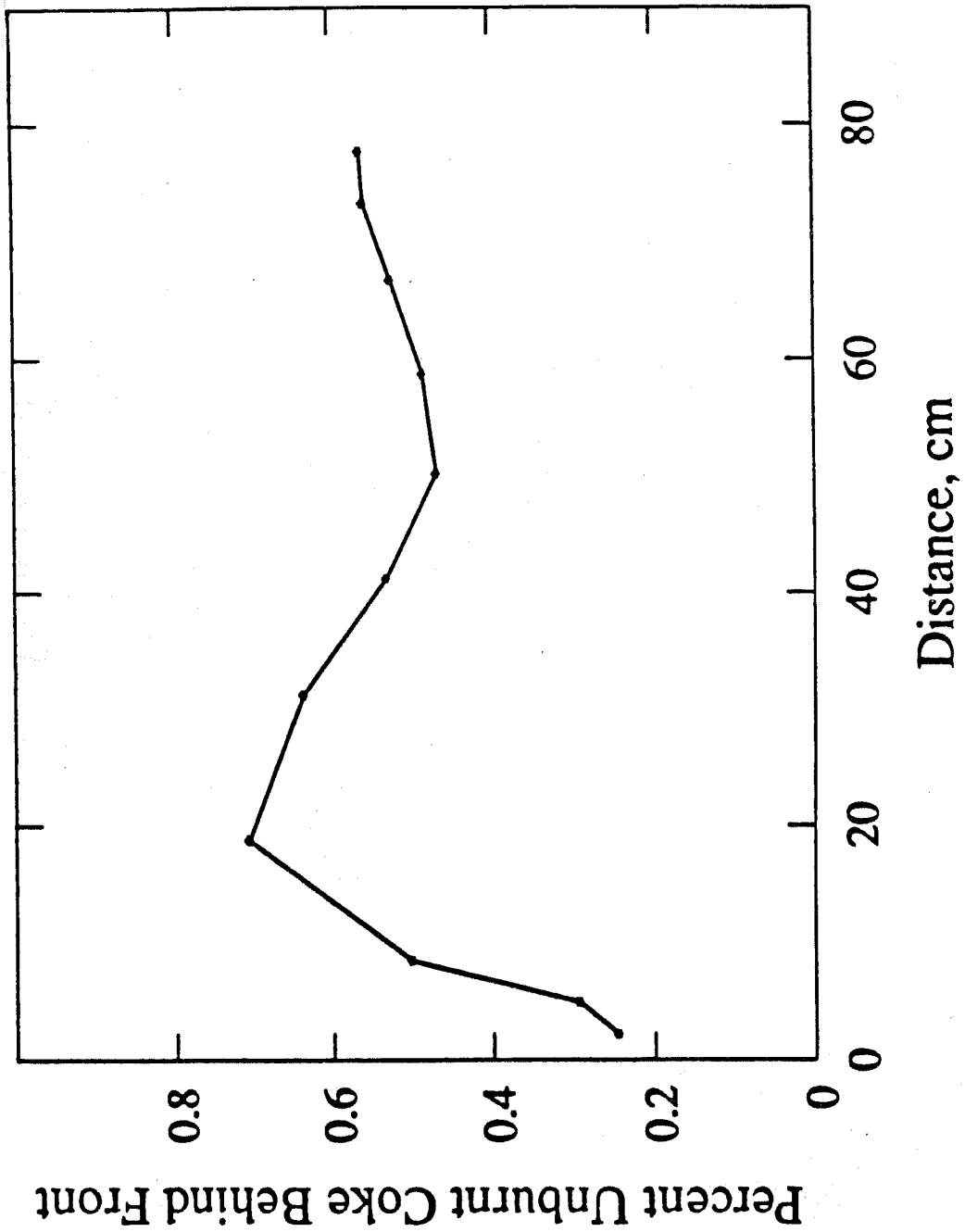


Figure 8.6 Carbonaceous Residue for the Control Run

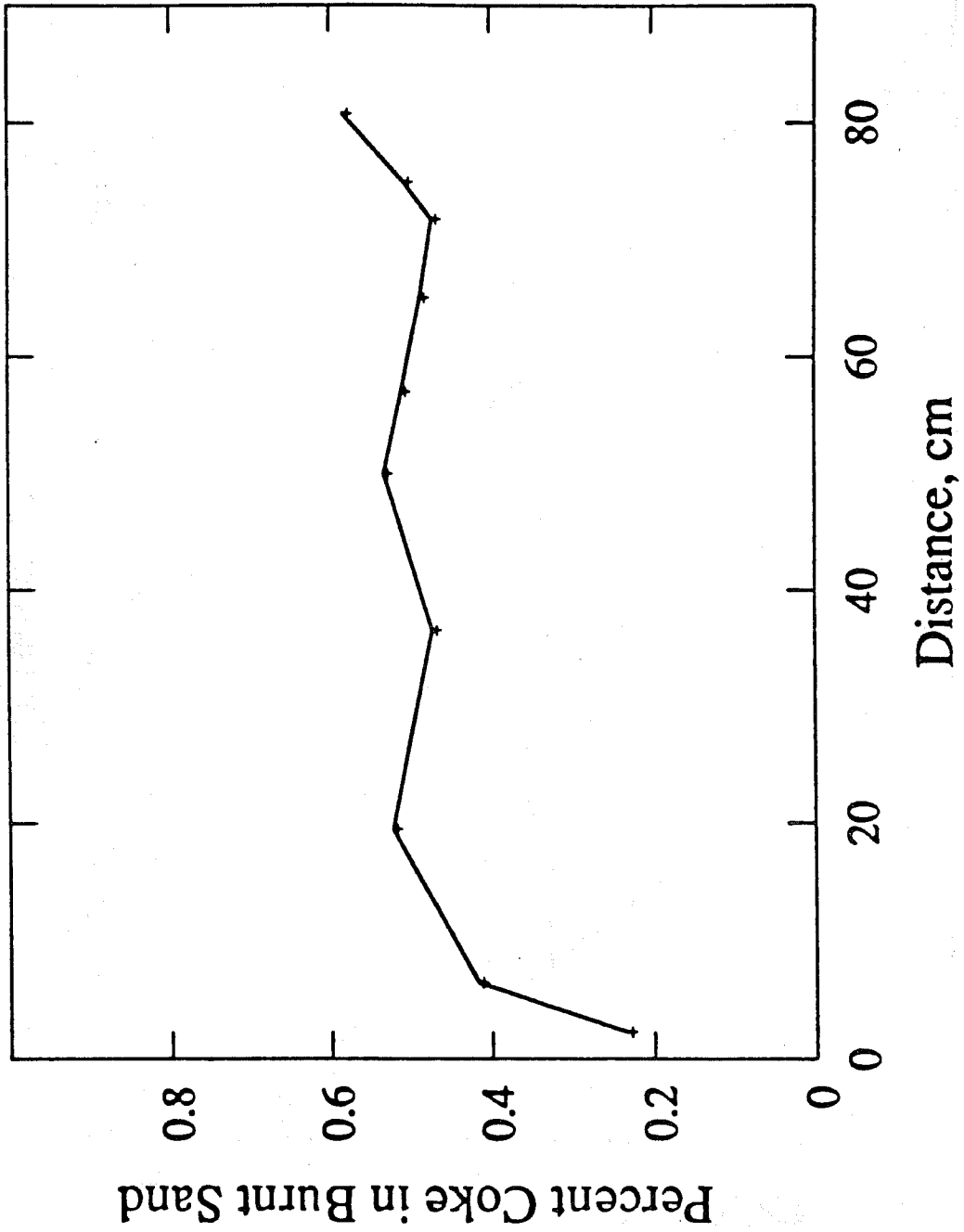


Figure 8.7 Carbonaceous Residue for the Ferrous Chloride ($FeCl_2 \cdot 4H_2O$) Run

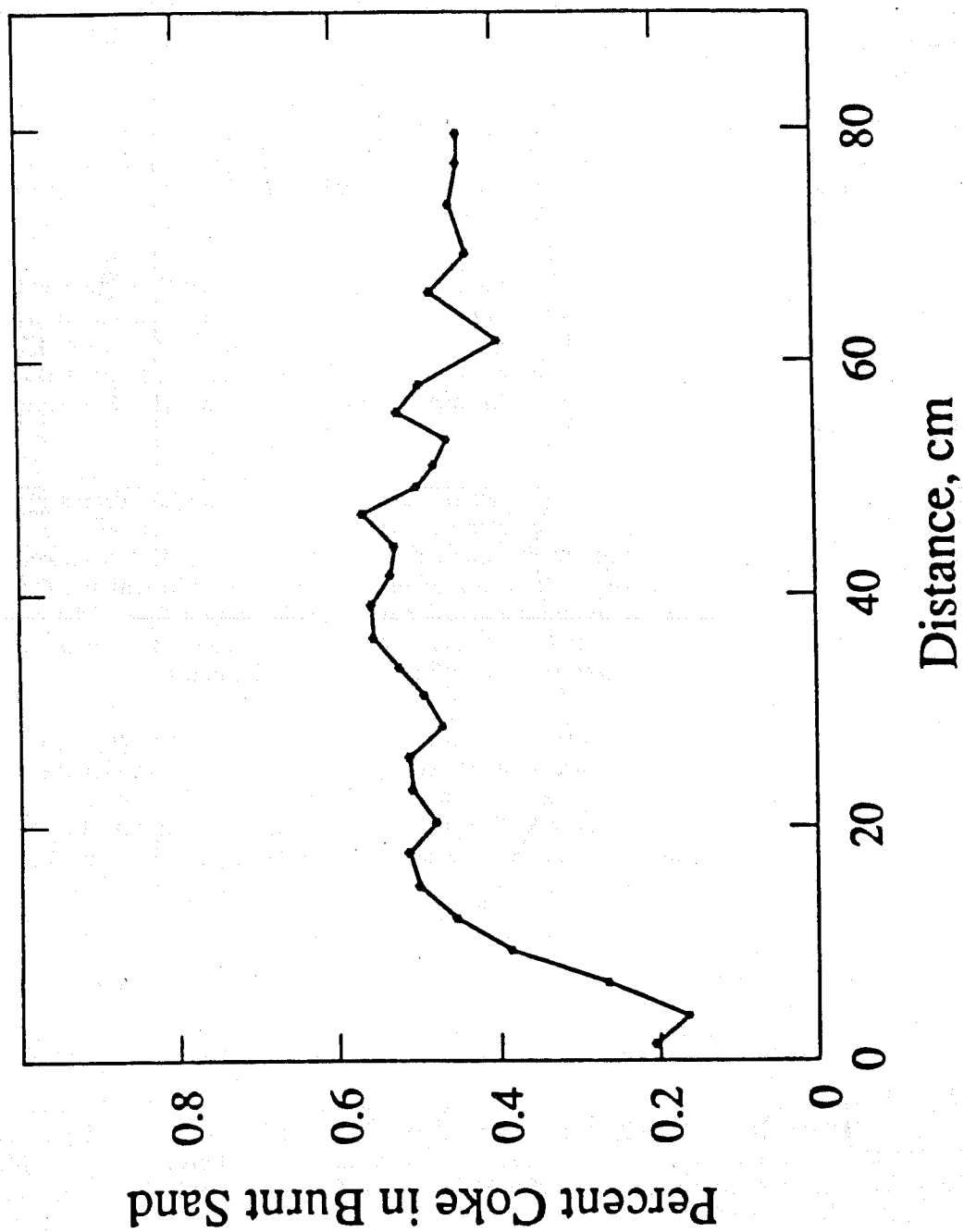


Figure 8.8 Carbonaceous Residue for the Zinc Chloride ($ZnCl_2$) Run

Since the amount of carbonaceous residue remaining unburned was about 0.5% of the weight of sand, about 65% to 68% of the available fuel was burned in all the runs.

When two to three samples from the same zone in the combustion tube were analyzed, the amounts of unburned carbonaceous residue were found to differ. The amounts were found to differ by about 20% to 40% of the mean values reported here.

8.1.7 Air-Oil Ratios

The air oil ratio is the ratio of the actual air requirements in standard cubic feet per barrel of crude oil produced. Computation of the air-oil ratio is important because it gives a measure of the actual amount of air which must be injected into the reservoir to produce one barrel of crude oil. The air requirements dictate the economics of oil recovery of an in-situ combustion process, because air compression costs are high. The air oil ratios reported here are specific to the operating conditions of the runs. Most field projects operate at 100% combustion efficiency, while most combustion tube experiments do not. Also the porosities, permeabilities, oil content, chemical composition of oil and rock of reservoirs are different from the samples studied in the laboratory.

Figure 8.9 shows the observed air-oil ratios for the four runs under stable conditions, when the heated oil flows. The air-oil ratio was computed using the data on the air actually injected and the crude oil produced. In computing the air-oil ratios, the density of the produced crude oil was measured. The values of the densities of the crude oils produced were 0.888 gm/cc for the control run, 0.876 gm/cc for ferrous chloride, 0.86 for stannic chloride and 0.8935 for zinc chloride.

From Figure 8.9 the order of increasing air-oil ratios was zinc chloride, ferrous chloride, stannic chloride and the control run. The average values of the air-oil ratios were 10,300 scf/bbl for zinc chloride, 11,500 scf/bbl for ferrous chloride, 12,400 scf/bbl for stannic chloride and 14,300 scf/bbl for the control run. The order of increasing air-oil ratio was not the same as the order of increasing actual air requirements of the reservoir (Figure 8.4). The order of increasing actual air requirements is stannic chloride, zinc chloride, ferrous chloride and control run. The control run had the highest air-oil ratio and actual air requirements.

The graphs of the actual air requirements and the air-oil ratios for the four runs (Figures 8.4 and 8.9) show that the observed variations are similar. For example, consider the graphs for the stannic chloride run. There is a decrease in the air-oil ratio and the actual air requirements between 3 and 4 hours and then both graphs tend to stabilize. Similarly for the zinc chloride run, the variations in the actual air requirement are similar to those seen in the air-oil ratio.

8.1.8 Heat of Combustion

The heat of combustion is important because the heat that is liberated is used to heat the crude oil and lower its viscosity. The heat of combustion of the fuel is determined using Equation A.9 in Appendix A. Figure 8.10 is a graph of the heat of combustion in terms of the heat generated per pound of fuel deposited. The values of heat of combustion averaged 11,900 BTU/lb of fuel burned for the control run, 12,500 BTU/lb of fuel for ferrous chloride, 14,500 BTU/lb of fuel for zinc chloride and 15,000 BTU/lb fuel for stannic chloride. The heat of combustion is a function of the nature of the fuel formed and the ratio of carbon oxides produced. The control run had the lowest heat of combustion as the fuel formed was essentially

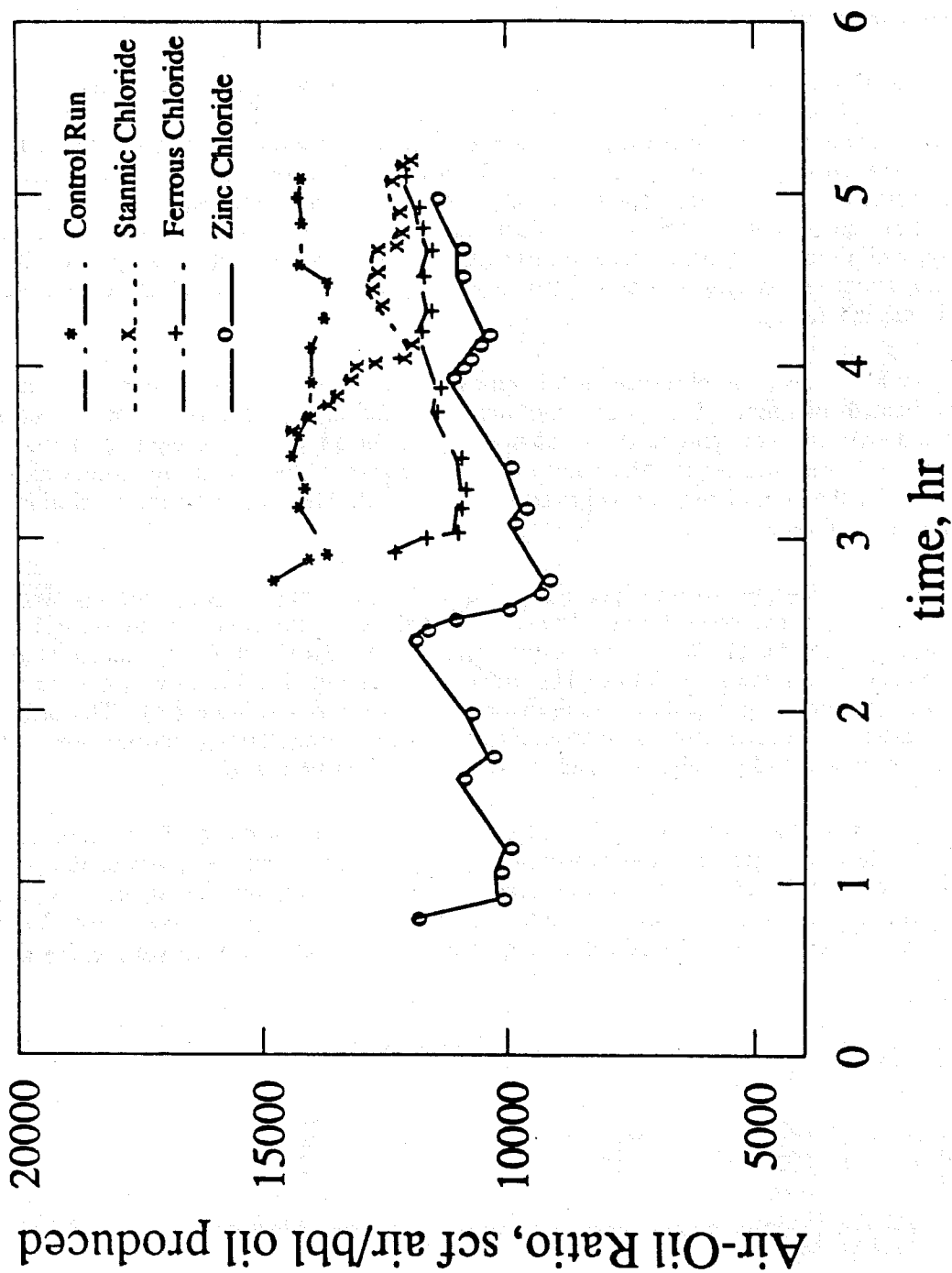


Figure 8.9 Air Oil Ratio

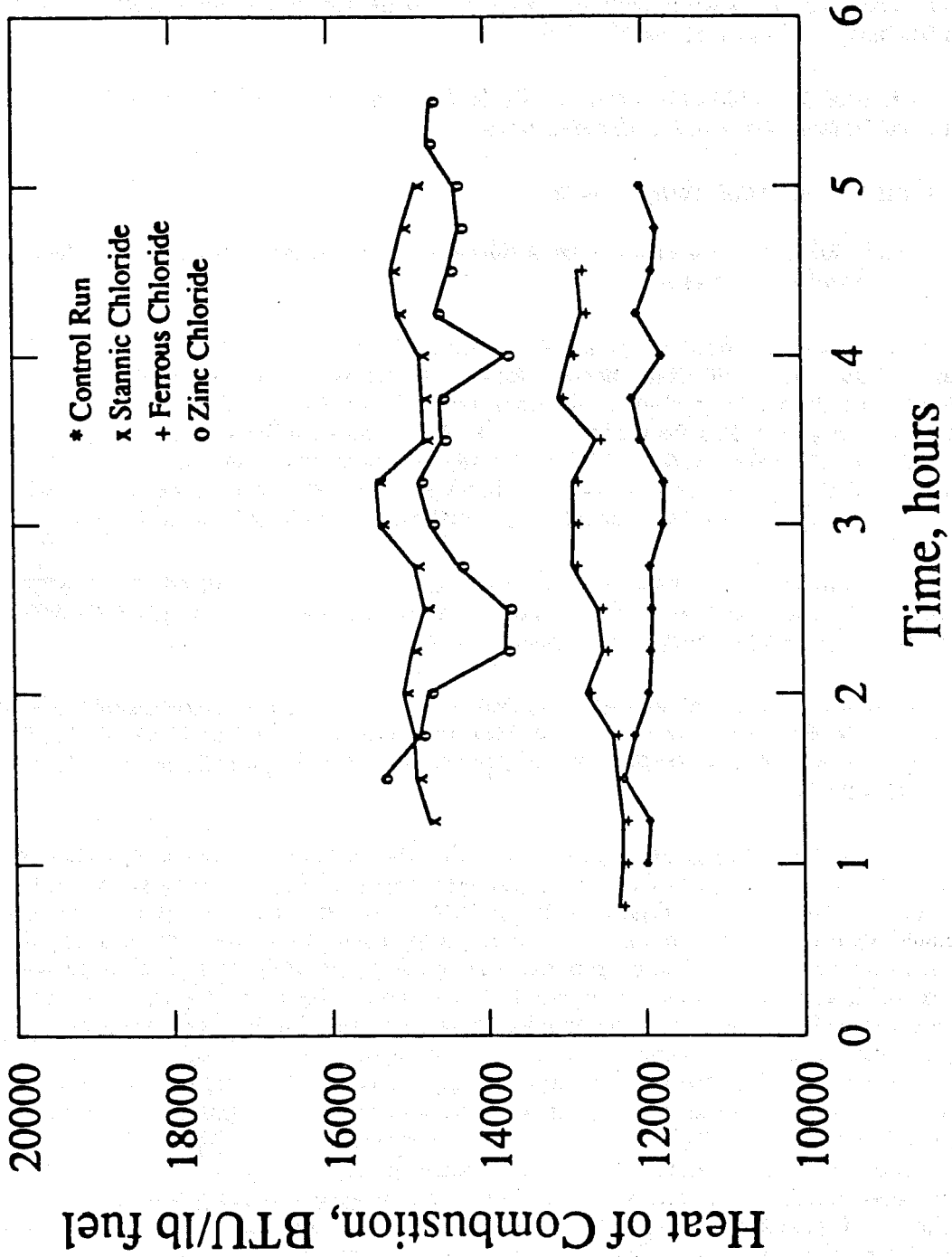


Figure 8.10 Heat of Combustion (BTU/lb of fuel burned)

carbon. Increasing values were observed for the ferrous chloride, zinc chloride and stannic chloride runs which deposited fuels having increasing fractions of hydrogen.

The graph of heat of combustion (Figure 8.10) shows that the order of increasing heat of combustion is the same as the H/C ratios (Figure 8.1). Also the variations in the heats of combustion are similar to the variations in the H/C ratio (Figure 8.1) and the air requirement (Figure 8.3). This is because all of these variables depend on the composition of the fuel burnt. The ratio of carbon dioxide to carbon monoxide had little effect on the heat of combustion because it did not vary significantly.

The heat of combustion strongly affects the combustion front temperature. The combustion front temperature data are analyzed next.

8.2 Combustion Front Temperature

In this subsection the data on the combustion front temperature reported in Section 7 and Figure 7.10 will be analyzed.

The combustion front temperature is a function of the amount of heat liberated and lost locally. The amount of heat liberated locally is related to the nature and amount of fuel formed. The greater the hydrogen to carbon ratio of the fuel, n , the greater would be the heat liberated locally, and thus the higher would be the combustion front temperature. The effect of the hydrogen to carbon ratio of the fuel on the amount of heat liberated can be seen in Equation A.9. The ratio of carbon oxides, m , has much smaller effect on the heat of combustion particularly in light of the rather small range in m seen in the experimental results.

Variations in the combustion front temperature are also a result of the variations in the amount of the fuel consumed. These can be due to local variations in saturation and porosity as a result of packing technique (discussed in Section 7).

Variations in combustion front temperature along the length of a combustion tube are also a function of the local heat loss. Heat loss variations would occur if the insulation in the annulus between the combustion tube and pressure shell was improperly packed. This idea will be investigated later.

All else being equal, one would expect that the combustion front temperature would be proportional to the amount of heat generated per pound of fuel and the amount of fuel available per pound of rock. Figures 8.11 to 8.14 show the total calculated amount of heat liberated locally for each run, and the measured combustion front temperatures along the length of the combustion tubes. The control run is shown in Figure 8.11, ferrous chloride is shown in Figure 8.12, stannic chloride in Figure 8.13 and zinc chloride in Figure 8.14. One would expect that with an increase in the amount of heat liberated locally, the combustion front temperature would increase. Figure 8.11 for the control run, shows a slight decrease in temperature after 40 cm. while the heat liberated slightly increases. This result is possibly due to an increase in the heat loss to the surroundings because of improper packing of insulation in the annulus. Figures 8.12 and 8.13 for ferrous chloride and stannic chloride show oscillating combustion front temperatures with about constant average amounts of heat liberated. These results may possibly be due to variations in the rates of heat loss due to unequal distribution of insulation. Figure 8.14 for the zinc chloride run shows variations with both the combustion front temperature and the amount of heat liberated. These variations are possibly due to differences in the nature and amount of fuel formed along the length of the combustion tube as discussed earlier in this section.

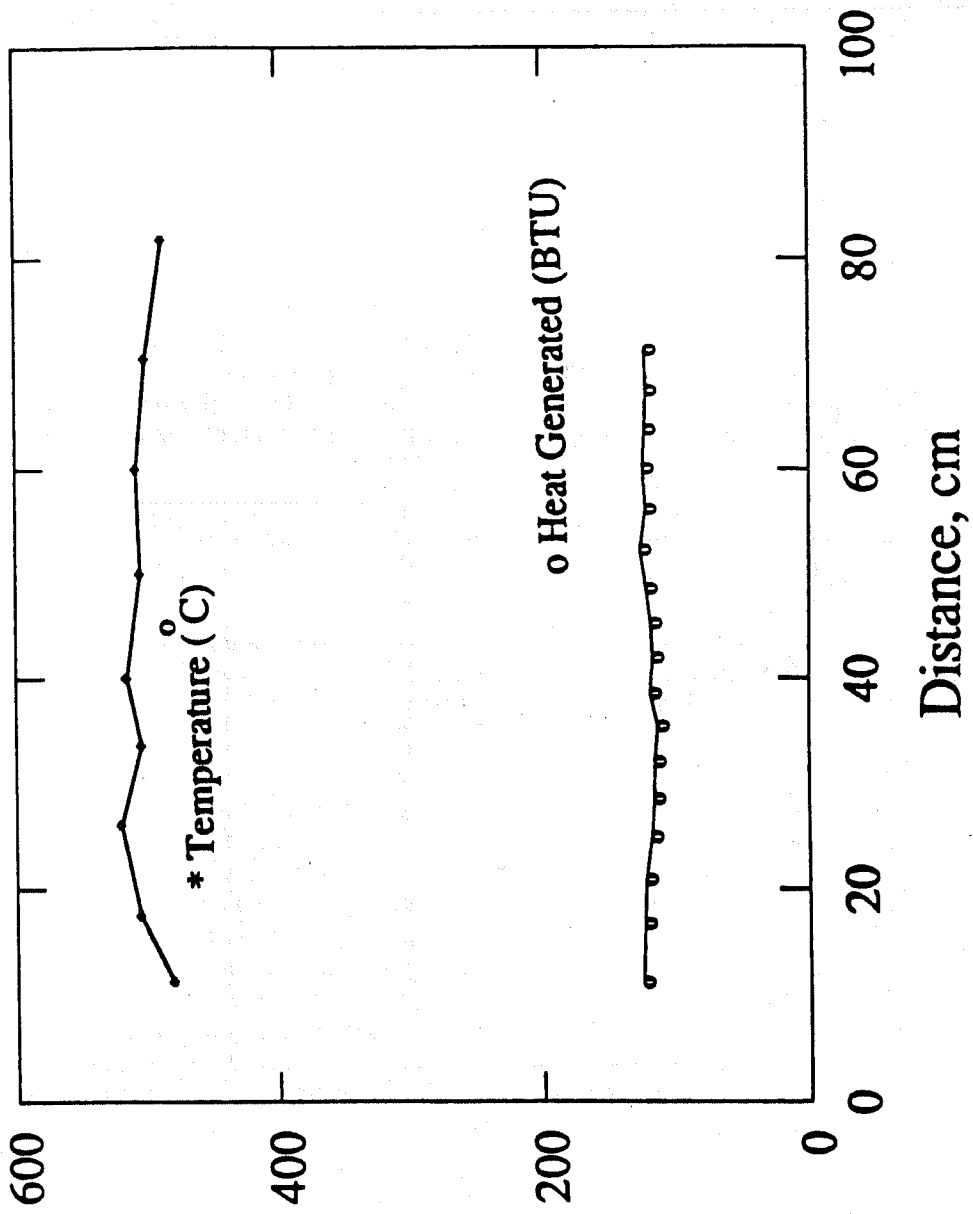


Figure 8.11 Front Temperature and Heat Liberated for the Control Run

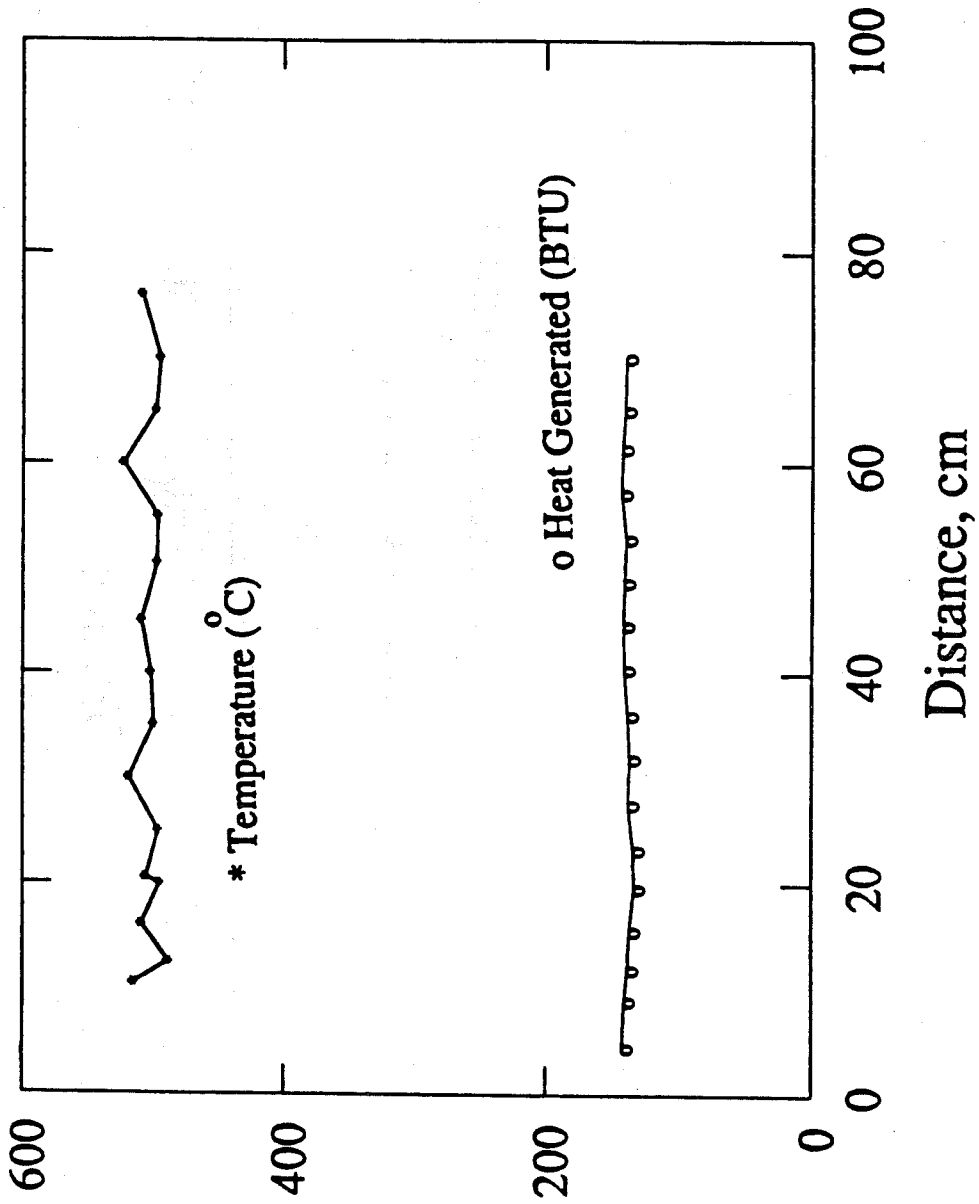


Figure 8.12 Front Temperature and Heat Liberated for the Ferrous Chloride ($FeCl_2 \cdot 4H_2O$) Run

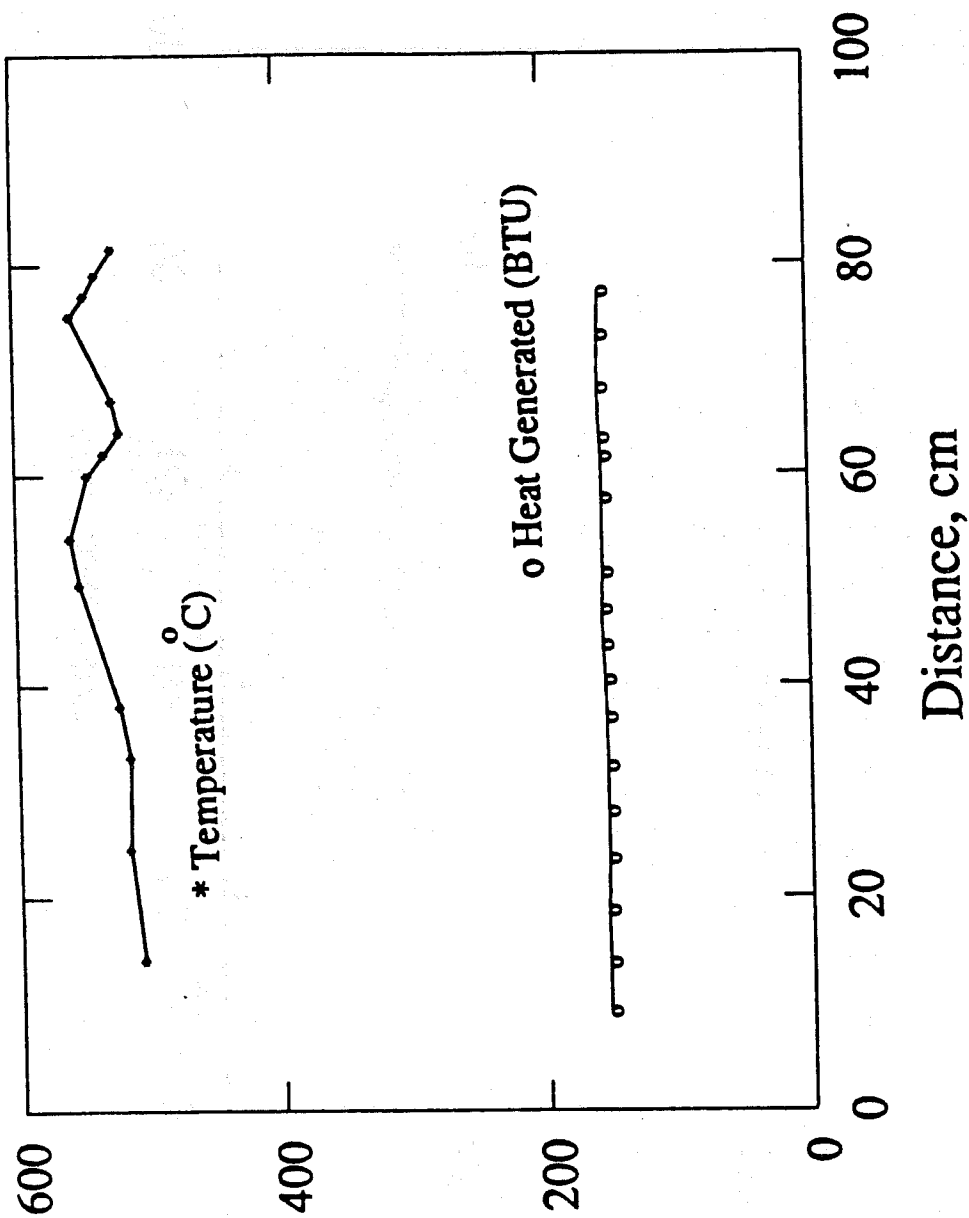


Figure 8.13 Front Temperature and Heat Liberated for the Stannic Chloride ($SnCl_4 \cdot 5H_2O$) Run

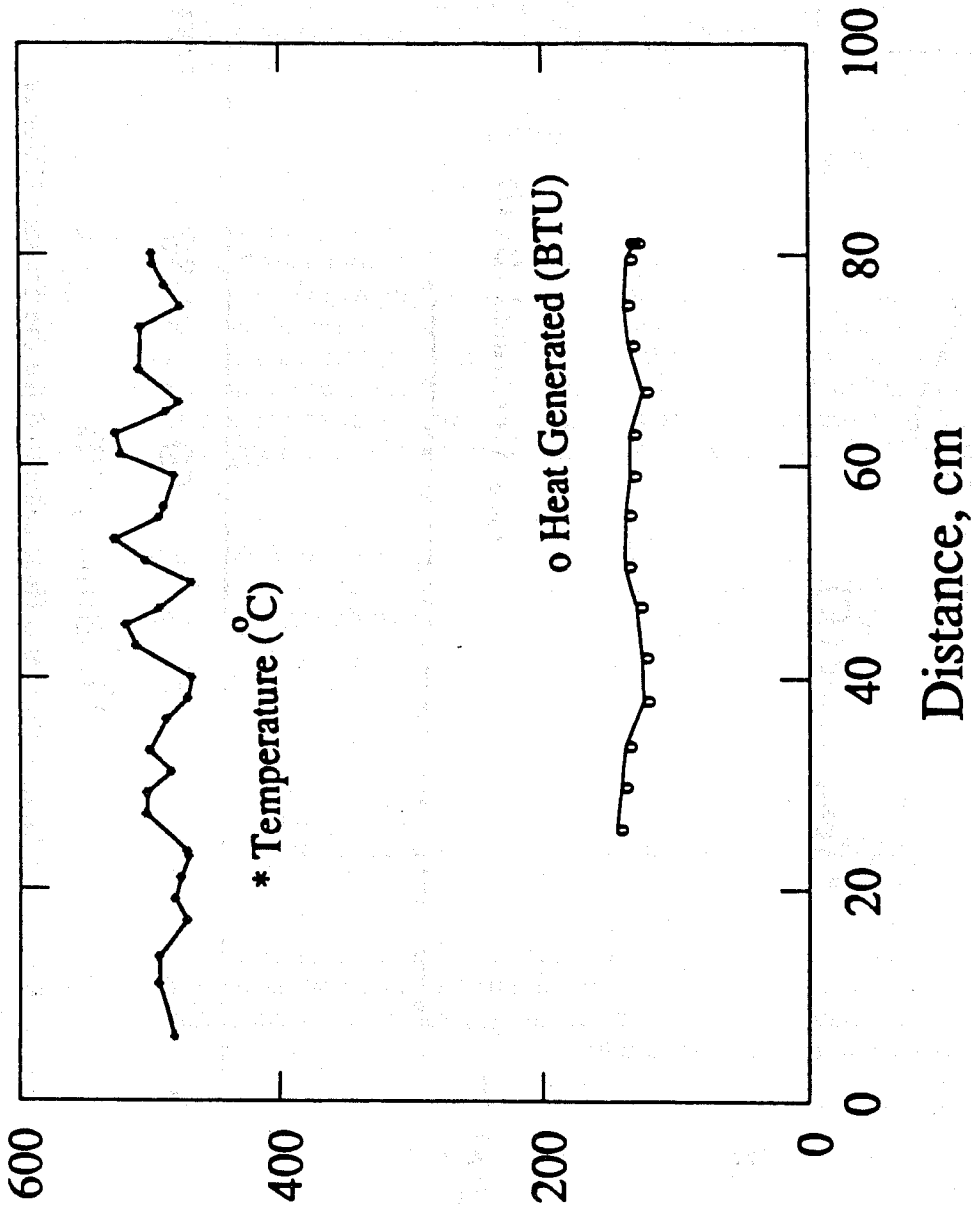


Figure 8.14 Front Temperature and Heat Liberated for the Zinc Chloride ($ZnCl_2$) Run

8.3 Combustion Front Velocity

The velocity of the combustion front is determined from data taken on the position of the front during the combustion tube runs.

Figure 8.15 shows the velocities of the combustion fronts for the four experiments. The combustion front velocities were higher with metallic additives. The combustion front velocities averaged 14.8 cm/hr for the control run, 16.6 cm/hr for stannic chloride, 17.0 cm/hr for ferrous chloride and 19.6 cm/hr for zinc chloride. An explanation for these observed velocities is given below.

Air flux, the oxygen utilization efficiency and the nature and amount of fuel formed all affect the combustion front velocity. If there is an increased amount of fuel available for burning, the velocity of the combustion front would decrease proportionately. The nature of the fuel formed affects the combustion front velocity by changing the amount of air required to burn the fuel. If the oxygen utilization efficiency decreases more air is needed, and thus the velocity of the combustion front drops.

The order of combustion front velocities is always opposite to the order of the calculated actual air requirements. Actual air requirements were computed using Equation A.16 in Appendix A. The control run had the highest actual air requirements of 275 scf/cu feet of reservoir. Actual air requirements were 241 scf/cu ft of reservoir for ferrous chloride, 241 scf/cu ft of reservoir for zinc chloride and 241 scf/cu ft of reservoir for stannic chloride. If the graphs of combustion front velocities (Figure 8.15) and the actual air requirements for each run (Figure 8.4) are compared, it is clear that the two sets of graphs are nearly mirror images of each other. Maximums in the combustion front velocity are matched by minimums in air requirements.

The oil recovery rates for the four runs, (Figures 7.11 to 7.15), also follow the same order as seen in the combustion front velocities. This result is expected from the fact that more oil will be produced if more of the reservoir is burned during a given time interval.

8.4 Discussion

In any experimental study, it is always a challenge to understand the variations in the data. In our case, variations were seen in the produced gas composition, combustion front temperature and fluid production data. This discussion focuses on an explanation of these variations.

Three factors were identified. They are: (1) inherent instabilities in the in-situ combustion process from the start of ignition until the time the heated oil began to flow, (2) variations in the packing technique for the sand pack, and (3) variations in the packing of the insulation in the annulus around the combustion tube.

8.4.1 Instabilities Early in In-Situ Combustion Type Runs

Early in the life of an in-situ combustion tube run, a number of instabilities are seen in the produced gas composition. Carbon dioxide, carbon monoxide and oxygen get dissolved in the crude oil ahead of the front. As a result the produced gas compositions show instabilities. In addition variations are seen in the combustion front temperatures. This can be a result of

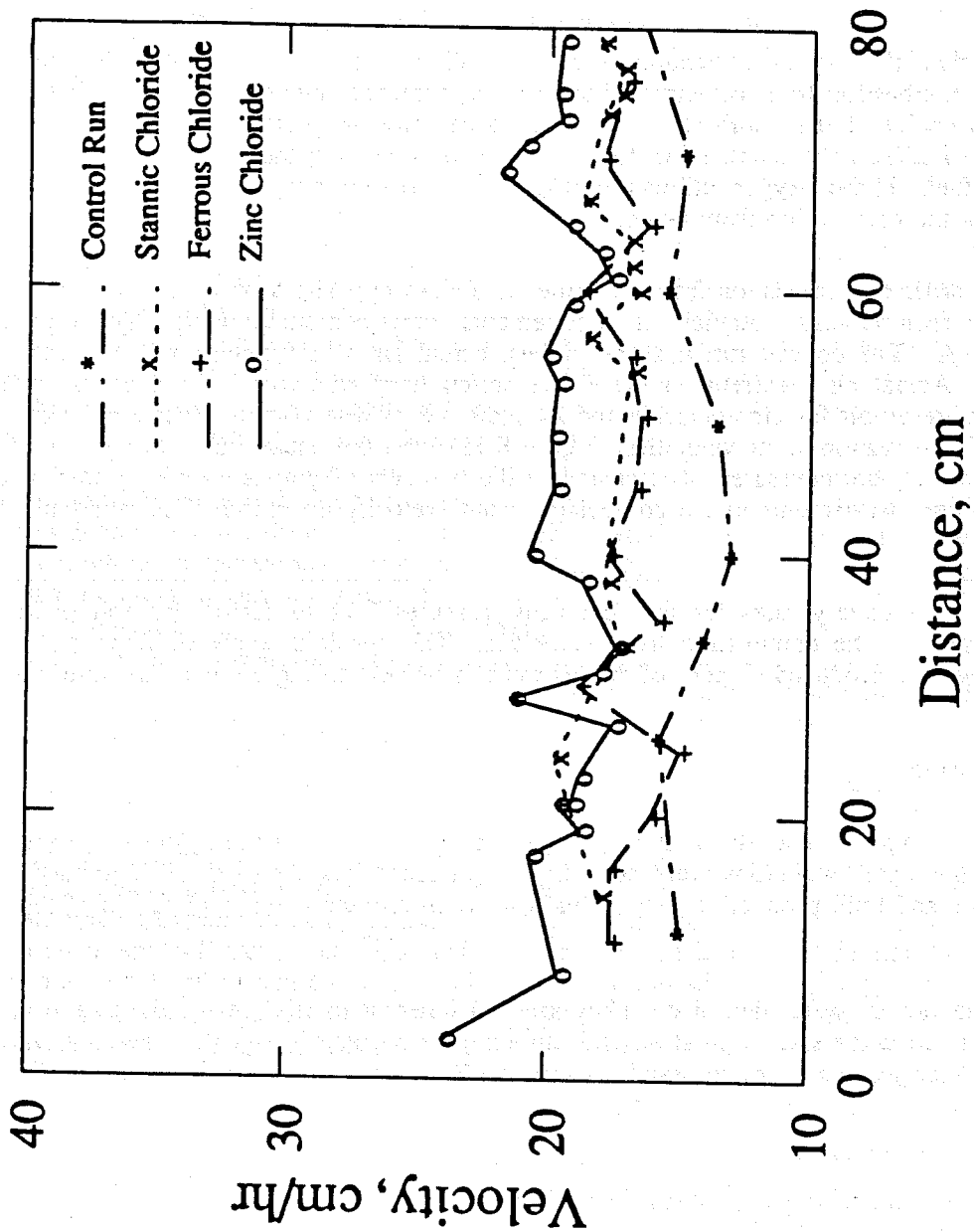


Figure 8.15 Velocities of the Combustion Front

unsteady state heat loss to the surroundings. Many investigators (Penberthy and Ramey, 1966; Andrade, 1984) compute a stabilization time for heat transfer. While this concept may be used, the real time for stabilization is the time the heated oil begins to flow. As oil is heated, the fluid that is produced is by drainage. As air is injected, it must build up sufficient oil saturation before oil begins to flow. The process that is taking place is similar to the building up of an oil bank ahead of a water injection front. When oil is being produced by drainage, its flow rate is small, however once the heated oil begins to flow, the rate rapidly increases, and remains relatively constant thereafter. The time at which this stabilization in rates is observed, should be taken to be the stabilization time in in-situ combustion tube experiments.

For example the graph of produced fluids for the control run (Figure 7.11), clearly indicates the time at which the heated oil begins to flow. This is at 2.7 hours. This is about the same time that gas composition stabilizes. The data should be analyzed after this time.

8.4.2 Packing Technique for Sand Pack

In the four combustion tube runs, two different methods were used for packing, which caused a number of differences in the data. These variations in packing were because two different persons packed the tubes. In packing the combustion tube for the ferrous and stannic chloride runs, large amounts of sample were taken and these were squeezed in with the help of a tamper. For the control run and zinc chloride, small amounts of the sand pack mixture were taken and these were vigorously tamped. Figure 7.5 illustrates the two techniques. These differences could have lead to local saturation and porosity variations, and also local differences in the amounts of fuel along the length of the combustion tube. For example, in the zinc chloride run, there are large variations in the gas compositions, combustion front temperatures and fluid production. These variations in gas compositions are manifested in the nature (Figure 8.1) and amount of fuel formed (Figure 8.5). The variations in the fuel formed affected the air requirement at 100% efficiency; while the variations in both the nature and amount of fuel formed affected the actual air requirements, which in turn affected the combustion front velocity and the oil recovery rates. Thus all these variables tended to be cyclic as a result of the packing techniques used.

8.4.3 Variations in Packing the Insulation

If the insulation in the annulus around the combustion tube is improperly packed, variations will be seen in the combustion front temperatures, even if the heat liberated remains constant. Let us consider the control run where the combustion front temperature decreased while the total heat liberated remained nearly constant. This behavior is possibly the result of packing the insulation poorly near the bottom of the tube. In the stannic chloride and zinc chloride runs, variations in the combustion front temperature were seen throughout the runs even while the heat liberated remained nearly constant (Figures 8.12 and Figure 8.13). This result may be due to uneven packing of the insulation in the annulus.

The next section includes a summary of the results and recommendations for future work.

9. CONCLUSIONS AND RECOMMENDATIONS

In this section the results obtained from the combustion tube experiments are summarized and recommendations are made for future work.

Del los Rios (1987), using Huntington Beach crude oil with ferrous chloride, stannic chloride and zinc chloride additives, determined the kinetic parameters (rate constants and energy of activation) for three reactions: (1) low temperature oxidation, (2) medium temperature reaction and (3) high temperature reaction. From the combustion tube experiments reported here, the effect of these additives on the nature of the fuel formed and on other combustion parameters were determined.

Table 9.1 summarizes the results obtained for Huntington Beach crude oil. The influence of the metallic additives on the nature of the fuel formed and the in-situ combustion characteristics are clearly evident. While the control run deposited a fuel that was essentially carbon, the metallic additives increased the atomic hydrogen to carbon ratio of the fuel from 0.07 with no additive to 0.13 with ferrous chloride, 0.61 with zinc chloride and 0.79 with stannic chloride. The H/C ratio and the ratio of carbon oxides affected the velocity of the burning front, the heat of combustion, the air requirements at 100% combustion efficiency, the air-oil ratio and the oil recovery rates. As a result of the increased hydrogen content of the fuel, the heat of combustion of the fuel increased with the additives. The air requirements at 100% combustion efficiency also increased in the order of increasing atomic H/C ratios of the fuels. The metallic additives caused an increase in the velocity of the burning front and the oil recovery rate. However these were also shown to depend on the actual air requirement, which in turn depends on the nature and the amount of fuel and the oxygen utilization efficiency.

Of the metals studied, stannic chloride caused the greatest changes. As its fuel had the highest H/C ratio, the heat of combustion and flame front temperatures were the highest. The air requirements for the stannic chloride run at 100% efficiency were also the highest. Thus the combustion front velocity and oil recovery rates were lowered.

Zinc chloride and ferrous chloride deposited a fuel with lower H/C ratios, and their heat of combustion and air requirements at 100% combustion efficiency were lower than seen with stannic chloride. Ferrous chloride caused the greatest amount of fuel deposition, consistent with the observations of De Los Rios (1987) and Racz (1985).

The fuel availability with zinc chloride was lower than the control run. This observation is inconsistent with results by De Los Rios who found a slight increase in the fuel deposition by zinc chloride. This discrepancy should be investigated by future researchers.

The above observations, that metallic additives cause changes in the nature and amount of the fuel formed, confirm that numerical simulations or designs of field tests when metallic salts will be present, should include these changes.

In this study, combustion tube experiments were performed using Ottawa sand and clay. Use of field cores would be more representative, and future work should use native core material.

Table 9.1
RESULTS OF COMBUSTION TUBE RUNS

Run Designation	Control	Ferrous Chloride	Stannic Chloride	Zinc Chloride
Oxygen Utilization Efficiency%	82.3	94.2	98.6	86.9
H/C Ratio of Fuel	0.07	0.13	0.79	0.61
Heat of Combustion (Btu/lb fuel)	11942.0	12490.0	14972.0	14481.0
Combustion Front Temperature (°C)	503.2	503	533.3	492.6
Fuel Consumption lbs fuel/100 lbs rock	1.4953	1.5461	1.5222	1.4107
Combustion Front Velocity (cm/hr)	14.8	17.0	16.6	19.6
Air Required at 100% Combustion Efficiency (scf/lb fuel)	130.6	135.75	150.4	147.4
Air Oil Ratio, scf/bbl	14,313	11,476	12,426	10,260
Actual Air Requirements (scf/cu.ft reservoir)	274.6	241.4	240.5	240.9
Density of Crude Oil Produced (gm/cc)	0.888	0.876	0.860	0.8935

The results obtained are specific to Huntington Beach crude. Crude oils may be affected to different extents by the same metallic additive, particularly when they are of significantly different composition or API gravity. Future work should study the effect of metals on differing crude oils using combustion tube studies coupled with differential thermal analysis and thermogravimetric analysis.

Metallic additives increase the fuel deposited and are particularly applicable to light oil reservoirs where the fuel deposited is often insufficient to sustain combustion. Metal salts in heavy oil reservoirs, which produce high levels of fuel, may render the process uneconomic because of high air requirements.

As observed from the cyclical variations in gas composition, combustion front temperature data, and oil recovery rates, zonal and local saturation variations affect the results. To avoid these variations it is recommended that the laboratory packing technique should aim at minimizing these saturation variations, both when mixing and when tamping the mixture into the combustion tube. The results of the stannic chloride run indicate that packing the tube by squeezing a larger sample into the combustion tube produces more uniform saturation distributions especially if the pack has been well mixed before packing.

Care should be taken to see that the packing of the external insulation is uniform and adequate. This will reduce variations in the combustion front temperatures, as a result of uneven heat loss.

When analyzing a combustion tube data, one must clearly identify the time at which the heated oil begins to flow. The data collected after this time is usually more representative of the steady state process.

The literature is nearly devoid of field studies on the application of metallic additives in in-situ combustion oil recovery. Metallic additives could be used to solve the problems of insufficient fuel deposition in light oil reservoirs. This process should be tried in the field after performing combustion tube studies on field cores with field crudes.

It is expected that this work will spark interest in the use of metallic additives in in-situ combustion oil recovery, particularly for those light oil reservoirs having problems of insufficient fuel deposition.

REFERENCES

Alexander, J.D., Martin, W.L., and Dew, J.N.: "Factors Affecting Fuel Availability and Composition During In Situ Combustion," J. Pet. Tech. (October 1962) 1154-1164.

Al-Saadoon, F.T.: "An Experimental and Statistical Study of Residual Oil Saturation After Gas, Water and Steam Drive, and Fuel Availability for the In-Situ Combustion Process," Ph.D. Dissertation, University of Pittsburgh, PA., 1970.

Andrade, G.M.: "An Investigation of Pressure Effects on Combustion Tube Runs," M.S. Thesis, Stanford University, CA (1984).

Arrhenius, S.: Z. Physik Chem. (1889), Vol. 4, 226.

American Society for Testing Materials Standard D-95, published by the AIME.

Bardon, C. and Gadelle, C.: "Essai de Laboratoire Pour L'Etude de la Combustion In-Situ," Institute Francais du Petrole, Paris (May 1977).

Benham, A.L. and Poettman, F.H.: "The Thermal Recovery Process - An Analysis of Laboratory Combustion Data," J. Pet. Tech. (September 1958) 83-85.

Bousaid, J.G.: "Oxidation of Crude Oil in Porous Media", Ph.D. Dissertation, Texas A & M University, TX (1967).

Burger, J.G. and Sahuquet, B.C.: "Combustion a Contre-Courant. Interpretation d'Essais par Modele Numerique Unidirectionnel," Rev. Institut Francais De Petrole (1971), Vol. 26, 399-422.

Burger, J.G. and Sahuquet, B.C.: "Chemical Aspects of In-Situ Combustion - Heat of Combustion Kinetics," Soc. Pet. Eng. J. (October 1972) 410-420.

Carcoana, A.N., Machedon, V.C., Pantazi, I. G., Petcovici, V.C., and Turta, A.T.: "In Situ Combustion - An effective method to enhance oil recovery in Romania", Eleventh World Petroleum Congress, London, 1983.

Dabbous, M.K. and Fulton, P.F.: "Low-Temperature-Oxidation Reaction Kinetics and Effects on the In-Situ Combustion Process," Soc. Pet. Eng. J. (June 1974) 253.

De Los Rios, C.: "The Effect of Metallic Additives on the Kinetics of Oil Oxidation Reactions in In-Situ Combustion," Engineers Degree Thesis, Stanford University, California (October 1987).

Dew, J.N. and Martin, W.L.: "Air Requirement for Forward Combustion," Pet. Eng. (December 1964) 82.; and (January 1965) 82-85.

Drici, O. and Vossoughi, S.: "Catalytic Effect of Heavy Metal Oxides on Crude Oil Combustion," paper 63a presented at the 1985 AIChE National Meeting and Petroleum Exposition, Houston, March 24-28.

Earlougher, R.C., Galloway, J.R., and Parsons, R.W.: "Performance of the Fry In-Situ Combustion Project," J. Pet. Tech. (May 1970) 551-557.

Fassihi, M.R.: "Analysis of Fuel Oxidation in In-Situ Combustion Oil Recovery," Ph.D. Dissertation, Stanford University, CA (1981).

Gureyev A.A. and Sablena, Z.A.: "The Role of Metals in Oxidation of Hydrocarbon Fuels in the Liquid Phase," Scientific Research Institute of Fuel and Lubricating Materials, Pergamon Press (1965).

Hardy, W.C., Fletcher, P.B., Shepard, J.C., Dittman, E.W., and Zadow, D.W.: "In-Situ Combustion in a Thin Reservoir Containing High-Gravity Oil," J. Pet. Tech. (February 1972) 199-208.

Martin, W.L., Alexander, J.D., and Dew, J.N.: "Process Variables of In-Situ Combustion," Trans., AIME (1958) Vol. 213, 28.

Moss, J.T., White, P.D. and McNeil, J.S. Jr.: "In-Situ Combustion Process- Results of a Five-Well Field Experiment in Southern Oklahoma", Trans. AIME (1959), Vol. 216, 28-35; J. Pet. Tech. (1959), 55-64.

McCarthy, H. Jr., Paiverneker, V.R., and Maycock, J.N.: "Determination of Kinetic Parameters from a Single Thermogram", Proceedings, Third International Conference on Thermal Analysis, Davos, Switzerland (1971), Vol. 1, 355.

Penberthy, W.L. Jr. and Ramey, H.J. Jr.: Design and Operation of Laboratory Combustion Tubes," Soc. Pet. Eng. J. (June 1966), 183-98.

Poettmann, F.H., Schilson, R.E., and Surkalo, H.: " Philosophy and Technology of In-Situ Combustion in Light Oil Reservoirs," World Oil (1967) Vol. 165, 487-497.

Racz.: " Development and Application of a Thermocatalytic In-Situ Combustion Process in Hungary," paper presented at the 1985 European Meeting on Improved Oil Recovery, Rome, Italy, April 16-18.

Satman, A.: "In-Situ Combustion Models for The Steam Plateau and for Fieldwide Oil Recovery," PhD Dissertation, Stanford University, CA (1979).

Showalter, W.E.: "Combustion-Drive Tests," Soc. Pet. Eng. Journal (March 1963), 53-58.

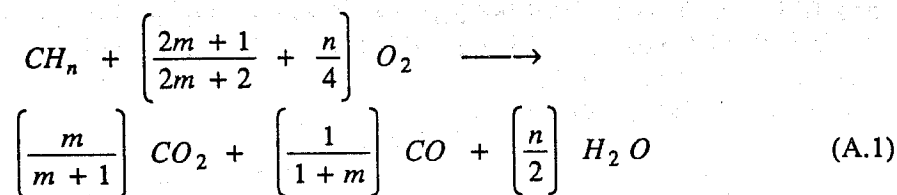
Sidqi, A., Ramey, H.J. Jr., Pettit, P., and Brigham, W.E.: The Reaction Kinetics of Fuel Formation for In-Situ Combustion," Stanford University Petroleum Research Institute, Stanford, CA, SUPRI TR-46, Report submitted to the U.S. Dept. of Energy, under contract No. DE-AC03-81SF 11564 (May 1985)

Weijdemans, J.: "Determination of the Oxidation Kinetics of the In-Situ Combustion Process," Report from Koninklijke/Shell Exploratie En Productie Laboratorium, Rijswijk, The Netherlands (1968).

Wilson, L.A., Reed, R.L., Clay, R.R. and Harrison, J.H.: "Some Effects on Pressure on Forward and Reverse Combustion," Soc. Pet. Eng. Journal (June 1963), 127-137.

APPENDIX A

The model of Dew and Martin (1964, 1965) was used to analyze of the influence of the metallic additives on the in-situ combustion of Huntington Beach crude oil. The model assumes that the high temperature oxidation reaction of the deposited fuel, CH_n , takes place according to the following equation:



In this equation, n is the hydrogen to carbon ratio of the deposited fuel, and m is the ratio of CO_2 to CO in the produced gases. Assuming that the water produced is completely removed by the dessicant, and that the produced gas contains only carbon dioxide, carbon monoxide, nitrogen and unburned oxygen, the mole fraction of nitrogen in the produced gas is determined from:

$$N_2 = 100 - (CO_2 + CO + O_2) \quad (A.2)$$

The ratio of hydrogen to carbon in the fuel can be determined by using the stoichiometric equation for the combustion of the fuel and a material balance on oxygen and nitrogen. Using the stoichiometric equation, the ratio of hydrogen to carbon in the fuel is given by:

$$n = 4 \frac{(\text{moles of oxygen converted water})}{(\text{atoms of carbon})} \quad (A.3)$$

The moles of oxygen converted to water is determined by a material balance on oxygen. The moles of oxygen in the injected air is given by:

$$n_{O_2} = \frac{0.21}{0.79} n_{N_2} \quad (A.4)$$

In the above equation, n_{O_2} is the number of moles of oxygen and n_{N_2} is the number of moles of nitrogen in the injected air. The constants 0.21 and 0.79 represent the mole fractions of oxygen and nitrogen in the injected air. Assuming that all the nitrogen injected is produced, use of Equation (A.2) leads to:

$$n_{O_2} = \frac{0.21}{0.79} \left[100 - (CO_2 + CO + O_2) \right] \quad (A.5)$$

The molar percentage of oxygen in the produced gas is $(CO_2 + 0.5 CO + O_2)$. The moles of oxygen converted to water is given by the difference between the moles of oxygen in the injected air and produced gas. Thus the atomic ratio of hydrogen to carbon of the fuel is given by using equations (A.3), (A.5) and the definition of the moles of oxygen in the produced gas.

$$n = \frac{106.33 + 2CO - 5.063 (CO_2 + CO + O_2)}{(CO_2 + CO)} \quad (A.6)$$

In deriving the above equation it is assumed that all of the oxygen consumed resulted in the production of carbon oxides and water. This assumption is not exact particularly at lower temperatures where a part of the oxygen reacts with the crude oil to form oxygenated compounds such as alcohols and phenols. The calculated hydrogen to carbon ratios also depend on the solubility of the combustion gases in the reservoir oil. During the early part of an in-situ combustion process, higher ratios are calculated, until the oil and water ahead of the combustion front are saturated with the combustion gases. The combustion efficiency, Y , defined as the fraction of the oxygen injected that is consumed, is given by:

$$Y = 1 - \frac{0.79}{0.21} \left[\frac{O_2}{N_2} \right] \quad (A.7)$$

The above equation is derived by using the material balance on nitrogen and the definition of oxygen utilization efficiency. In this equation, 0.79 and 0.21 are the mole fractions of nitrogen and oxygen in the injected air. Combustion efficiencies determined in the laboratory are specific to the conditions under which the experiment is performed. However most field projects on California crude operate at nearly 100% combustion efficiency. Thus comparisons should be made on this basis. The amount of air required to burn a pound of fuel at 100% combustion efficiency, F_{aF} in scf/lb fuel is obtained by using the stoichiometric equation and converting the moles of oxygen to the volume of air at standard conditions of temperature and pressure. The air required at 100% combustion efficiency is given by:

$$F_{aF} = 902.38 \frac{\left[\frac{2m + 1}{m + 1} + \frac{n}{2} \right]}{12 + n} \quad (A.8)$$

The factor $(12 + n)$ converts moles of the deposited fuel to pounds of fuel since $(12 + n)$ is the molecular weight of the fuel. The constant 902.38 arises from the value $379 / 2 * 0.21$ where 379 converts the moles of air to standard cubic feet of air and 0.21 is used to convert the moles of oxygen to moles of air. The heat generated on combustion of the fuel is determined by summing the heats of formation of carbon monoxide, carbon dioxide and water. The heat of combustion, H_c , in Btu/lb is given by:

$$H_c = \frac{174000 m}{(m + 1)(12 + n)} + \frac{52500}{(m + 1)(n + 12)} + \frac{123000 n}{2 (12 + n)} \quad (A.9)$$

In the above equation, the values 174,000, 52,500, and 123,000 are the heats of formation of carbon dioxide, carbon monoxide and water in Btu/lb mole.

The amount of heat generated per standard cubic foot of air consumed at 100% efficiency, H_a , is derived by dividing the heat of combustion per pound of fuel by the air required to burn that pound of fuel:

$$H_a = \frac{H_c}{F_{aF}} \quad (A.10)$$

Computations of the amount of fuel deposited are made by performing a material balance over nitrogen to determine the total flow rate of the produced gas. From the composition of the produced gas, the volumetric flow rate and the molar flow rate of the carbon oxides in the produced gas can be determined. Knowing the molecular weight of the fuel, $12 + n$, the weight of the fuel deposited can be determined. The steps to determine the fuel availability are explained in the next few paragraphs.

At any time, t , a material balance on nitrogen flowing through the combustion tube yields:

$$q_{in} [N_2]_{in} = q_{out} [N_2]_{out} \quad (A.11)$$

In this equation $[N_2]_{in}$ and $[N_2]_{out}$ are the mole fractions of nitrogen in the inlet and outlet gas, while q_{in} and q_{out} are their volumetric flow rates. The volumetric flow rate of the gas entering the combustion tube is measured in standard liters per minute. Hence q_{out} is also calculated in standard liters per minute. The values of q_{in} and $[N_2]_{in}$ are known while $[N_2]_{out}$ can be determined using equation (A.2). During time period from t_1 to t_2 hours, the front moves from location x_1 to location x_2 . During this period, the total standard cubic feet of carbon oxides, $[Q_{out}]_{CO_x}$, that flow out of the combustion tube is given by:

$$[Q_{out}]_{CO_x} = \frac{60}{(28.32)(100)} q_{out} [t_2 - t_1] [CO + CO_2] \quad (A.12)$$

In the above equation, the factor 60 is used to convert hours to minutes, the constant 28.32 is used to convert liters to standard cubic feet, and 100 is used to convert the concentration of carbon oxides from percentages to volume fractions.

Knowing that one pound mole of gas occupies 379 cubic feet at standard conditions of temperature and pressure, the moles of carbon oxides flowing out of the combustion tube can be determined. From the stoichiometric equation, the number of moles of the fuel burned is the same as the moles of carbon oxides produced. Thus the weight of the fuel burnt can be determined as the molecular weight of the fuel is known. Using the above argument, the pounds of the fuel burnt during time increment t_1 to t_2 is:

$$W = \frac{[Q_{out}]_{CO_x} [12 + n]}{379} \quad (A.13)$$

The incremental fuel availability, M_R , in pounds of fuel per cubic feet of rock, is obtained by dividing the weight of the fuel burned by the incremental cubic feet of rock burned during time interval t_1 to t_2 . Thus M_R is determined by:

$$M_R = \frac{28317 W}{A [x_2 - x_1] [1 - \phi]} \quad (A.14)$$

In this equation A is the cross sectional area of the combustion tube in square centimeters, x_1 and x_2 are the positions of the front in centimeters at time t_1 and t_2 hours, and ϕ is the porosity of the sand pack. The denominator is the incremental volume of the reservoir rock burned in square centimeters while the factor 28,317 in the numerator converts cubic centimeters to cubic feet.

Laboratory data has shown that the amount of fuel burned is not affected by the porosity variations over a practical range and can be represented on the basis of pounds of rock (Dew and Martin, 1964, 1965). It is therefore standard practice to report the fuel deposited in terms of pounds of fuel deposited per 100 lb of reservoir rock, W_R , for a given crude oil and reservoir rock. W_R can be computed using M_R (lb of fuel/cubic feet of rock) and the sand grain density of the reservoir rock, ρ_R (lb/cubic feet). The equation used is:

$$W_R = M_R \frac{100}{\rho_R} \quad (\text{A.15})$$

In addition to computing the fuel deposition, one determines the air requirements. The number of the standard cubic feet of air actually required per cubic feet of reservoir at the operating efficiency, a_R , is determined from:

$$a_R = \frac{M_R F_{aF} (1 - \phi)}{Y} \quad (\text{A.16})$$

In an in-situ combustion process, it is standard practice to determine the amount of the air required to be injected to produce one barrel of crude oil. This amount is called the air-oil ratio. It is determined using the data on the actual amount of air injected and the actual amount of crude oil produced.

These computations were performed on the data collected during the laboratory runs.

